DISS. ETH No. 16811

Late Quaternary changes in nitrogen fixation and climate variability recorded by sediments from the Gulf of Mexico and the Caribbean Sea

A dissertation submitted to the

ETH ZURICH

for the degree of

Doctor of Natural Sciences

presented by

ANNA NELE MECKLER

Dipl.-Geoökologin Univ., University of Bayreuth
born 22 April 1977 in Frankfurt am Main
citizen of Germany

accepted on the recommendation of

Prof. Dr. Hans R. Thierstein, examiner
Prof. Dr. Gerald H. Haug, co-examiner
Prof. Dr. Judith A. McKenzie, co-examiner
Prof. Dr. Nicolas Gruber, co-examiner

2006

Table of Contents

Seite Leer /
Blank leaf

Abstract

The availability of nitrate limits primary productivity in many parts of the ocean. Therefore, changes in the size of the marine nitrogen reservoir potentially have a large impact on oceanic uptake of CO_2 and thereby on global climate. Glacial-interglacial variations in the marine nitrogen pool could hence have played a role in the large observed variations in atmospheric CO_2 content. However, while it is well established that the most important sink of nitrate, denitrification, was less active in glacial times, only little has been known about concurrent changes in the major source, namely N_2 fixation. Both processes can be traced back in time by studying the nitrogen isotopic composition ($\delta^{15}N$) of sedimentary organic matter (OM).

The aim of this thesis is to determine changes in N_2 fixation from glacials to interglacials based on high-resolution $\delta^{15}N$ records obtained from two exceptional sites in the Gulf of Mexico (Orca Basin) and the Caribbean Sea (Cariaco Basin). Both sites are characterized by anoxic bottom water and excellent OM preservation despite being located in areas of active N_2 fixation. In the Orca Basin, however, the signal is influenced by varying input of terrigenous OM, which is assessed using bulk parameters (C/N, $\delta^{13}C$, %detritus), biomarker measurements, and optical kerogen analyses. All proxies indicate larger input of terrigenous OM during glacial and deglacial times, although the results are equivocal in some aspects. Furthermore, the findings suggest that the history of deglacial meltwater flow to the Gulf of Mexico, especially during the Younger Dryas period, is not yet fully understood. Taking the influence of terrigenous OM in the glacial section into account, the $\delta^{15}N$ record revealed that present N_2 fixation is at least of glacial magnitude but probably stronger.

In Cariaco Basin, high-resolution records from the last deglaciation and Termination V (the initiation of the interglacial MIS 11 at around 430 ka) complement existing low-resolution data. A close similarity of the signals during the two terminations suggests systematic changes in the regional nitrogen cycle. The observed deglacial $\delta^{15}N$ decreases in Cariaco Basin are best explained by increasing N_2 fixation during interglacials, since these changes occur much later than local influences due to rising sea level. The results from both sites therefore suggest a deglacial increase in N_2 fixation in the western North Atlantic, which probably responded to an enhanced global loss of nitrate through denitrification lowering the global nutrient N:P ratio. The late Holocene $\delta^{15}N$ decrease in Cariaco Basin, however, calls for an additional influence, such as increased iron input. Common features of the records from Orca and Cariaco Basin and data from denitrification zones are an early Holocene decrease in $\delta^{15}N$, which likely reflects a change in mean ocean nitrate $\delta^{15}N$, and stable $\delta^{15}N$ values after around 3 ka, indicating that the marine N budget is currently stable.

First tests towards coccolith-bound $\delta^{15}N$ measurements and initial determinations of the abundance of proposed cyanobacterial biomarkers indicate that further work is needed to establish such methods, which would allow assessing variations in N_2 fixation without interferences by terrigenous OM, diagenetic overprint, or additional nitrogen cycle processes such as denitrification.

In a second part of this thesis, Holocene climate variability in North America is studied to assess the link between climatic changes in mid-latitudes and those in low latitudes, such as the Caribbean. Variations in the relative contribution of terrigenous elements in sediments from Pigmy Basin, Gulf of Mexico, are interpreted as changes in Mississippi input, which reflects fluctuations in the hydrological cycle over North America. Mississippi input was largest during generally dry conditions in much of the catchment. Although some potential influences such as climate conditions in the eastern part of the catchment or changes in sediment distribution in the Gulf of Mexico are currently not well constrained, this observation is best explained by more extreme climate conditions facilitating erosion during overall drier times, which were generally associated with strong summer insolation.

With regard to the influence of the nitogen cycle on glacial-interglacial variations in atmospheric CO_2 content, this work suggests that a deglacial increase in N_2 fixation in the western North Atlantic balanced some of the increased global nitrogen loss through denitrification. Alternative methods need to be further developed to complete the picture with data from other ocean basins.

Zusammenfassung

In großen Teilen des Ozeans ist Primärproduktion durch die Verfügbarkeit von Nitrat limitiert. Daher können Veränderungen in der Gesamtmenge marinen Stickstoffs einen großen Einfluss auf die Aufnahme von CO_2 durch den Ozean und damit auf das globale Klima ausüben. So könnten die erheblichen glazial-interglazialen CO_2-Schwankungen unter anderem durch Änderungen im marinen Stickstoffvorrat hervorgerufen worden sein. Während bekannt ist, dass die Hauptsenke für Nitrat, die Denitrifizierung, in Glazialen weniger aktiv war, weiß man bislang wenig über Veränderungen in der Hauptquelle, der N_2 Fixierung. Beide Prozesse können aus der Isotopenzusammensetzung von Stickstoff ($\delta^{15}N$) in sedimentärem organischem Material (OM) abgeleitet werden.

Ziel der vorliegenden Arbeit ist es, glazial-interglaziale Veränderungen der N_2 Fixierung zu rekonstruieren. Die hochaufgelösten $\delta^{15}N$ Daten stammen von zwei aussergewöhnlichen Becken im Golf von Mexico (Orca Becken) und der Karibik (Cariaco Becken), die sich durch anoxisches Tiefenwasser und vorzügliche Erhaltung des OM auszeichnen, obwohl sie in Gegenden aktiver N_2 Fixierung liegen. Im Orca Becken wurde das Signal allerdings zusätzlich von wechselndem Eintrag terrigenen OMs beeinflusst, welcher hier mittels gesamtsedimentärer Parameter (C/N, $\delta^{13}C$, %Detritus), Biomarkern und optischer Kerogenanalysen bestimmt wurde. Alle Indikatoren zeigen erhöhten Eintrag von terrigenem OM im glazialen Sediment, wobei sie nicht in allen Details übereinstimmen. Desweiteren deuten die Ergebnisse darauf hin, dass der zeitliche Ablauf des Schmelzwassereintrags in den Golf von Mexico noch nicht hinlänglich untersucht ist, vor allem während der Jüngeren Dryas. Unter Einbeziehung des zusätzlichen Einflusses terrigenen OMs in den glazialen Abschnitten zeigen die $\delta^{15}N$ Daten, dass die heutige N_2 Fixierung mindestens so aktiv, wahrscheinlich aber stärker ist als im Glazial.

Im Cariaco Becken ergänzen die hochauflösenden Daten für die Terminationen I (vor ca. 18 ka) und V (Übergang zum Interglazial MIS11 vor ca. 430 ka) einen bestehenden, niedriger aufgelösten Datensatz. Die Ähnlichkeit des Signals während dieser Übergänge deutet auf systematische Veränderungen im regionalen Stickstoffkreislauf hin. Die abnehmenden $\delta^{15}N$ Werte beruhen wahrscheinlich auf zunehmender N_2 Fixierung in Interglazialen, da sie deutlich später erfolgten als lokale Veränderungen im Zusammenhang mit Meeresspiegelanstiegen. In beiden Becken weisen die Daten demnach auf zunehmende N_2 Fixierung in Interglazialen hin, was wahrscheinlich mit vermehrtem globalem Verlust von Stickstoff durch Denitrifizierung und daraus folgenden Veränderungen im N:P Verhältnis des globalen Nährstoffvorrats zusammenhängt. Der späte Zeitpunkt der holozänen Abnahme von $\delta^{15}N$ im Cariaco Becken spricht allerdings für einen weiteren Einflussfaktor, wie zum Beispiel Eiseneintrag. Die Zeitreihen

von Orca und Cariaco Becken zeigen Gemeinsamkeiten mit Daten aus Denitrifizierungsgebie ten: Eine globale früh-holozäne Abnahme von $\delta^{15}N$ deutet auf eine Veränderung des mittleren globalen $\delta^{15}N$ von Nitrat hin, während konstante Werte während der letzten 3 ka Stabilität des Stickstoffreservoirs über diesen Zeitraum anzeigen.

Erste Tests zur Messung von $\delta^{15}N$ an Coccolithen sowie zur Abundanz von cyanobakteriellen Biomarkern zeigen, dass weitere Entwicklungsarbeit an Methoden dieser Art nötig ist, um Veränderungen der N_2 Fixierung unabhängig von Einflüssen wie terrigenem OM, diagenetischen Veränderungen oder anderen Prozessen des N Kreislaufs wie Denitrifizierung rekonstruieren zu können.

In einem zweiten Teil dieser Arbeit werden holozäne Klimaveränderungen in Nordamerika rekonstruiert, um den Zusammenhang zwischen dem Klima der mittleren Breiten und dem der Subtropen (z.B. Karibik) zu untersuchen. Veränderungen des Gehalts an terrigenen Elementen in Sedimenten des Pigmy Beckens, Golf von Mexico, werden dabei als wechselnder Eintrag des Mississippi interpretiert, der mit den hydrologischen Bedingungen in Nordamerika zusammenhängt. Der Mississippi-Eintrag war am stärksten unter überwiegend trockenen Bedingungen im Einzugsgebiet. Obwohl einige potentielle Einflussfaktoren, wie das Klima im östlichen Einzugsgebiet oder Veränderungen der Sedimentverteilung im Golf von Mexico, momentan nicht gut abschätzbar sind, ist die wahrscheinlichste Erklärung ein vermehrtes Auftreten extremer Ereignisse in Zeiten genereller Trockenheit, was zu verstärkter Erosion führte. Diese Phasen waren tendenziell mit erhöhter Solareinstrahlung verbunden.

Im Bezug auf den Einfluss des Stickstoffkreislaufes auf die glazial-interglazialen CO_2-Schwankungen deuten die Ergebnisse darauf hin, dass Steigerungen der N_2 Fixierung im westlichen Nordatlantik vermehrten globalen N-Verlusten durch Denitrifizierung entgegenwirkten. Neue Methoden sind erforderlich, um das Bild mit Daten aus anderen Teilen des Ozeans zu vervollständigen.

Chapter 1

Introduction

1.1. Why study the marine nitrogen cycle?

In most parts of today's ocean, primary productivity is considered to be limited by the availability of dissolved ('fixed') nitrogen. This is reflected in the extensive areas of the surface ocean that are depleted in nitrate (Figure 1.1A). Through this importance for marine primary production, the availability of nitrate represents one control for the oceanic uptake of CO_2. Since CO_2 is an important greenhouse gas, this link furthermore implies a potentially large climate impact of changes in the marine nitrogen cycle. Nonetheless, the factors that regulate the size of the marine pool of fixed nitrogen are still only poorly understood. Facing the increasing anthropogenic emissions of CO_2 and our influence on the nutrient cycles, there is a strong need to better understand the important feedback mechanisms within the carbon and nutrient cycles.

Valuable information can be gained by studying past changes in the various components of this system, for example during large deglacial climatic shifts. Measurements of gas concentrations in ice cores have shown that the CO_2 content of the atmosphere underwent large fluctua-

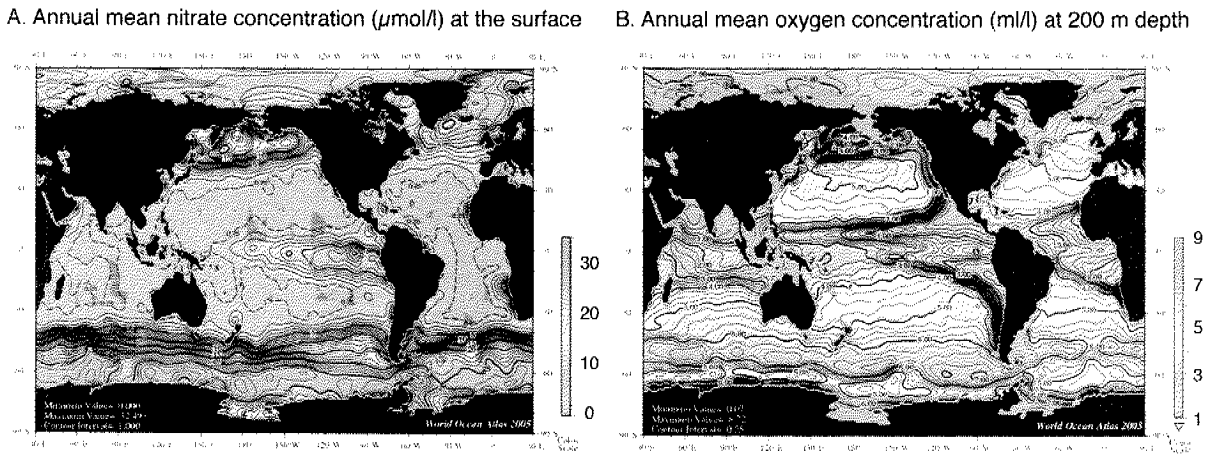

Figure 1.1. A. Map of the ocean showing nitrate concentrations at the surface. Note the large areas depleted in nitrate (blue color) in the subtropical gyres. B. Oxygen concentrations at 200 m depth showing the major oxygen minimum zones (blue color) in the eastern tropical north and south pacific and the Arabian Sea, hosting most of the water column denitrification. From World Ocean Atlas 2005 (http://www.nodc.noaa.gov/OC5/indprod.html).

tions on glacial-interglacial timescales, with much lower concentrations in glacials compared to interglacials [e.g., *Barnola et al.*, 1987; *Siegenthaler et al.*, 2005]. This fact certainly contributed to the large glacial-interglacial differences in climate. A variety of hypotheses exist to explain the observed magnitude in deglacial CO_2 concentration change, one of which focuses on changes in the marine nitrogen reservoir [*Falkowski*, 1997; *Broecker and Henderson*, 1998]. In this proposed scenario, glacial drawdown of CO_2 occurred due to enhanced marine primary productivity in areas that are currently limited by the availability of nitrogen. It is therefore important to assess how stable the marine nitrogen inventory has been on glacial-interglacial timescales.

1.2. Current understanding

1.2.1. Main sinks and sources of fixed nitrogen

Nitrate is the most stable form of fixed nitrogen in the ocean under aerobic conditions. In oxygen-deficient environments, however, nitrate is used instead of oxygen as an electron acceptor for the remineralization of organic matter. Thereby, nitrate is transformed to the gases N_2O and N_2, which are lost to the atmosphere. This bacterially mediated process is called denitrification and constitutes the most important sink of fixed nitrogen from the ocean. Denitrification occurs both in the oxygen minimum zones of the water column and in sediments. The major oxygen minimum zones are located in the upwelling areas of the Eastern Tropical North and South Pacific and the Arabian Sea (Figure 1.1B).

The most important source of nitrogen to the ocean is nitrogen fixation, which is performed by specialized organisms called diazotrophs. These are capable of using N_2 gas instead of dissolved nitrogen forms, converting N_2 to organic nitrogen, which is eventually added to the marine nitrogen pool. This way, diazotrophs have a competitive advantage in areas where fixed nitrogen is rare, such as the oligotrophic subtropical gyres. On the other hand, these organisms are considered as not competitive under nitrogen-replete conditions, because N_2 fixation is energetically very costly.

1.2.2. Potential controlling factors

As denitrification substitutes for aerobic remineralization, its rate is mostly controlled by the prevailing oxygen concentrations. In the water column, this is determined by the prior oxygen saturation state ('ventilation') of the respective water mass and the local oxygen consumption

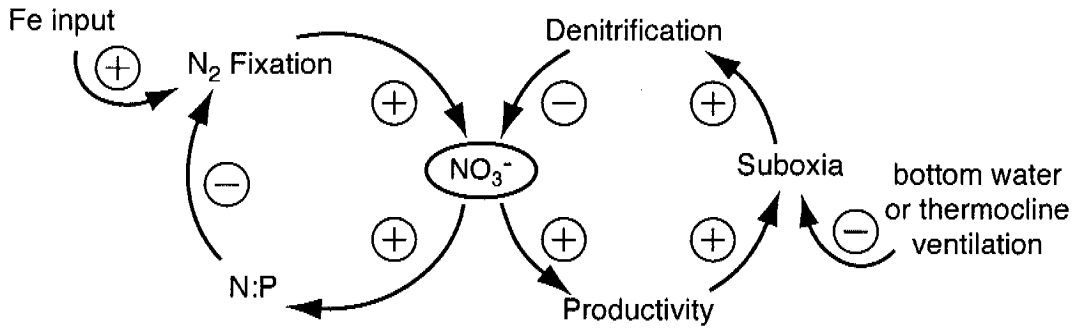

Figure 1.2. Proposed controlling factors and feedbacks involving the most important source and sink of fixed nitrogen, N_2 fixation and denitrification, respectively. Modified after *Deutsch et al.* [2004].

rate, a function of organic matter flux. In upwelling areas, denitrification could be self-controlling [*Codispoti*, 1989], as strong denitrification leaves less nitrate to be upwelled and to fuel productivity at the surface, which in turn decreases the oxygen demand at depth (Figure 1.2, right side). This feedback can be imagined to work for both sedimentary and water column denitrification, but is probably more efficient in the water column system [*Deutsch et al.*, 2004].

A second proposed feedback mechanism within the nitrogen cycle involves both denitrification and N_2 fixation . Whenever nitrogen is removed from the system by denitrification and the global oceanic nutrient N/P ratio sinks considerably below the ratio required by primary producers (Redfield Ratio), diazotrophs should profit, as they can use the excess phosphate [*Redfield et al.*, 1963; *Haug et al.*, 1998; *Tyrrell*, 1999]. Since N_2 fixation is a net source of nitrogen to the system, such an internal feedback mechanism would tend to keep the nitrogen budget in balance (Figure 1.2, left side). Other potential controlling factors for N_2 fixation are temperature, light, stratification of the water column, and the availability of iron, which is an essential part of the enzymes required for this process [e.g., *Karl et al.*, 2002; *Kustka et al.*, 2003; *LaRoche and Breitbarth*, 2005].

1.2.3. Reconstruction of past changes

An important tool for reconstructing changes within the nitrogen cycle is the isotopic composition of nitrogen in sedimentary organic matter. The nitrogen isotopic composition is reported in the delta notation ($\delta^{15}N$), which is based on the ratio of the two isotopes in the sample compared to that in the standard (air):

$$\delta^{15}N\ (‰) = (({}^{15}N/{}^{14}N \text{ of sample} / {}^{15}N/{}^{14}N \text{ of air}) - 1) * 1000$$

During denitrification, the light ^{14}N is preferentially removed, causing the remaining nitrate to become enriched in the heavy isotope [*Cline and Kaplan*, 1975]. This fractionation is only observable, however, were nitrate is not transformed completely. Sedimentary denitrification, which is limited by the diffusion of nitrate, can therefore not be traced this way [e.g., *Brandes and Devol*, 1997; *Lehmann et al.*, 2004]. N_2 fixation adds nitrogen with an isotopic composition similar to that of atmospheric nitrogen [*Wada and Hattori*, 1991], which is 0 ‰ by convention. This input is significantly lighter than the mean ocean isotopic composition of nitrate, which is currently around 5 ‰ [*Sigman et al.*, 2000], due to the fractionation during water column denitrification. At a given site, the isotopic composition of nitrate reflects the combination of mean ocean nitrate $\delta^{15}N$ and the effect of local influences such as water column denitrification or N_2 fixation. Through uptake of nitrate by primary producers, the signal is transferred to the sedimentary record.

Using this approach, it could be shown that in all three areas with major water column denitrification, sedimentary $\delta^{15}N$ values increased from glacials to interglacials [e.g., *Altabet et al.*, 1995; *Ganeshram et al.*, 1995; *De Pol-Holz et al.*, 2006], which likely reflects lower water column denitrification rates in glacial times. If so, this could imply that the ocean was losing less fixed nitrogen in glacials, resulting in a larger N reservoir. Changes in sedimentary denitrification cannot be as well constrained. However, a large part probably occurs in organic-rich shelf sediments. Since most of the shelf area was exposed in glacial times, sedimentary denitrification was likely also reduced, augmenting an increase in the N reservoir [*Christensen*, 1994]. It is unclear to date whether the proposed feedback mechanisms within the nitrogen cycle counteracted this deglacial increase in denitrification and if so, to which extent.

1.2.4. The other side of the balance – changes in N_2 fixation

While several high-resolution $\delta^{15}N$ records are available from denitrification zones, little is known about global changes in N_2 fixation. The reason is twofold: Firstly, due to the large fractionation effect of water column denitrification, this signal dominates sedimentary $\delta^{15}N$ records in the East Pacific and the Arabian Sea, even though N_2 fixation might occur in these regions as well. And secondly, diagenetic effects have been observed to alter the isotopic signal in regions with low accumulation rates and well-oxygenated bottom water [*Altabet and Francois*, 1994; *Sigman*, 1997]; conditions that characterize areas where one would expect the clearest signal of N_2 fixation.

Based on the potential feedback between denitrification and N_2 fixation, one might expect N_2 fixation to have been weaker in glacial times, responding to the reduced nitrogen loss through denitrification. This would have reduced the glacial increase of the marine N pool. On the other

hand, it has been proposed that the increased dust content of the glacial atmosphere delivered more iron to the ocean and stimulated N_2 fixation [*Falkowski*, 1997; *Broecker and Henderson*, 1998], which would have further increased the glacial N reservoir. The relative importance of these potential controls for past changes in N_2 fixation can only be determined with high-resolution $\delta^{15}N$ records from N_2 fixation areas.

1.3. Exceptional sites in the subtropical North Atlantic

One aim of this thesis is to establish high-resolution $\delta^{15}N$ records from sites located in areas with current N_2 fixation and distant from the major denitrification zones. This could be accomplished due to the special character of the sites investigated. Orca Basin in the Gulf of Mexico (Figure 1.3) can be considered as a natural sediment trap. Due to its dense, hypersaline bottom water fed by surrounding salt diapirs, the deep part of Orca Basin is anoxic. This results in excellent preservation of organic material, despite the location in an oligotrophic area with active N_2 fixation.

Cariaco Basin off Venezuela also contains anoxic bottom water due to a shallow sill restricting exchange with the open Caribbean. An earlier study focusing on long-term glacial-interglacial changes in Cariaco Basin revealed that $\delta^{15}N$ values were lower during interglacials, interpreted as increased N_2 fixation either within or outside the basin [*Haug et al.*, 1998]. A detailed assessment of the interglacial increases in N_2 fixation in comparison with other high-resolution data sets promises valuable information about forcing factors and timing.

Besides this unusual potential for reconstructions of variations in N_2 fixation, the sites are also prone to local influences due to the deglacial change in sea level. The open Gulf of Mexico experienced increased input of terrigenous organic matter by the Mississippi River during glacial and deglacial times [e.g., *Newman et al.*, 1973; *Northam et al.*, 1981; *Jasper and Gagosian*, 1990]. This could potentially have affected the sedimentary nitrogen isotopic signal and therefore needs to be assessed. Low sea level further isolated the Cariaco Basin, causing large changes in hydrography and nutrient cycling [e.g., *Peterson et al.*, 1991]. Fortunately, a large body of different proxy data is by now available for the last deglaciation, which allows constraining this potential additional influence on $\delta^{15}N$.

1.4. Climate variability

Climate in the Caribbean is strongly influenced by the seasonal movement of the rain belt associated with the Intertropical Convergence Zone (ITCZ; Figure 1.3). This results in a rainy season during northern hemispheric summer and a dry season during northern hemispheric winter, which is characterized by strong trade wind-induced upwelling. The average position of the ITCZ has varied over time. In the early Holocene its mean position is thought to have

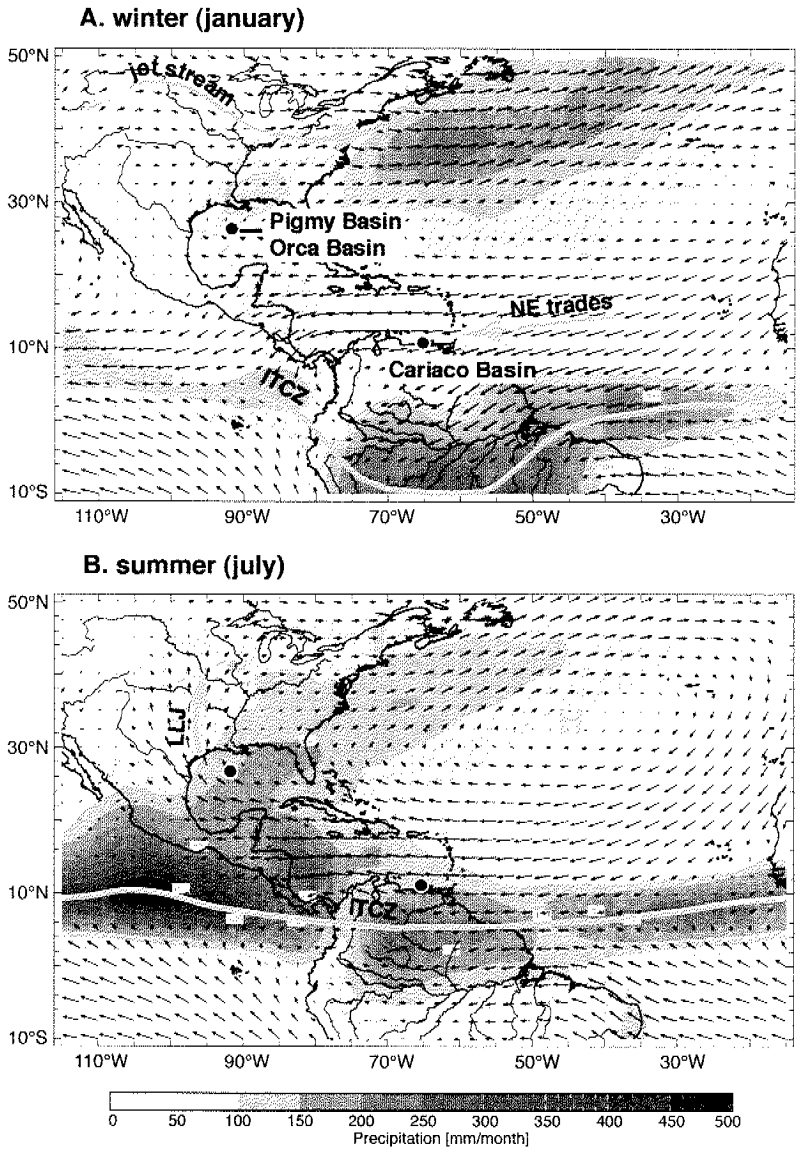

Figure 1.3. General atmospheric circulation and precipitation (shading) patterns in winter (A) and summer (B). Black dots indicate locations of the study sites in the Gulf of Mexico (Orca Basin and Pigmy Basin) and off Venezuela (Cariaco Basin). Black arrows represent surface winds. Climate in North America is mainly influenced by the path of the upper-tropospheric jet stream (winter) and the locations of the subtropical high pressure systems in the Atlantic and the Pacific (summer). LLJ is low level jet, important for transporting moisture to central North America. In the Caribbean, the dominant factor is the seasonal movement of the Intertropical Convergence Zone (ITCZ) with the associated trade winds. Maps taken from http://iridl.ldeo.columbia.edu/maproom.

been further north than today, due to stronger northern hemispheric summer insolation. The shift in ITCZ position is for example reflected the composition of Cariaco Basin sediments, which show a mid-Holocene maximum in titanium concentration [*Haug et al.*, 2001]. This was interpreted as increased input of riverine material due to prolonged rainy seasons. Similar effects of this Holocene climate shift have also been observed in other regions. For example, in North Africa the mid-Holocene change to drier conditions resulted in the re-establishment of the Saharan desert after an early Holocene humid period [*deMenocal et al.*, 2000]. The impact of such climatic changes on N_2 fixation reflected in the Cariaco Basin $\delta^{15}N$ record is assessed in the present study.

How did such variations in tropical climate relate to climate in higher latitudes, such as North America? The Gulf of Mexico is an important moisture source for central North America [e.g., *Higgins et al.*, 1997; *Hu and Feng*, 2001], constituting a potential link between low and mid-latitude climate. However, influences from the north such as the position of the jet stream are also important factors for North American climate (Figure 1.3). In this context, the large input of terrigenous material by the Mississippi River to the Gulf of Mexico and its contribution to the sediments becomes a useful source of information. Analogous to the above-mentioned Ti record from Cariaco Basin, the elemental composition of Holocene sediments from Pigmy Basin in the Gulf of Mexico (Figure 1.3) can be used for reconstructing variations in the hydrological cycle over North America. Pigmy Basin is located just to the north of Orca Basin on the Louisiana slope. As the Mississippi River drains a very large catchment area, covering almost half of the conterminous United States, the signal in the Gulf of Mexico probably integrates over small-scale changes and shifts in climate patterns. It can therefore complement existing paleoclimate records from archives on the continent.

1.5. Objectives and thesis outline

The aims of this thesis are i) to assess changes in North Atlantic N_2 fixation during deglaciations and to determine the forcing factors for such changes and ii) to investigate the hydrologic variability in North America in response to Holocene climate variations. In this context, the main objectives are to

- establish high-resolution $\delta^{15}N$ records from Orca Basin and Cariaco Basin covering the last deglaciation and, in Cariaco Basin, an earlier glacial termination for comparison
- assess of the contribution of terrigenous organic matter in Orca Basin sediments and its influence on the $\delta^{15}N$ record taking a multi-proxy approach.

- test alternative methods for studying changes in N_2 fixation and circumventing interference by terrigenous organic matter
- study Holocene variations in sediment input by the Mississippi River and its implications for North American climate

The present thesis is organized as follows:

In **Chapter 2**, the $\delta^{15}N$ record from Orca Basin, Gulf of Mexico for the last deglaciation is presented and discussed. This is the first high-resolution record from an area with active N_2 fixation. The influence of terrigenous nitrogen during the glacial and deglacial part of the record is examined using bulk $\delta^{13}C_{org}$ and C/N ratios and a correction scheme for this input is proposed based on an observed anti-correlation of C/N and $\delta^{15}N$.

The contribution of terrigenous organic matter to Orca Basin sediments as well as its composition is further investigated in **Chapter 3**, employing a combination of optical kerogen analyses and measurements of biomarker concentrations and compound-specific carbon isotopes on selected samples.

Subject of **Chapter 4** are high-resolution $\delta^{15}N$ records from Cariaco Basin in the Caribbean Sea for the last deglaciation and for Termination V, complementing the existing, low-resolution data set. Thereby, local influences are deciphered from global and regional influences through comparisons with other proxy data from Cariaco Basin and $\delta^{15}N$ records from other parts of the oceans, including the one from Orca Basin.

Motivated by the complexity of bulk sedimentary $\delta^{15}N$ values due to varying organic matter sources and overlying influences by different forcing factors, **Chapter 5** describes initial tests performed towards alternative methods for determining changes in N_2 fixation and measurements of $\delta^{15}N$ bound to calcareous nannofossils. Based on these first results, the most promising approaches for future work are proposed.

In **Chapter 6**, the Holocene elemental record from Pigmy Basin in the Gulf of Mexico is presented and its usefulness for reconstructing Mississippi River input is assessed. The implications for climate variability in North America are discussed and the signal is compared to climate reconstructions from North America and the Caribbean, revealing common patterns and discrepancies.

Chapter 7 summarizes the most important findings of this thesis and provides an outlook.

References

Altabet, M. A., and R. Francois (1994), Sedimentary Nitrogen Isotopic Ratio as a Recorder for Surface Ocean Nitrate Utilization, *Global Biogeochem. Cycles*, *8*, 103-116.

Altabet, M. A., R. Francois, D. W. Murray, and W. L. Prell (1995), Climate-Related Variations in Denitrification in the Arabian Sea from Sediment N-15/N-14 Ratios, *Nature*, *373*, 506-509.

Barnola, J. M., D. Raynaud, Y. S. Korotkevich, and C. Lorius (1987), Vostok Ice Core Provides 160,000-Year Record of Atmospheric CO2, *Nature*, *329*, 408-414.

Brandes, J. A., and A. H. Devol (1997), Isotopic fractionation of oxygen and nitrogen in coastal marine sediments, *Geochim. Cosmochim. Acta*, *61*, 1793-1801.

Broecker, W. S., and G. M. Henderson (1998), The sequence of events surrounding Termination II and their implications for the cause of glacial-interglacial CO2 changes, *Paleoceanography*, *13*, 352-364.

Christensen, J. P. (1994), Carbon Export from Continental Shelves, Denitrification and Atmospheric Carbon-Dioxide, *Cont. Shelf Res.*, *14*, 547-576.

Cline, J. D., and I. R. Kaplan (1975), Isotopic fractionation of dissolved nitrate during denitrification in the eastern tropical North Pacific Ocean, *Mar. Chem.*, *3*, 271-299.

Codispoti, L. A. (1989), Phosphorus vs. nitrogen limitation of new and export production, in *Productivity of the Ocean: Past and Present*, edited by W. H. Berger, et al., pp. 377-394, John Wiley, Hoboken, N.J.

De Pol-Holz, R., O. Ulloa, L. Dezileau, J. Kaiser, F. Lamy, and D. Hebbeln (2006), Melting of the Patagonian Ice Sheet and deglacial perturbations of the nitrogen cycle in the eastern South Pacific, *Geophys. Res. Lett.*, *33*, L04704, doi:10.1029/2005GL024477.

deMenocal, P., J. Ortiz, T. Guilderson, J. Adkins, M. Sarnthein, L. Baker, and M. Yarusinsky (2000), Abrupt onset and termination of the African Humid Period: rapid climate responses to gradual insolation forcing, *Quaternary Science Reviews*, *19*, 347-361.

Deutsch, C., D. M. Sigman, R. C. Thunell, A. N. Meckler, and G. H. Haug (2004), Isotopic constraints on glacial/interglacial changes in the oceanic nitrogen budget, *Global Biogeochem. Cycles*, 18, GB4012, doi:10.1029/2003GB002189.

Falkowski, P. G. (1997), Evolution of the nitrogen cycle and its influence on the biological sequestration of CO2 in the ocean, *Nature*, *387*, 272-275.

Ganeshram, R. S., T. F. Pedersen, S. E. Calvert, and J. W. Murray (1995), Large Changes in Oceanic Nutrient Inventories from Glacial to Interglacial Periods, *Nature*, *376*, 755-758.

Haug, G. H., K. A. Hughen, D. M. Sigman, L. C. Peterson, and U. Rohl (2001), Southward migration of the intertropical convergence zone through the Holocene, *Science*, *293*, 1304-1308.

Haug, G. H., T. F. Pedersen, D. M. Sigman, S. E. Calvert, B. Nielsen, and L. C. Peterson (1998), Glacial/interglacial variations in production and nitrogen fixation in the Cariaco Basin during the last 580 kyr, *Paleoceanography*, *13*, 427-432.

Higgins, R. W., Y. Yao, and X. L. Wang (1997), Influence of the North American monsoon system on the US summer precipitation regime, *Journal of Climate*, *10*, 2600-2622.

Hu, Q., and S. Feng (2001), Climatic role of the southerly flow from the Gulf of Mexico in inter-annual variations in summer rainfall in the central United States, *Journal of Climate*, *14*, 3156-3170.

Jasper, J. P., and R. B. Gagosian (1990), The Sources and Deposition of Organic-Matter in the Late Quaternary Pygmy Basin, Gulf of Mexico, *Geochim. Cosmochim. Acta*, *54*, 1117-1132.

Karl, D., A. Michaels, B. Bergman, D. Capone, E. Carpenter, R. Letelier, F. Lipschultz, H. Paerl, D. M. Sigman, and L. Stal (2002), Dinitrogen fixation in the world's oceans, *Biogeochemistry*, *57*, 47-98.

Kustka, A. B., S. A. Sanudo-Wilhelmy, E. J. Carpenter, D. Capone, J. Burns, and W. G. Sunda (2003), Iron requirements for dinitrogen- and ammonium-supported growth in cultures of Trichodesmium (IMS 101): Comparison with nitrogen fixation rates and iron: carbon ratios of field populations, *Limnol. Oceanogr.*, *48*, 1869-1884.

LaRoche, J., and E. Breitbarth (2005), Importance of the diazotrophs as a source of new nitrogen in the ocean, *Journal of Sea Research*, *53*, 67-91.

Lehmann, M. F., D. M. Sigman, and W. M. Berelson (2004), Coupling the N-15/N-14 and O-18/O-16 of nitrate as a constraint on benthic nitrogen cycling, *Mar. Chem.*, *88*, 1-20.

Newman, J. W., P. L. Parker, and E. W. Behrens (1973), Organic Carbon Isotope Rations in Quaternary Cores from Gulf of Mexico, *Geochim. Cosmochim. Acta*, *37*, 225-238.

Northam, M. A., D. J. Curry, R. S. Scalan, and P. L. Parker (1981), Stable Carbon Isotope Ratio Variations of Organic-Matter in Orca Basin Sediments, *Geochim. Cosmochim. Acta*, *45*, 257-260.

Peterson, L. C., J. T. Overpeck, N. G. Kipp, and J. Imbrie (1991), A high-resolution late quaternary upwelling record from the anoxic Cariaco Basin, Venezuela, *Paleoceanography*, *6*, 99-119.

Redfield, A. C., B. H. Ketchum, and F. A. Richards (1963), The influence of organisms on the composition of seawater, in *The Sea*, edited by M. N. Hill, pp. 26-77, Wiley Interscience, Hoboken, N.J.

Siegenthaler, U., T. F. Stocker, E. Monnin, D. Luthi, J. Schwander, B. Stauffer, D. Raynaud, J. M. Barnola, H. Fischer, V. Masson-Delmotte, and J. Jouzel (2005), Stable carbon cycle-climate relationship during the late Pleistocene, *Science*, 310, 1313-1317.

Sigman, D. M. (1997), The Role of Biological Production in Pleistocene Atmospheric Carbon Dioxide Variations and the Nitrogen Isotope Dynamics of the Southern Ocean, PhD thesis, Woods Hole Oceanographic Institution.

Sigman, D. M., M. A. Altabet, D. C. McCorkle, R. Francois, and G. Fischer (2000), The delta N-15 of nitrate in the Southern Ocean: Nitrogen cycling and circulation in the ocean interior, *J. Geophys. Res. Oceans*, *105*, 19599-19614.

Tyrrell, T. (1999), The relative influences of nitrogen and phosphorus on oceanic primary production, *Nature*, *400*, 525-531.

Wada, E., and A. Hattori (1991), *Nitrogen in the Sea: Forms, Abundances and Rate Processes*, CRC Press, Boston.

Seite Leer /
Blank leaf

Chapter 2

A new N isotope record from Orca Basin, Gulf of Mexico – Evidence for feedbacks in the marine nitrogen cycle*

Abstract

For a sediment core from Orca Basin in the oligotrophic Gulf of Mexico, we report measurements of bulk nitrogen isotopic composition ($\delta^{15}N$) and other parameters extending back to the last ice age. The $\delta^{15}N$ is very low (2.2 to 2.5 ‰ versus air) in most of the record. Glacial $\delta^{15}N$ is similar to that in the Holocene part of the core, whereas a peak reaching 4.0 ‰ occurs during deglaciation. However, the interpretation of the glacial part of the record is complicated by a larger terrigenous input, indicated by higher C/N and lower $\delta^{13}C$ of organic matter. An attempt to correct for this input using the observed relationship of C/N and $\delta^{15}N$ for the glacial data suggests a marine glacial $\delta^{15}N$ of roughly 4.0 ‰, decreasing toward the Holocene. A robust observation is that, at this site, glacial $\delta^{15}N$ was higher than or similar to present-day values, but not lower. Therefore, a proposed larger glacial dust input apparently did not lead to enhanced N_2 fixation in this region. If an overall deglacial decrease in sinking flux $\delta^{15}N$ did occur, it is best explained by an increase in N_2 fixation within the Atlantic in response to a deglacial increase in global ocean denitrification. In the case of similar glacial and Holocene $\delta^{15}N$, the Orca record resembles records from the western Pacific, which suggest no glacial/interglacial change in global ocean nitrate $\delta^{15}N$. The deglacial $\delta^{15}N$ peak may be explained by a transient deglacial maximum in the fraction of global ocean denitrification occurring in the water column as opposed to the sediments.

*in review for *Paleoceanography* as A.N. Meckler, D.M. Sigman, B. Plessen, G.H. Haug, A new N isotope record from Orca Basin, Gulf of Mexico - Evidence for feedbacks in the marine nitrogen cycle.

2.1. Introduction

Nitrogen is considered the limiting nutrient for primary productivity in vast parts of the present day ocean. Hence, the marine nitrogen cycle represents one control of primary productivity and thus oceanic uptake of CO_2, implying a potentially large impact on global climate. The major source of nitrogen to the ocean is nitrogen fixation by diazotrophic organisms, whereas denitrification is its most important sink. Despite extensive research, it is still not clear whether the marine nitrogen budget is currently in balance and whether it has been stable in the past. Several hypotheses to explain the large variations in atmospheric CO_2 on glacial/interglacial timescales involve changes in the marine nitrogen budget.

Stable nitrogen isotopes provide an important tool for assessing changes in the sinks and sources of oceanic nitrogen. During N_2 fixation, little isotopic fractionation is observed [*Wada and Hattori*, 1991], resulting in a $\delta^{15}N$ for newly fixed N of –2 to 0 ‰ ($\delta^{15}N$ (‰) = (($^{15}N/^{14}N$ of sample / $^{15}N/^{14}N$ of air) – 1) * 1000). During denitrification, on the other hand, preferentially light nitrogen gas escapes the ocean, leaving isotopically enriched nitrate behind [*Cline and Kaplan*, 1975; *Liu and Kaplan*, 1989]. The enrichment can only be expressed, however, if not all available nitrate is consumed by this process [*Thunell et al.*, 2004]. Hence, denitrification in sediments, where nitrate supply is limited by diffusion, usually does not affect the isotopic composition of marine nitrate [*Brandes and Devol*, 1997; 2002; *Sebilo et al.*, 2003; *Lehmann et al.*, 2004], whereas water column denitrification in the oxygen minimum zones does increase the $\delta^{15}N$ of mean ocean nitrate. The average isotopic composition of oceanic nitrate is ultimately controlled the relative global importance of water column versus sedimentary denitrification [*Brandes and Devol*, 2002], as well as by the completeness with which nitrate is consumed in zones of water column denitrification [*Deutsch et al.*, 2004]. In most of the tropical and subtropical ocean, the $\delta^{15}N$ of N sinking out of the euphotic zone depends mainly on the $\delta^{15}N$ of the nitrogen source. Therefore, sedimentary $\delta^{15}N$ should record both the $\delta^{15}N$ of mean ocean nitrate and local processes such as water column denitrification or N_2 fixation.

A number of N isotope records exist from the major denitrification zones in the eastern tropical north and south Pacific and the Arabian Sea [e.g., *Altabet et al.*, 1995; *Ganeshram et al.*, 1995; *Pride et al.*, 1999; *Emmer and Thunell*, 2000; *Kienast et al.*, 2002; *De Pol-Holz et al.*, 2006]. These records reveal lower $\delta^{15}N$ during glacial times, suggesting decreased water column denitrification. The observed pattern led *Ganeshram et al.* [1995] and *Altabet et al.* [1995] to the hypothesis that the global nitrate reservoir was larger in glacial times, potentially fuelling higher primary productivity. This was augmented by probably decreased sedimentary denitrification due to the lower sea level, exposing large shelf areas [*Christensen*, 1994]. However, glacial-interglacial changes in productivity appear to be dominated by regional processes, with no clear glacial/interglacial trend across the tropics and subtropics, where the major nutrient supply

controls export production [*Sigman and Haug*, 2003, and references therein]. Furthermore, large changes in the marine nitrate reservoir would affect the mean isotopic composition of nitrate, except under very specific circumstances [*Deutsch et al.*, 2004]. In the only N isotope record to date that is proposed to reflect mainly the mean ocean nitrate composition, no significant glacial/interglacial change has been observed [*Kienast*, 2000].

Hence, the current evidence suggests that internal feedback mechanisms regulate the marine nitrogen budget, balancing the increase in water column denitrification upon deglaciations. Two such mechanisms have been proposed, one involving denitrification [*Codispoti*, 1989] and one involving nitrogen fixation [*Redfield et al.*, 1963; *Haug et al.*, 1998; *Tyrrell*, 1999]. The former focuses on the negative impact of denitrification on productivity due to the loss of nitrate, which will ultimately lead to decreased oxygen consumption and hence reduce denitrification toward pre-perturbation levels. The latter invokes the idea that the energetically costly process of nitrogen fixation is only of advantage in nitrate-deplete, phosphate-bearing waters. Therefore, this nitrogen source increases as denitrification increases, so as to buffer the nitrogen loss. Whether one or both of these feedbacks are important and how strong they are, however, is an open question. Nitrogen isotopic records from outside the direct influence of denitrification zones would greatly improve our understanding of past changes in the ocean N budget.

In this context, we analyzed the nitrogen isotopic composition in a sediment core from the Orca Basin in the oligotrophic Gulf of Mexico. In this region as well as in the open subtropical North Atlantic, nitrogen fixation is probably responsible for the low $\delta^{15}N$ of thermocline nitrate (~2.5‰) [*Knapp et al.*, 2005]. The importance of N_2 fixation is supported by elevated N:P ratios observed in the subtropical North Atlantic thermocline [*Michaels et al.*, 1996; *Gruber and Sarmiento*, 1997; *Karl et al.*, 2002]. Diazotrophic organisms, mostly *Trichodesmium*, have been repeatedly observed and studied in the Caribbean, Gulf of Mexico and subtropical North Atlantic [e.g., *Goering et al.*, 1966; *Carpenter and Price*, 1977; *Carpenter and Romans*, 1991; *Tyrrell et al.*, 2003; *Carpenter et al.*, 2004].

Orca Basin is an intraslope basin off the coast of Louisiana and about 300 km southwest of the Mississippi mouth (Figure 2.1). The 400 km^2 large basin has a maximum depth of 2400 m and is surrounded by diapiric highs rising to 1800 m water depth [*Shokes et al.*, 1977]. Hence, the water column above ~1800 m over the Orca Basin is indistinguishable from the surrounding Gulf of Mexico. The lowermost 200 m of the basin are filled with dense, hypersaline brine [*Sackett et al.*, 1979]. The strong density stratification results in anoxic bottom water below the brine-seawater interface leading to excellent preservation of organic matter in the sediments. Denitrification occurs in the basin just above 2200 m [*Van Cappellen et al.*, 1998]. However, as Orca Basin is not an upwelling site and the vertical distance from the denitrification zone to the surface is great, the isotopic signal from this denitrification cannot be transferred to the surface water and will hence not be recorded in the organic matter sinking out of the surface ocean and

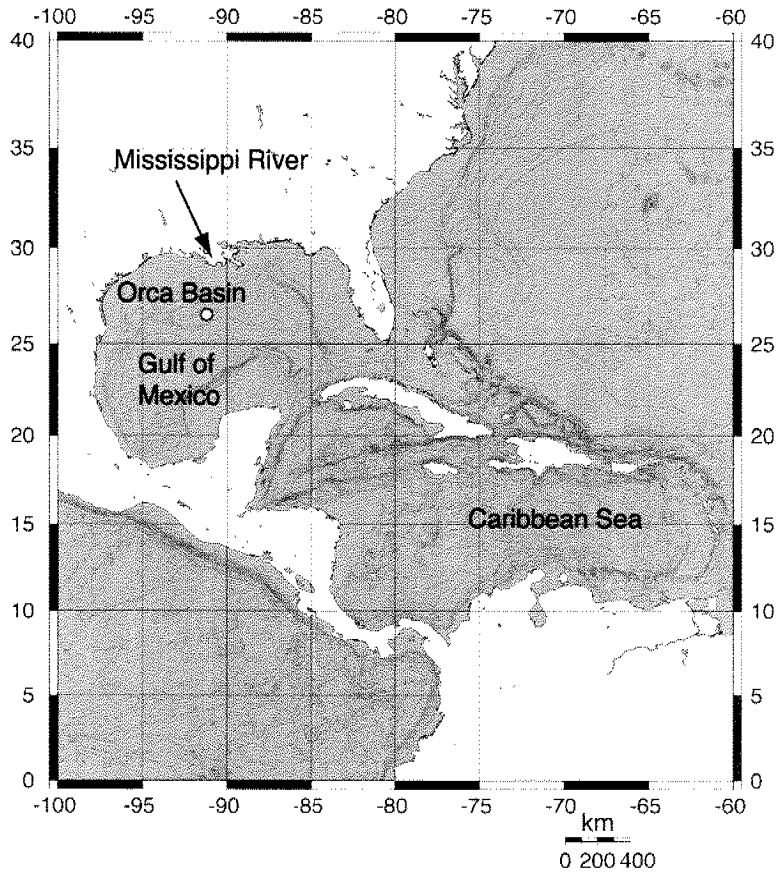

Figure 1. Map of the core location in the Gulf of Mexico. Core MD02-2550 was taken from the slope of Orca Basin, in a water depth of 2249 m at 26°56.77N and 91°20.74W. The basin is located about 300 km offshore the Mississippi River mouth.

accumulating in the sediments. The brine probably built up around 8000 years before present (BP) due to lateral leakage from a salt deposit [*Addy and Behrens*, 1980]. Laminated sections of the sediment occurring deeper in the core indicate earlier sub- to anoxic intervals as well, and it is possible that the brine leakage has continuously supported low dissolved O_2 in the basin. Therefore, Orca Basin offers the unique combination of good organic matter preservation in an open ocean oligotrophic setting.

A weakness of the location in the sense of this study is its proximity to the continental margin, and to the mouth of Mississippi River in particular (Figure 2.1). As a result of this proximity, one would expect an input of terrestrial organic matter, and this input has likely changed through time. Below, we describe C/N and carbon isotopic evidence for greater terrestrial inputs during the last ice age and through deglaciation. Moreover, in the course of the last deglaciation, a large meltwater pulse from the Mississippi is recorded in Orca Basin sediments by negative oxygen isotope excursions, starting at around 16 ka and lasting until around 13 ka (calender age) [*Leventer et al.*, 1983; *Flower and Kennett*, 1990; *Flower et al.*, 2004]. Other cores from the Louisiana slope indicate several other meltwater floods between 16 and 8.5 ka (^{14}C age) [*Aharon*, 2003].

Table 2.1. Radiocarbon dates for MD02-2550 measured on foraminifera (*G. ruber*; pink and white variety for CAMS dates, pink var. only for ETH dates). Conversion to calendar years BP was performed with the software CALIB 5.0 [*Stuiver and Reimer*, 1993] using the calibration curve Marine04 [*Hughen et al.*, 2004].

Lab number	Sample depth (cm)	Radiocarbon age	Calibrated age range (1 sigma)	calendar age (median) (year before present)
CAMS 100668	167.0-167.5	3120 ± 45	2830-2962	2900
CAMS 100669	175.0-175.5	3025 ± 40	2745-2832	2790
CAMS 100670	190.0-190.5	6510 ± 35	6957-7084	7020
CAMS 100671	210.0-210.5	7450 ± 40	7865-7953	7910
CAMS 100672	230.0-230.5	8050 ± 35	8451-8549	8500
CAMS 100673	250.0-250.5	8330 ± 40	8850-8987	8910
CAMS 100674	270.5-271.0	8815 ± 40	9451-9514	9480
CAMS 100675	290.0-290.5	9285 ± 40	10101-10195	10140
CAMS 100676	307.5-308.0	9790 ± 40	10577-10683	10640
ETH 28012	374.5-377.0	11170 ± 85	12743-12862	12800
ETH 28013	434.0-436.0	12910 ± 85	14394-14880	14610
ETH 28014	563.5-565.5	14470 ± 110	16538-17007	16770
ETH 28015	902.0-904.0	20340 ± 160	23676-24110	23880

2.2. Material and Methods

The 9.09 m long giant box core MD02-2550 was taken during IMAGES cruise VIII (PAGE) in 2002. Its chronology is based on 13 radiocarbon dates on foraminifera (Table 2.1 and Figure 2.2). The oldest 4 dates were measured on *G. ruber* (pink variety) at the AMS radiocarbon laboratory at ETH Zurich and the younger dates were measured on *G. ruber* (both pink and white variety) at the CAMS, Lawrence Livermore National Laboratory [*LoDico et al.*, 2006; Flower

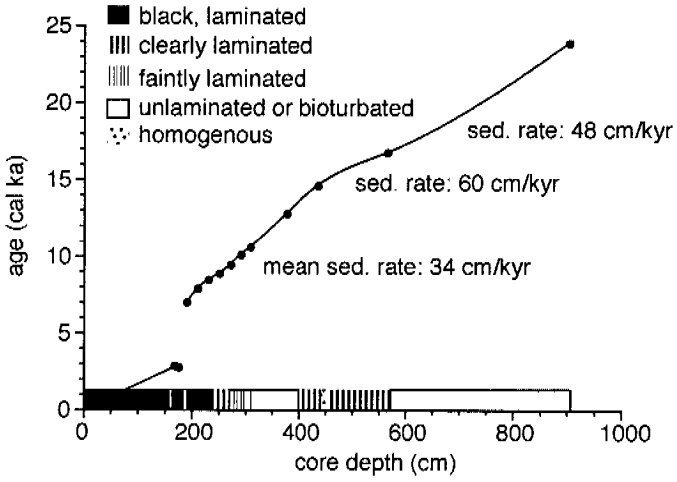

Figure 2. Age model for core MD02-2550 based on 13 ^{14}C dates on foraminifera (*G. ruber*), converted to calendar ages with the CALIB software [*Stuiver and Reimer*, 1993] (version 5.0) using the calibration curve Marine04 [*Hughen et al.*, 2004]. A hiatus was observed between 2.8 and 7.0 ka. Also shown is the lithology of the core as described in the text.

and Quinn, unpublished data]. All ages were converted to calendar years with the CALIB software [*Stuiver and Reimer*, 1993] (version 5.0; http://calib.qub.ac.uk/calib), using the calibration curve Marine04 [*Hughen et al.*, 2004] with a reservoir age of around 400 years ($\Delta R = 0$). In the Holocene section, a large hiatus of around 4.2 kyr (from 2.8 to 7.0 ka) was discovered, but could be well constrained by ^{14}C dates. The age model is constructed by fitting a smoothing spline to the age points below 190 cm. In the top part of the core, the age model is based on the two dates at 167 cm and 175 cm and the assumption of zero-age at the core top. The calculated sedimentation rates vary from 20 cm ka^{-1} to 60 cm ka^{-1}, the highest rates being associated with the glacial section and the meltwater pulse. This compares well to sedimentation rates determined previously in neighboring core EN32-PC6 (40 cm ka^{-1}) [*Leventer et al.*, 1983].

The upper 232 cm of the core consist of clearly laminated black sediment, with the exception of two light gray intervals at 161-162 cm and 185-192 cm. The latter coincides with the top of the hiatus observed in ^{14}C dates. The black color is due to metastable iron sulfides, and the change to black color has been interpreted as the onset of brine accumulation [*Addy and Behrens*, 1980]. However, laminated sediment suggesting anoxic conditions can also be found below this depth. From 232-268 cm, the sediment is clearly laminated, but it lacks the black color. Laminations are less clear and not continuous from 268 to 300 cm and deteriorate further from 300-394 cm. From 394 to 567 cm clear laminations reappear, interrupted by a homogenous interval at 437-456 cm. Smear slide examinations showed that this homogenous interval corresponds to the deglacial peak in the percentage of reworked nannofossils, which has been described by Marchitto and Wei [1995] for neighboring core EN32-PC4. Below 567 cm the sediment is bioturbated. However, bundles of black layers were observed in the bottom section of the core, at 852-863 cm, 875-884 cm, and 896-906 cm. The sediment is rich in well preserved microfossils such as foraminifera and pteropods. Recovery of completely intact sargassum at several depths in the core furthermore attests to the excellent preservation of organic material.

Total organic carbon (TOC) was determined by substracting inorganic carbon concentrations, measured on a *Stroehlein Coulomat 702,* from total carbon concentrations, measured on a *LECO CNS2000* elemental analyzer. The precision was better than 1% of the mean for both total carbon and inorganic carbon based on duplicate measurements. Total nitrogen (TN) content and $\delta^{15}N$ were measured with a *Carlo-Erba CN2500* elemental analyzer on-line to a *Thermo-Finnigan DELTAplusXL* mass spectrometer using the reference standards IAEA N1 and N2. All samples were measured at least in duplicate and precision was in most cases better than 0.2 ‰ for $\delta^{15}N$ and better than 5% of the mean value for TN. In some samples, TN was additionally determined on the *LECO CNS2000*, the results being indistinguishable from those of the on-line elemental analyzer. $\delta^{13}C$ of organic material was obtained by acidifying samples weighed into silver cups and subsequent drying at 70°C without a rinsing step, followed by

combustion and isotopic analysis with the same system. Values are reported relative to VPDB based on reference standards USGS24 and CH-7, and precision was better than 0.2‰.

2.3. Results

The nitrogen isotopic record from Orca Basin (Figure 2.3) yields several important observations. First, the sediment $\delta^{15}N$ is overall very low (varying around 2.5 ‰) compared to the mean isotopic composition of oceanic nitrate (~5‰) [*Sigman et al.*, 2000], but is similar to the $\delta^{15}N$ of today's nitrate in the thermocline of the subtropical Atlantic [*Knapp et al.*, 2005]. Second, there is not much difference between glacial and Holocene sediment $\delta^{15}N$. Third, the record exhibits a pronounced deglacial peak in $\delta^{15}N$ centered at 11-9 ka, with maximum values of around 3.7 ‰.

Apart from these most obvious observations, there are several second-order features in the record. The glacial part of the core (24.0-16.8 ka) is characterized by low but variable $\delta^{15}N$ values, ranging from 2.0 to 2.8 ‰ with a short interval of higher values (up to 3.4 ‰) between 18 and 17 ka. During the laminated interval between 16.8 - 13.4 ka $\delta^{15}N$ values are mostly below 2.8 ‰, with a minimum of around 1.8 ‰ during and after the deposition of a homogenous interval in the core. After about 13.4 ka $\delta^{15}N$ rises towards the deglacial maximum, with an initial shoulder during the Younger Dryas period of values around 3.1 ‰. After 9 ka, the values decrease to almost late Holocene values within less than 3 ka. A small secondary peak is located at around 8 ka.

The period of low $\delta^{15}N$ between 16.8 and 13.4 ka coincides with the time of major meltwater input into the Gulf of Mexico, as seen by a negative excursion in $\delta^{18}O$ (Figure 2.3). During this interval, TOC concentrations are much higher, with values reaching 1.1 to 1.6 weight%, and the sediment is clearly laminated. The TOC maximum is interrupted by a short minimum coincident with the homogenous interval. In contrast, TOC concentrations are relatively stable during both LGM and Holocene, ranging between 0.6 and 1.0 weight%.

We measured $\delta^{13}C$ and C/N ratios to assess the contribution of terrigenous organic material (Figure 2.3). Both parameters suggest higher terrestrial input during the glacial, indicated by lighter $\delta^{13}C$ (around -26 ‰) and higher C/N ratios (12 to 14) as compared to the Holocene section. However, the two proxies differ in the details of this trend. Whereas $\delta^{13}C$ exhibits a more or less constant increase in values toward the Holocene, the C/N ratios peak between 16.8 to 14.5 ka. On the other hand, $\delta^{13}C$ displays a negative peak during the Younger Dryas interval (13.0 to 11.5 ka), when C/N shows little change.

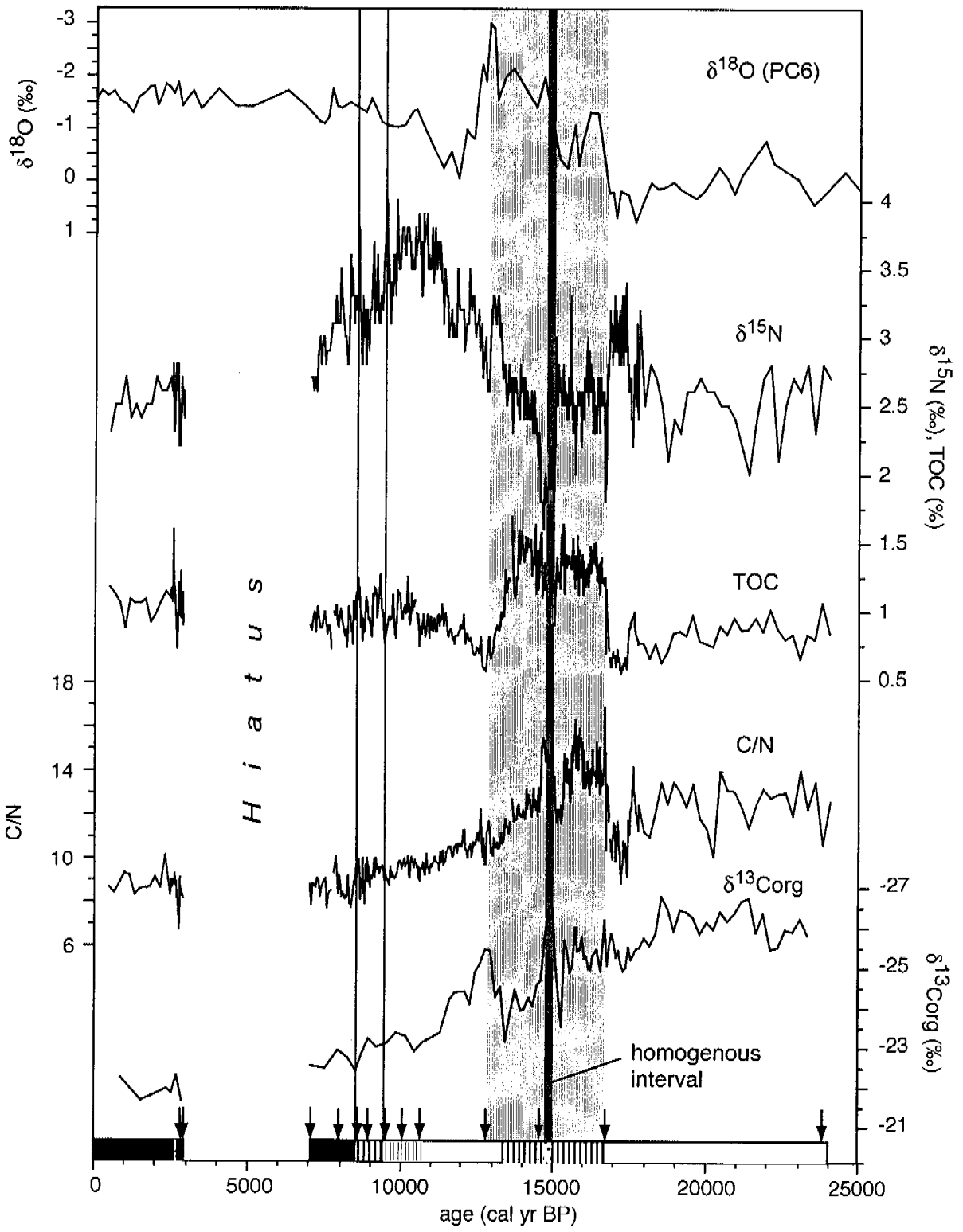

Figure 2.3. Profiles for $\delta^{15}N$, TOC, C/N and $\delta^{13}C$ versus age from MD02-2550 (this study) in comparison to $\delta^{18}O$ from neighboring core EN32-PC6 [*Leventer et al.*, 1983]. Note the reversed scale for $\delta^{18}O$ and $\delta^{13}C$. For MD02-2550, lithology changes are shown at the bottom (symbols as in Figure 2.2) and arrows specify depths of ^{14}C age control. Light shading indicates time of meltwater flow, corresponding to high TOC, low $\delta^{15}N$, and well-laminated sediment.

2.4. Discussion

2.4.1. Potential influences on $\delta^{15}N$

The $\delta^{15}N$ record from Orca Basin is based on bulk sediment measurements, which implies that it could be influenced by different processes. The potential influences at this site are diagenetic changes, terrestrial input (both organic and inorganic nitrogen), local to regional changes in N_2 fixation rates, and changes in the global mean isotopic composition of nitrate. The open Gulf of Mexico is an oligotrophic regime, so that changes in the completeness of nitrate consumption are unlikely.

Since the redox conditions in the water column varied in the course of the history of Orca Basin, changes in diagenetic alteration could potentially influence the $\delta^{15}N$ record. However, the fact that lithologic changes (from bioturbated to laminated and to black sediment) in the core do not consistently coincide with shifts in the isotopic composition makes such alteration unlikely. Hence, from the last ice age to the present, the Orca Basin seems to belong to the high-accumulation, organic-rich sites where little or no diagenetic alteration of the $\delta^{15}N$ record can be observed.

Terrestrial organic nitrogen and inorganic nitrogen usually both have a lower $\delta^{15}N$ than marine organic nitrogen [e.g., *Peters et al.*, 1978; *Meyers*, 1997; *Calvert et al.*, 2001; *Schubert and Calvert*, 2001]. Therefore, a stronger contribution of these nitrogen sources could lower the bulk sediment $\delta^{15}N$, as will be discussed in the following. However, we expect this influence to be almost negligible after around 11 ka, when sea level was already much higher than during the LGM and the peak meltwater inflow into the Gulf of Mexico had ended. Hence, the high deglacial $\delta^{15}N$ and the subsequent Holocene $\delta^{15}N$ decrease are most probably a signal of changes in the marine N cycle.

Today, the Orca Basin is located about 300 km south of the mouth of the Mississippi River, preventing much of the terrestrial organic material from reaching the site [*Trefry et al.*, 1994; *Goni et al.*, 1997; *Wang et al.*, 2004]. However, with lowered sea level during the LGM, this source of material was probably much more important. This has been shown in previous studies in the Gulf of Mexico, reporting higher concentrations of terrestrial organic matter in glacial sediments on the basis of carbon isotopic composition and biomarker concentrations [*Newman et al.*, 1973; *Northam et al.*, 1981; *Jasper and Gagosian*, 1990; 1993]. Our results for $\delta^{13}C$ and C/N agree very well with these previous findings. Furthermore, the higher sedimentation rates in the glacial section of our core also point toward an increased input of detrital material.

Although often used as proxies for terrestrial input, both $\delta^{13}C$ and C/N ratios can be influenced by several other factors. The deglacial increase in $\delta^{13}C$ in Gulf of Mexico sediments,

for example, has also been attributed to a shift in the vegetation of the Mississippi drainage area. [*Goni et al.*, 1998] proposed that during glacial periods C3 grasses, which have a lower $\delta^{13}C$ than tropical C4 grasses, were more abundant than today. The $\delta^{13}C$ minimum during the Younger Dryas (13.0 – 11.5 ka), which is not accompanied by higher C/N, could be due to such a vegetation change, as might be part of the glacial-Holocene trend. Diagenetic alteration of $\delta^{13}C$ due to differential degradation of organic compounds with different isotopic composition might also lower the $\delta^{13}C$ of bulk organic matter [e.g., *Benner et al.*, 1987; *Lehmann et al.*, 2002]. Unlike for $\delta^{15}N$, the lower $\delta^{13}C$ values are consistently associated with non-laminated sediment and therefore we cannot exclude this possibility at the moment.

C/N ratios, on the other hand, depend on the relative contribution of nitrogen-rich organic compounds, which can be more labile. Hence, this ratio may also change during degradation. In addition, significant amounts of inorganic nitrogen, typically bound to clay minerals, can lower the C/N ratio. The potential influence of inorganic nitrogen will therefore be discussed first. As noted above, the $\delta^{13}C$ increase is much more continuous than the C/N decrease. However, inorganic nitrogen could be responsible for the divergence before 16.8 ka, lowering the glacial C/N values. We would need to subtract about 0.010 to 0.015 weight % from TN for that part of the record to see a trend similar to that of $\delta^{13}C$. One might take this weight percentage of TN as a rough estimate of the inorganic nitrogen contribution. However, as already mentioned, the stronger trend in $\delta^{13}C$ could also be partly attributed to vegetation shifts or diagenetic effects.

We explore these complications and the influence of terrestrial organic matter on $\delta^{15}N$ further using correlation plots of the different parameters. In a TN-TOC plot (Figure 2.4a), inorganic nitrogen produces a positive intercept on the ordinate. When grouping the data by age, the glacial data before 16.8 ka show a positive intercept of the regression line, whereas all other data groups have intercepts closer to zero. This may reflect an important inorganic nitrogen contribution prior to 16.8 ka, which could also explain the offset of C/N and $\delta^{13}C$ in this part of the record (Figure 2.4b), as explained above. The contribution of inorganic nitrogen suggested by the intercept in the TOC-TN plot is 0.03 weight %, which would be around half of the total nitrogen in this interval, much more than suggested by the comparison of C/N and $\delta^{13}C$. However, the uncertainties of both these estimates are large. In addition to the positive intercept (Figure 2.4a), the slope of the regression line of the glacial data group is less steep than those of the other groups, which might imply a different, perhaps more refractory nature of the glacial organic matter. Both a higher contribution of inorganic nitrogen and a different nature of the organic matter may result from the greater input of detrital material during the glacial sea level low stand. In contrast, the regression line in TN/TOC space for the data from the Younger Dryas period is not consistent with an inorganic N contribution (Figure 2.4a), although $\delta^{13}C$ and C/N values diverge during this time as in the glacial (Figures 2.3 and 2.4b). Hence, inorganic

nitrogen does not seem to be an explanation for the divergence between these two common tracers of terrestrial organic matter input during the Younger Dryas.

After 11.5 ka, $\delta^{15}N$ does not show strong covariations with C/N (Figure 2.4c) or $\delta^{13}C$, both of which vary little during the Holocene. Therefore, the pronounced decrease in $\delta^{15}N$ after about 10 ka cannot be explained by changes in the contribution of terrestrial material. In contrast, the glacial data show a clear negative correlation with C/N (Figure 2.4c), consistent with a significant input of terrestrial organic matter (high C/N and low $\delta^{15}N$) in this portion of the core. The same is true for $\delta^{13}C$, which is positively correlated to $\delta^{15}N$ in the glacial data

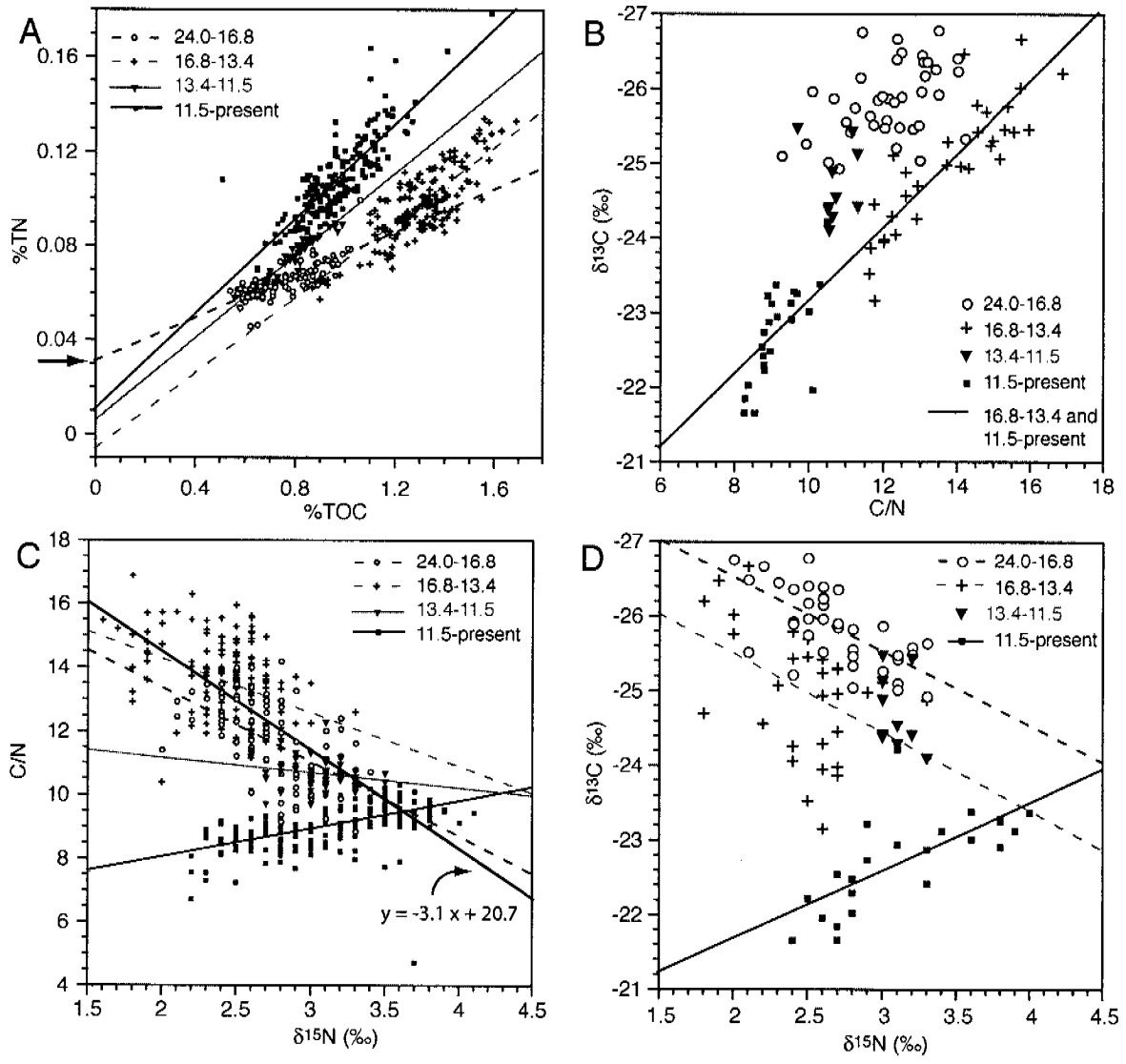

Figure 2.4. A. Total nitrogen versus total organic carbon, grouped by age (in ka) and the respective regression lines. Only the oldest data group (24.0-16.8 ka) shows a significant intercept (arrow), indicating inorganic nitrogen contribution. B. $\delta^{13}C$ versus C/N for the same age groups as in A. The regression line through the data from 16.8 to 13.4 ka and 11.5 to present is added to show the offset of the glacial and Younger Dryas data from the general relationship of $\delta^{13}C$ and C/N. C. C/N versus $\delta^{15}N$ for the four age groups with respective regression lines. Also shown is the regression line with parameters for all data older than 11.5 ka. The slope of this line is used to correct $\delta^{15}N$ for terrestrial inputs (see text and Figure 2.5). D. $\delta^{13}C$ versus $\delta^{15}N$.

(Figure 2.4d), although the correlation is less clear due to fewer paired $\delta^{13}C$ and $\delta^{15}N$ measurements. The strong correlation between $\delta^{15}N$ and C/N makes this relationship the best available basis for attempting to correct the $\delta^{15}N$ record for terrestrial inputs. As described above, the C/N data suffer from ambiguities involving a possible inorganic N contribution. Inorganic nitrogen would work to lower the glacial C/N ratios to some extent, erasing the signal of terrestrial organic matter input while most likely contributing low-$\delta^{15}N$ N to the sediment [*Schubert and Calvert*, 2001]. Therefore, the correlation between $\delta^{15}N$ and C/N yields a conservative estimate for the impact of terrestrial inputs, especially before 16.8 ka. The carbon isotope data would suggest a larger correction (Figure 2.4d), but the uncertainties involving C3 versus C4 plants warn against this approach.

In order to roughly estimate the $\delta^{15}N$ of marine organic matter, we use the correlation between bulk $\delta^{15}N$ and C/N. Thereby, we move the data points along the regression line for all data older than 11.5 ka to a C/N of 9, the mean value of the Holocene data group ($\delta^{15}N_{corr}$ = ((9 - C/N) / -3.1) + $\delta^{15}N$; Figure 2.5). Because using individual regression lines for different age groups does not change the general picture, we applied the same correction to the whole record. A more thorough analysis would require determining the endmember values and calculating the exact mixing line. However, as we do not have constraints for the N isotopic composition

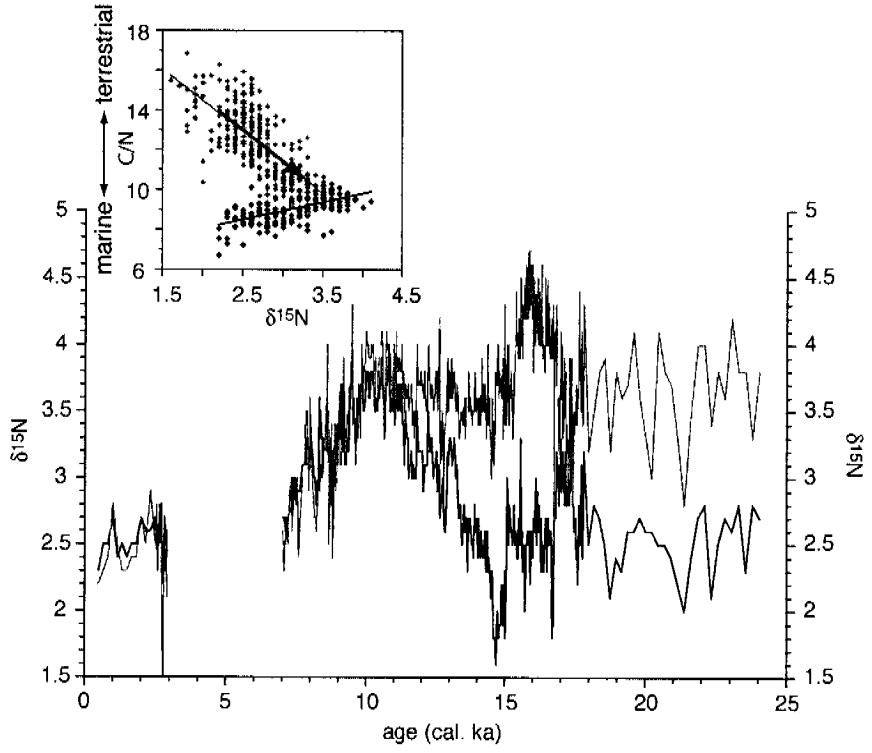

Figure 2.5. Correction of $\delta^{15}N$ for terrestrial organic nitrogen inputs using the regression of C/N versus $\delta^{15}N$ before 11.5 ka and shifting data along the regression line to C/N = 9 (inset). Corrected data are plotted in grey on top of original data (black).

of the endmembers and our measured values are probably in an intermediate range, the linear approximation should be sufficient for our purpose. The calculation shows that, if terrigenous organic matter influences the glacial $\delta^{15}N$ values, then the $\delta^{15}N$ of marine organic matter might have been as high as or even higher than during the deglacial $\delta^{15}N$ peak observed in the uncorrected record, with values 1.0 to 1.5 ‰ higher than Holocene values (Figure 2.5). Interestingly, with this correction, an earlier $\delta^{15}N$ peak appears during the meltwater spike, starting around 17.5 ka and decreasing after 15.5 ka before present. However, as mentioned above, inorganic nitrogen inputs might cause an underestimation of the marine sinking flux $\delta^{15}N$, especially before 16.8 ka.

2.4.2. Global comparison and implications

The low $\delta^{15}N$ of the Orca Basin sediments suggests a strong influence of N_2 fixation at this location, both today and in the past. This signal may be produced directly at the site, by N_2 fixation in the surface layer and the direct export of the resulting low-$\delta^{15}N$ organic matter to the seafloor. However, it can also be produced more regionally and indirectly: newly fixed N may be remineralized in the thermocline, producing low $\delta^{15}N$ nitrate in the thermocline that is subsequently mixed into the euphotic zone, leading to a low $\delta^{15}N$ in the sinking flux. The relative importance of these two routes by which the sinking flux may acquire the low-$\delta^{15}N$ signature of the N_2 fixation depends on the fraction of new production in any given year that is supplied by in situ N_2 fixation as opposed to nitrate mixed up from below. In the northern Sargasso Sea (i.e. at the Bermuda Atlantic Time-series Site), the similarity between the $\delta^{15}N$ of thermocline nitrate and sinking N suggests that the "indirect" route is more important there [*Altabet*, 1988; *Knapp et al.*, 2005]. However, the case may be different in the Gulf of Mexico.

One hypothesis explaining the lower glacial atmospheric CO_2 concentrations focuses on stimulation of N_2 fixation by increased dust and thereby iron input, increasing the marine N reservoir and hence productivity in glacial times [*Falkowski*, 1997]. The basis for this hypothesis is the high iron content of the enzyme nitrogenase [*Rueter et al.*, 1992], which is required for N_2 fixation. However, the question if and where N_2 fixation is limited by iron availability is still a matter of discussion [e.g., *Hood et al.*, 2000; *Lenes et al.*, 2001; *Sanudo-Wilhelmy et al.*, 2001; *Kustka et al.*, 2003; *Mills et al.*, 2004]. Based on the Orca Basin record, we conclude that glacial N_2 fixation was not enhanced in the region, as glacial-age $\delta^{15}N$ was similar to or higher than Holocene $\delta^{15}N$, but not lower. A greater ice age input of dust and iron to the tropical and subtropical Atlantic seems likely [*Mahowald et al.*, 1999]. Thus, the lack of a glacial enhancement in N_2 fixation suggests that, in this region and on the timescales we are investigating, Fe input is not the determining factor for N-fixation rates. This might be due to the presently already very high iron input into this region.

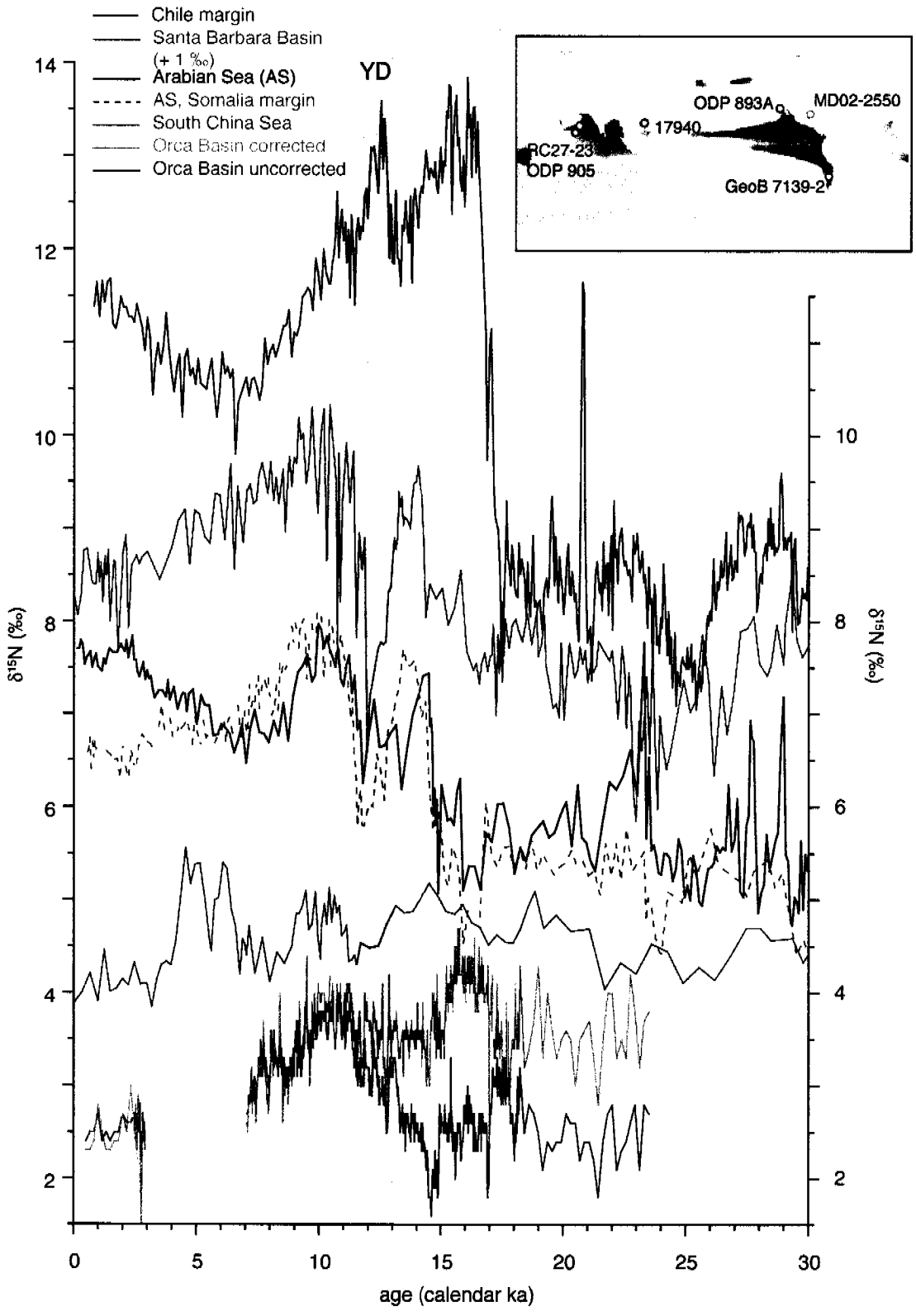

Figure 2.6. Global comparison of $\delta^{15}N$ records. Core locations are shown in the inset, together with the major oxygen minimum zones (dark grey). Shown are records (from top) from the Chile margin (GeoB 7139-2) [*De Pol-Holz et al.*, 2006], Santa Barbara Basin (ODP893A) [*Emmer and Thunell*, 2000], the Arabian Sea (RC27-23 [*Altabet et al.*, 2002] and ODP 905 [*Ivanochko et al.*, 2005]), and from the South China Sea (17940) [*Kienast*, 2000], as well as both the uncorrected and the corrected record from Orca Basin (this study). Note that the Santa Barbara Basin record is shifted upwards by 1 ‰ for better comparison. Grey shading indicates the time of the Younger Dryas period.

An established deglacial change in the marine nitrogen cycle, however, was the increase in denitrification in the oxygen minimum zones. This shift is well documented by several high-resolution nitrogen isotope records, showing a deglacial increase in $\delta^{15}N$, with a superimposed deglacial peak or double peak (Figure 2.6). In the Eastern North Pacific and the Arabian Sea, the strongest increase is observed at around 15 ka, the peak is interrupted by low Younger Dryas values, and the early Holocene decrease commences at round 10 - 9 ka [e.g., *Pride et al.*, 1999; *Emmer and Thunell*, 2000; *Altabet et al.*, 2002; *Ivanochko et al.*, 2005]. In the Eastern South Pacific, the trends appear similar, but suggest a southern hemispheric timing, with the increase in $\delta^{15}N$ starting already at around 18 - 17 ka and a temporary minimum during the Antarctic cold reversal [*Higginson and Altabet*, 2004; *De Pol-Holz et al.*, 2006]. A record from the South China Sea has been interpreted as reflecting mean ocean nitrate $\delta^{15}N$, leading to the conclusion of relative constancy in nitrate $\delta^{15}N$ from the last ice age through deglaciation and into the Holocene [*Kienast*, 2000]. With the Orca Basin record, we now have a high-resolution record from an oligotrophic regime that is even more distant from the Indo-Pacific regions of water column denitrification and that potentially records changes in N_2 fixation. Hence, we can use the data in comparison with the other available records to assess the interplay of denitrification and N_2 fixation and/or changes in mean ocean nitrate $\delta^{15}N$ in detail.

The uncorrected bulk sediment $\delta^{15}N$ record from the Orca Basin exhibits no glacial-to-Holocene trend, similar to the South China Sea record. Hence, taken at face value, the data suggest no long-term change in local to regional N_2 fixation, such that the isotopic signature of mean ocean nitrate would explain the glacial/interglacial constancy of the record [*Kienast*, 2000]. However, as discussed above, it is likely that the glacial part of the record is influenced by low-$\delta^{15}N$ terrestrial nitrogen so that the marine nitrogen $\delta^{15}N$ was higher than indicated by the bulk sediments. The overall last glacial-to-Holocene decrease we see in the corrected $\delta^{15}N$ record therefore does suggest a deglacial increase in N_2 fixation in this region. Hence, if we believe the correction scheme for terrestrial N inputs, the Orca Basin $\delta^{15}N$ record indicates that local and/or regional N_2 fixation responded to globally increased denitrification and can therefore be seen as a counterpart to the records from the oxygen minimum zones representing denitrification. The corrected record suggests that, today, the thermocline nitrate $\delta^{15}N$ is more divergent from mean ocean nitrate $\delta^{15}N$ in both the denitrification zones and nitrogen fixing regions than it was during glacial times. This observation supports the notion that the rates of both N outputs and inputs increased upon deglaciation, assuming a more or less constant nitrate reservoir.

The final decrease in $\delta^{15}N$, however, seems to start only after 10 ka, much later than the abrupt intensification of denitrification at around 17 ka in the Eastern South Pacific and 15 ka in the northern hemisphere. This is surprising with regard to the relatively short residence time of nitrate in the ocean (3 kyr or less) [*Gruber and Sarmiento*, 1997; *Brandes and Devol*, 2002] and

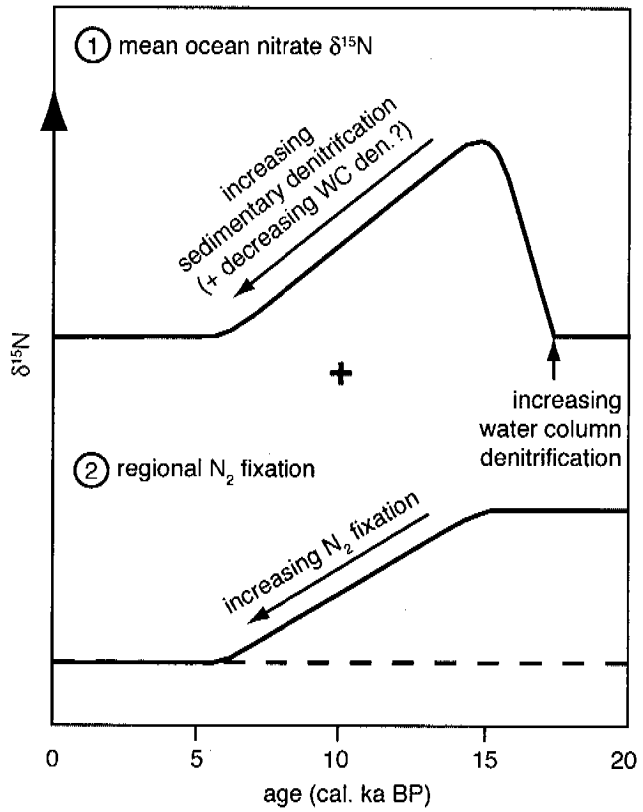

Figure 2.7. Conceptual drawing of potential influences on the Orca Basin $\delta^{15}N$ record. Top curve: Changes in mean ocean nitrate $\delta^{15}N$ due to variable proportion of water column (WC) denitrification. Rapid increases in WC denitrification occurred between 17 ka (southern hemisphere) and 15 ka (northern hemisphere; Figure 2.6). Decreasing proportion of WC denitrification is due to increasing sedimentary denitrification (probably paced by sealevel rise) [*Christensen*, 1994], and potentially a slow decrease in WC denitrification in response to a decreasing oceanic nitrate concentration [*Codispoti*, 1989]. Bottom curve: The corrected Orca Basin record (Figure 2.5) would call for a regional increase in N_2 fixation to explain the general last-glacial-to-Holocene $\delta^{15}N$ decrease (solid line). The timing and rapidity is not well constrained due to the overprint of whole ocean nitrate changes, but changes occurred some time between 15 and 5 ka.

the routes of ocean circulation that would transport a denitrification-driven decrease in nitrate-to-phosphate ratio into the North Atlantic thermocline. An explanation could be that the hypothesized deglacial increase in N_2 fixation is confounded with transient changes in the mean $\delta^{15}N$ of nitrate. This value is ultimately controlled by the fraction of global denitrification occurring in the water column (fw), an increase of which causes an increase in the $\delta^{15}N$ of nitrate [*Brandes and Devol*, 2002]. A deglacial peak could result from water column denitrification increasing earlier and/or faster than sedimentary denitrification, the latter probably being paced by sea level rise and the establishment of appropriate sedimentary environments on the shelves.

In addition, the overall strength of denitrification and the size of the marine N reservoir affect the isotopic composition of nitrate [*Deutsch et al.*, 2004]. If a larger fraction of nitrate is consumed by water column denitrification in the suboxic zone, the $\delta^{15}N$ of the residual nitrate will increase. At the same time, since less nitrate leaves the suboxic zone, the impact on the $\delta^{15}N$

of mean ocean nitrate decreases. A significant decrease in the marine nitrate reservoir would therefore lower the mean ocean nitrate $\delta^{15}N$. In principle, such a signal could be counteracted by an increase in fw, resulting in unchanged mean nitrate $\delta^{15}N$ such as observed in the South China Sea. However, as was shown by the box model study of *Deutsch et al.* [2004], an expected $\delta^{15}N$ increase in the oxygen minimum zones for such a scenario is not consistent with the Holocene $\delta^{15}N$ decrease observed in numerous records from these regions, suggesting relative constancy in the marine nitrogen budget. In short, we tentatively conclude that the Orca Basin record represents a composite of a regional deglacial increase in N_2 fixation and a transient deglacial maximum in mean ocean nitrate $\delta^{15}N$, driven by changes in fw (Figure 2.7).

Due to the different timing of the denitrification increase in the different oxygen minimum zones and also because there is not yet a firm constraint on the timing and magnitude of sedimentary denitrification changes, the effect on the isotopic composition of mean ocean nitrate is difficult to predict. However, the deglacial strengthening of denitrification is so pronounced that it should cause an increase in fw and thus in the mean ocean nitrate $\delta^{15}N$ as well. Following these deglacial increases, fw and thus global ocean nitrate $\delta^{15}N$ will then decrease as sedimentary denitrification increases due to sea level rise. Indeed, some features of the Orca Basin $\delta^{15}N$ record are remarkably similar to the denitrification-influenced records, suggesting a global signal. The early Holocene peak occurs at the same time as the second part of the deglacial peak observed in the records from the northern hemisphere. Furthermore, although the details of the corrected record should not be over-interpreted due to the large uncertainties involved, the earlier peak appearing in the corrected record coincides with the increase in Eastern South Pacific denitrification. The fact that, in the uncorrected data, the $\delta^{15}N$ peak begins later than one would expect is a further indication that the initiation of this peak is masked by terrestrial N inputs during the period of maximum meltwater influx.

2.5. Conclusions

In conclusion, the Orca Basin data adds to previous evidence for proposed feedbacks within the nitrogen cycle that stabilize the marine N budget on glacial-interglacial timescales. Interference by terrestrial nitrogen input during glacial times does not permit us to draw a definitive picture of changes in N_2 fixation in the subtropical North Atlantic. However, two end-member interpretations of the record support the notion that, in the face of climate-driven changes in water column denitrification, negative feedbacks work to stabilize the global ocean N reservoir. If we take the Orca Basin record at face value, glacial $\delta^{15}N$ was similar to Holocene values, implying that the global marine N budget cannot have changed by much since the deglaciation [*Kienast*, 2000; *Deutsch et al.*, 2004]. In this case, the deglacial peak in Orca Basin

probably represents transitory changes in the fraction of global denitrification occurring in the water column (fw) during deglaciation. The main feedback mechanism keeping the global N budget in balance could have been either the denitrification feedback, or changes in N_2 fixation that were not focused in the Atlantic. The Orca Basin record would therefore mainly reflect global changes in nitrate isotopic composition.

However, we have several indications that the glacial $\delta^{15}N$ of the marine sinking flux in the Orca Basin was higher than measured in the bulk sediment and therefore higher than during the Holocene. In this case, the most plausible explanation for the deglacial $\delta^{15}N$ decrease is an increase in local or regional N_2 fixation. This would be consistent with strong global feedbacks in the ocean N budget, with increases in denitrification such as has been observed in the Indo-Pacific leading to an increase in N_2 fixation in regions such as the Atlantic. If correct, one must then ask whether the Atlantic was unique in hosting the N_2 fixation response to the deglacial increase in denitrification, or whether this N_2 fixation response was widespread among the different basins. If iron inputs are a critical limiter of N_2 fixation across the global ocean, then one might predict that the N_2 fixation reponse was dominated by the Atlantic, where iron is relatively plentiful.

Global changes in mean ocean nitrate isotopic composition are likely responsible for the deglacial peak(s) evident in the Orca Basin record. These peaks are reminiscent of $\delta^{15}N$ peaks observed in records underlying regions of water column denitrification, and they may record a deglacial maximum in the globally averaged fraction of denitrification occurring in the water column as opposed to the sediments [*Brandes and Devol*, 2002; *Deutsch et al.*, 2004].

While the data from the Orca Basin provide important constraints, certain aspects of the interpretation are clearly compromised by the uncertainties associated with the potential for large terrestrial N inputs during the glacial and deglacial sections. Thus, although the Orca Basin setting yields for good preservation of sedimentary organic matter, minimizing the effects of isotopic alteration, its location on the margin introduces terrestrial N inputs as a confounding factor. Looking forward, it may prove difficult to find a coring site monitoring the subtropical oligotrophic ocean that hosts good organic matter preservation without risk of terrigenous N input. The tropical and subtropical ocean away from upwelling regions is therefore a particularly worthy target for approaches that seek to remove both terrigenous and diagenetic overprints from the isotopic composition of sedimentary organic matter, using either compound-specific or microfossil-bound $\delta^{15}N$ analyses [e.g., *Altabet and Curry*, 1989; *Shemesh et al.*, 1993; *Sachs and Repeta*, 1999; *Sigman et al.*, 1999].

Acknowledgements

We would like to thank Laurent Labeyrie, Yvon Balut, and the crew of R/V *Marion Dufresne* for a successful cruise in the Gulf of Mexico. Ben Flower is thanked for sharing radiocarbon dates, and H.-C. Lan for preparing the samples dated at ETH. P. Meier, U. Kegel, and G. Schettler are gratefully acknowledged for their help with sample preparation and measurements. This work was funded by the Swiss National Science Foundation.

References

Addy, S. K., and E. W. Behrens (1980), Time of Accumulation of Hypersaline Anoxic Brine in Orca Basin (Gulf of Mexico), *Mar. Geol.*, *37*, 241-252.

Aharon, P. (2003), Meltwater flooding events in the Gulf of Mexico revisited: Implications for rapid climate changes during the last deglaciation, *Paleoceanography*, *18*, 1079, doi:10.1029/2002PA000840.

Altabet, M. A. (1988), Variations in Nitrogen Isotopic Composition between Sinking and Suspended Particles - Implications for Nitrogen Cycling and Particle Transformation in the Open Ocean, *Deep-Sea Res. Part I*, *35*, 535-554.

Altabet, M. A., and W. B. Curry (1989), Testing models of past ocean chemistry using foraminifera 15N/14N, *Global Biogeochem. Cycles*, *3*, 107-119.

Altabet, M. A., M. J. Higginson, and D. W. Murray (2002), The effect of millennial-scale changes in Arabian Sea denitrification on atmospheric CO2, *Nature*, *415*, 159-162.

Altabet, M. A., R. Francois, D. W. Murray, and W. L. Prell (1995), Climate-Related Variations in Denitrification in the Arabian Sea from Sediment N-15/N-14 Ratios, *Nature*, *373*, 506-509.

Benner, R., M. L. Fogel, E. K. Sprague, and R. E. Hodson (1987), Depletion of C-13 in Lignin and Its Implications for Stable Carbon Isotope Studies, *Nature*, *329*, 708-710.

Brandes, J. A., and A. H. Devol (1997), Isotopic fractionation of oxygen and nitrogen in coastal marine sediments, *Geochim. Cosmochim. Acta*, *61*, 1793-1801.

Brandes, J. A., and A. H. Devol (2002), A global marine-fixed nitrogen isotopic budget: Implications for Holocene nitrogen cycling, *Global Biogeochem. Cycles*, *16*, 1120, doi:10.1029/2001GB001856.

Calvert, S. E., T. F. Pedersen, and R. E. Karlin (2001), Geochemical and isotopic evidence for post-glacial palaeoceanographic changes in Saanich Inlet, British Columbia, *Mar. Geol.*, *174*, 287-305.

Carpenter, E. J., and C. C. Price (1977), Nitrogen-Fixation, Distribution, and Production of Oscillatoria-(Trichodesmium) Spp in Western Sargasso and Caribbean Seas, *Limnol. Oceanogr.*, *22*, 60-72.

Carpenter, E. J., and K. Romans (1991), Major Role of the Cyanobacterium Trichodesmium in Nutrient Cycling in the North-Atlantic Ocean, *Science*, *254*, 1356-1358.

Carpenter, E. J., A. Subramaniam, and D. G. Capone (2004), Biomass and primary productivity of the cyanobacterium Trichodesmium spp. in the tropical N Atlantic ocean, *Deep-Sea Res. Part I*, *51*, 173-203.

Christensen, J. P. (1994), Carbon Export from Continental Shelves, Denitrification and Atmospheric Carbon-Dioxide, *Cont. Shelf Res.*, *14*, 547-576.

Cline, J. D., and I. R. Kaplan (1975), Isotopic fractionation of dissolved nitrate during denitrification in the eastern tropical North Pacific Ocean, *Mar. Chem.*, *3*, 271-299.

Codispoti, L. A. (1989), Phosphorus vs. nitrogen limitation of new and export production, in *Productivity of the Ocean: Past and Present*, edited by W. H. Berger, et al., pp. 377-394, John Wiley, Hoboken, N.J.

De Pol-Holz, R., O. Ulloa, L. Dezileau, J. Kaiser, F. Lamy, and D. Hebbeln (2006), Melting of the Patagonian Ice Sheet and deglacial perturbations of the nitrogen cycle in the eastern South Pacific, *Geophys. Res. Lett.*, *33*, L04704, doi:10.1029/2005GL024477.

Deutsch, C., D. M. Sigman, R. C. Thunell, A. N. Meckler, and G. H. Haug (2004), Isotopic constraints on glacial/interglacial changes in the oceanic nitrogen budget, *Global Biogeochem. Cycles*, *18*, GB4012, doi:10.1029/2003GB002189.

Emmer, E., and R. C. Thunell (2000), Nitrogen isotope variations in Santa Barbara Basin sediments: Implications for denitrification in the eastern tropical North Pacific during the last 50,000 years, *Paleoceanography*, *15*, 377-387.

Falkowski, P. G. (1997), Evolution of the nitrogen cycle and its influence on the biological sequestration of CO2 in the ocean, *Nature*, *387*, 272-275.

Flower, B. P., and J. P. Kennett (1990), The Younger Dryas cool episode in the Gulf of Mexico, *Paleoceanography*, *5*, 949-961.

Flower, B. P., D. W. Hastings, H. W. Hill, and T. M. Quinn (2004), Phasing of deglacial warming and laurentide ice sheet meltwater in the Gulf of Mexico, *Geology*, *32*, 597-600.

Ganeshram, R. S., T. F. Pedersen, S. E. Calvert, and J. W. Murray (1995), Large Changes in Oceanic Nutrient Inventories from Glacial to Interglacial Periods, *Nature*, *376*, 755-758.

Goering, J. J., R. C. Dugdale, and D. W. Menzel (1966), Estimates of in Situ Rates of Nitrogen Uptake by Trichodesmium Sp in Tropical Atlantic Ocean, *Limnol. Oceanogr.*, *11*, 614-620.

Goni, M. A., K. C. Ruttenberg, and T. I. Eglinton (1997), Source and contribution of terrigenous organic carbon to surface sediments in the Gulf of Mexico, *Nature*, *389*, 275-278.

Goni, M. A., K. C. Ruttenberg, and T. I. Eglinton (1998), A reassessment of the sources and importance of land-derived organic matter in surface sediments from the Gulf of Mexico, *Geochim. Cosmochim. Acta*, *62*, 3055-3075.

Gruber, N., and J. L. Sarmiento (1997), Global patterns of marine nitrogen fixation and denitrification, *Global Biogeochem. Cycles*, *11*, 235-266.

Haug, G. H., T. F. Pedersen, D. M. Sigman, S. E. Calvert, B. Nielsen, and L. C. Peterson (1998), Glacial/interglacial variations in production and nitrogen fixation in the Cariaco Basin during the last 580 kyr, *Paleoceanography*, *13*, 427-432.

Higginson, M. J., and M. A. Altabet (2004), Initial test of the silicic acid leakage hypothesis using sedimentary biomarkers, *Geophys. Res. Lett.*, *31*, L18303, doi:10.1029/2004GL020511.

Hood, R. R., A. F. Michaels, and D. G. Capone (2000), Answers sought to the enigma of marine nitrogen fixation, *EOS, Trans. AGU*, *81*, 133-139.

Hughen, K. A., et al. (2004), Marine04 marine radiocarbon age calibration, 0-26 cal kyr BP, *Radiocarbon*, *46*, 1059-1086.

Ivanochko, T. S., R. S. Ganeshram, G. J. A. Brummer, G. Ganssen, S. J. A. Jung, S. G. Moreton, and D. Kroon (2005), Variations in tropical convection as an amplifier of global climate change at the millennial scale, *Earth Planet. Sc. Lett.*, *235*, 302-314.

Jasper, J. P., and R. B. Gagosian (1990), The Sources and Deposition of Organic-Matter in the Late Quaternary Pygmy Basin, Gulf of Mexico, *Geochim. Cosmochim. Acta*, *54*, 1117-1132.

Jasper, J. P., and R. B. Gagosian (1993), The Relationship between Sedimentary Organic-Carbon Isotopic Composition and Organic Biomarker Compound Concentration, *Geochim. Cosmochim. Acta*, *57*, 167-186.

Karl, D., A. Michaels, B. Bergman, D. Capone, E. Carpenter, R. Letelier, F. Lipschultz, H. Paerl, D. M. Sigman, and L. Stal (2002), Dinitrogen fixation in the world's oceans, *Biogeochemistry*, *57*, 47-98.

Kienast, M. (2000), Unchanged nitrogen isotopic composition of organic matter in the South China Sea during the last climatic cycle: Global implications, *Paleoceanography*, *15*, 244-253.

Kienast, S. S., S. E. Calvert, and T. F. Pedersen (2002), Nitrogen isotope and productivity variations along the northeast Pacific margin over the last 120 kyr: Surface and subsurface paleoceanography, *Paleoceanography*, *17*, 1055, doi:10.1029/2001PA000650.

Knapp, A. N., D. M. Sigman, and F. Lipschultz (2005), N isotopic composition of dissolved organic nitrogen and nitrate at the Bermuda Atlantic time-series study site, *Global Biogeochem. Cycles*, *19*.

Kustka, A. B., S. A. Sanudo-Wilhelmy, E. J. Carpenter, D. Capone, J. Burns, and W. G. Sunda (2003), Iron requirements for dinitrogen- and ammonium-supported growth in cultures of Trichodesmium (IMS 101): Comparison with nitrogen fixation rates and iron: carbon ratios of field populations, *Limnol. Oceanogr.*, *48*, 1869-1884.

Lehmann, M. F., D. M. Sigman, and W. M. Berelson (2004), Coupling the N-15/N-14 and O-18/O-16 of nitrate as a constraint on benthic nitrogen cycling, *Mar. Chem.*, *88*, 1-20.

Lehmann, M. F., S. M. Bernasconi, A. Barbieri, and J. A. McKenzie (2002), Preservation of organic matter and alteration of its carbon and nitrogen isotope composition during simulated and in situ early sedimentary diagenesis, *Geochim. Cosmochim. Acta*, *66*, 3573-3584.

Lenes, J. M., et al. (2001), Iron fertilization and the Trichodesmium response on the West Florida shelf, *Limnol. Oceanogr.*, *46*, 1261-1277.

Leventer, A., D. F. Williams, and J. P. Kennett (1983), Relationships between Anoxia, Glacial Meltwater and Microfossil Preservation in the Orca Basin, Gulf of Mexico, *Mar. Geol.*, *53*, 23-40.

Liu, K. K., and I. R. Kaplan (1989), The Eastern Tropical Pacific as a Source of N-15-Enriched Nitrate in Seawater Off Southern-California, *Limnol. Oceanogr.*, *34*, 820-830.

LoDico, J. M., B. P. Flower, and T. M. Quinn (2006), Sub-Centennial Scale Climatic and Hydrologic Variability in the Gulf of Mexico during the Early Holocene, *Paleoceanography, (in press).*

Mahowald, N., K. Kohfeld, M. Hansson, Y. Balkanski, S. P. Harrison, I. C. Prentice, M. Schulz, and H. Rodhe (1999), Dust sources and deposition during the last glacial maximum and current climate: A comparison of model results with paleodata from ice cores and marine sediments, *J. Geophys. Res. Atmos.*, *104*, 15895-15916.

Marchitto, T. M., and K. Y. Wei (1995), History of Laurentide Meltwater Flow to the Gulf-of-Mexico During the Last Deglaciation, as Revealed by Reworked Calcareous Nannofossils, *Geology*, *23*, 779-782.

Meyers, P. A. (1997), Organic geochemical proxies of paleoceanographic, paleolimnologic, and paleoclimatic processes, *Org. Geochem.*, *27*, 213-250.

Michaels, A. F., D. Olson, J. L. Sarmiento, J. W. Ammerman, K. Fanning, R. Jahnke, A. H. Knap, F. Lipschultz, and J. M. Prospero (1996), Inputs, losses and transformations of nitrogen and phosphorus in the pelagic North Atlantic Ocean, *Biogeochemistry*, *35*, 181-226.

Mills, M. M., C. Ridame, M. Davey, J. La Roche, and R. J. Geider (2004), Iron and phosphorus co-limit nitrogen fixation in the eastern tropical North Atlantic, *Nature*, *429*, 292-294.

Newman, J. W., P. L. Parker, and E. W. Behrens (1973), Organic Carbon Isotope Rations in Quaternary Cores from Gulf of Mexico, *Geochim. Cosmochim. Acta*, *37*, 225-238.

Northam, M. A., D. J. Curry, R. S. Scalan, and P. L. Parker (1981), Stable Carbon Isotope Ratio Variations of Organic-Matter in Orca Basin Sediments, *Geochim. Cosmochim. Acta*, *45*, 257-260.

Peters, K. E., R. E. Sweeney, and I. R. Kaplan (1978), Correlation of Carbon and Nitrogen Stable Isotope Ratios in Sedimentary Organic-Matter, *Limnol. Oceanogr.*, *23*, 598-604.

Pride, C., R. Thunell, D. M. Sigman, L. Keigwin, M. Altabet, and E. Tappa (1999), Nitrogen isotopic variations in the Gulf of California since the last deglaciation: Response to global climate change, *Paleoceanography*, *14*, 397-409.

Redfield, A. C., B. H. Ketchum, and F. A. Richards (1963), The influence of organisms on the composition of seawater, in *The Sea*, edited by M. N. Hill, pp. 26-77, Wiley Interscience, Hoboken, N.J.

Rueter, J. G., D. A. Hutchins, R. W. Smith, and N. L. Unsworth (1992), Iron nutrition in Trichodesmium, in *Marine Pelagic Cyanobacteria: Trichodesmium and other*

Diazotrophs, edited by E. J. Carpenter, et al., pp. 289-306, Kluwer Academic, Dordrecht.

Sachs, J. P., and D. J. Repeta (1999), Oligotrophy and nitrogen fixation during eastern Mediterranean sapropel events, *Science*, *286*, 2485-2488.

Sackett, W. M., J. M. Brooks, B. B. Bernard, C. R. Schwab, H. Chung, and R. A. Parker (1979), Carbon Inventory for Orca Basin Brines and Sediments, *Earth Planet. Sc. Lett.*, *44*, 73-81.

Sanudo-Wilhelmy, S. A., et al. (2001), Phosphorus limitation of nitrogen fixation by Trichodesmium in the central Atlantic Ocean, *Nature*, *411*, 66-69.

Schubert, C. J., and S. E. Calvert (2001), Nitrogen and carbon isotopic composition of marine and terrestrial organic matter in Arctic Ocean sediments: implications for nutrient utilization and organic matter composition, *Deep-Sea Res. Part I*, *48*, 789-810.

Sebilo, M., G. Billen, M. Grably, and A. Mariotti (2003), Isotopic composition of nitrate-nitrogen as a marker of riparian and benthic denitrification at the scale of the whole Seine River system, *Biogeochemistry*, *63*, 35-51.

Shemesh, A., S. A. Macko, C. D. Charles, and G. H. Rau (1993), Isotopic Evidence for Reduced Productivity in the Glacial Southern-Ocean, *Science*, *262*, 407-410.

Shokes, R. F., P. K. Trabant, B. J. Presley, and D. F. Reid (1977), Anoxic, Hypersaline Basin in Northern Gulf of Mexico, *Science*, *196*, 1443-1446.

Sigman, D. M., and G. H. Haug (2003), The Biological Pump in the Past, in *Treatise on Geochemistry*, edited by H. D. Holland and K. K. Turekian, pp. 491-528, Pergamon, Oxford.

Sigman, D. M., M. A. Altabet, R. Francois, D. C. McCorkle, and J. F. Gaillard (1999), The isotopic composition of diatom-bound nitrogen in Southern Ocean sediments, *Paleoceanography*, *14*, 118-134.

Sigman, D. M., M. A. Altabet, D. C. McCorkle, R. Francois, and G. Fischer (2000), The delta N-15 of nitrate in the Southern Ocean: Nitrogen cycling and circulation in the ocean interior, *J. Geophys. Res. Oceans*, *105*, 19599-19614.

Stuiver, M., and P. J. Reimer (1993), Extended C-14 Data-Base and Revised Calib 3.0 C-14 Age Calibration Program, *Radiocarbon*, *35*, 215-230.

Thunell, R. C., D. M. Sigman, F. Muller-Karger, Y. Astor, and R. Varela (2004), Nitrogen isotope dynamics of the Cariaco Basin, Venezuela, *Global Biogeochem. Cycles*, *18*, GB3001, doi:10.1029/2003GB002185.

Trefry, J. H., S. Metz, T. A. Nelsen, R. P. Trocine, and B. J. Eadie (1994), Transport of Particulate Organic-Carbon by the Mississippi River and Its Fate in the Gulf-of-Mexico, *Estuaries*, *17*, 839-849.

Seite Leer /
Blank leaf

Chapter 3

Terrigenous organic matter input to sediments from Orca Basin, Gulf of Mexico – a combined optical and biomarker approach*

Abstract

In this study we assessed changes in the contribution of terrigenous organic matter (OM) to the Gulf of Mexico over the course of the last deglaciation. To this end, we combined optical kerogen analyses with biomarker measurements and compound-specific carbon isotope analyses on terrigenous n-alkanes. These analyses complement existing records of bulk sedimentary parameters. The results confirmed previous findings that terrigenous input was much larger in glacial times, and additionally revealed that much of the glacial OM is reworked. In contrast, the Holocene sediments contain mainly marine OM, which is exceptionally well preserved. The Holocene sediments are therefore a well-suited archive for reconstructions of marine ecosystem changes, whereas the complex nature of OM in the glacial and deglacial part of the core hampers such studies if they are based on bulk analyses. During the deglaciation, terrigenous input was generally high due to large meltwater fluxes, whereby discrepancies between different proxies call for additional influences, such as differential transport. The beginning of the Younger Dryas period around 12.5 ka was characterized by a peak in terrigenous input, although it is generally believed that meltwater flow was rerouted away from the Mississippi at this time. Hence, the results revealed that the history of deglacial meltwater inflow to the Gulf of Mexico is not yet fully understood.

*in preparation as A.N. Meckler, C.J. Schubert, P.A. Hochuli, D. Birgel, Terrigenous organic matter input to sediments from Orca Basin, Gulf of Mexico - a combined optical and biomarker approach.

3.1. Introduction

Sedimentary organic matter (OM) is in most places composed of a mixture of autochthonous marine particles and allochthonous particles derived from land plants, which are already degraded to a varying degree. The composition of OM deposited in the Gulf of Mexico has been shown to vary on glacial-interglacial timescales due to the proximity of the Mississippi River mouth changing with sea level. Evidences for increased terrestrial input in glacial times are lower $\delta^{13}C$ values of OM and higher C/N ratios [e.g., *Newman et al.*, 1973; *Northam et al.*, 1981; *Jasper and Gagosian*, 1990], as well as higher abundances of terrigenous biomarkers [*Jasper and Gagosian*, 1993]. Furthermore, during deglaciations the inflow of large volumes of meltwater from the Laurentide Ice Sheet delivered terrigenous OM and nutrients into the Gulf of Mexico, which likely left an imprint on the composition of sedimentary OM [*Jasper and Gagosian*, 1993]. Detailed assessment of such effects, however, has been hampered by the low resolution of the earlier records.

For the last deglaciation, the timing of this so-called meltwater spike was reconstructed using the oxygen isotopic composition ($\delta^{18}O$) of foraminiferal calcite (a proxy for salinity) in sediments from Orca Basin, located on the continental slope [*Leventer et al.*, 1983]. While the oxygen isotopic record from Orca Basin is used as standard record for the timing of deglacial meltwater inflow to the Gulf of Mexico, it has recently been challenged by another $\delta^{18}O$ record, stacked from individual data sets from cores located closer to the shore [*Aharon*, 2003]. This latter record, although similar in the general picture, did not agree with that from Orca Basin in all aspects, which will be discussed later. Such discrepancies in meltwater input reconstructions based on foraminiferal $\delta^{18}O$ call for an independent assessment of deglacial meltwater fluxes into the Gulf of Mexico. Due to the potentially large effect of the associated terrigenous input on the composition of sedimentary OM, changes in OM composition could be useful as an alternative proxy for reconstructing meltwater input.

In addition, information about the composition of OM aids in the interpretation of bulk geochemical analyses (e.g., nitrogen isotopes), when they are used to reconstruct changes in the marine ecosystem. A varying contribution of terrigenous OM can significantly alter the signal and therefore needs to be assessed. For Orca Basin, it has been shown that varying terrigenous input likely affected the N isotopic composition in the glacial part of the sediments, revealed by a negative correlation of C/N and $\delta^{15}N$ [*Meckler et al.*, submitted; see previous chapter]. This has, in that part of the core, serious implications for the applicability of bulk $\delta^{15}N$ as proxy for changes in the marine nitrogen cycle. The results of the two bulk parameters used in that study to assess terrigenous input (C/N and bulk organic $\delta^{13}C$) did not agree in several intervals, such as during the meltwater spike and the Younger Dryas period (around 13 – 11.5 ka before present). The reason is that both $\delta^{13}C_{org}$ and C/N can be influenced by a number of other factors

besides the OM source. In this study, we therefore performed a more detailed assessment of OM in the same core from Orca Basin, employing both microscopic kerogen analysis and biomarker measurements.

Within the kerogen fraction, certain types of terrigenous organic matter can be identified, such as pollen grains, spores, or phytoclasts (wood, cuticles), in contrast to marine components such as dinoflagellate cysts (dinocysts) and other algal remains [*Tyson*, 1995]. Additionally, the contribution of reworked OM can be estimated based on the abundance of reworked palynomorphs (pollen grains, spores, or dinocysts) and to some extent the amount of opaque phytoclasts [*Tyson*, 1995, and references therein]. The latter particles can also be derived from contemporary biomass burning, however. It has to be noted that much of the OM appears as amorphous in normal light observations and is therefore often not clearly attributable.

Measuring the concentrations of characteristic organic compounds (biomarkers) from each realm is another way to obtain proxies for terrigenous and marine contributions to sedimentary OM, which are more specific than bulk parameters due to the various influences on the latter. Typical terrestrial compounds are for example long-chain n-alkanes and n-alcohols, derived from leaf waxes of higher plants [*Eglinton and Hamilton*, 1967]. Marine derived compounds are for example the sterols brassicasterol (24-methylcholesta-5,22E-dien-3β-ol), produced by diatoms and other algae, and dinosterol (4,23,24-Trimethyl-5α(H)-Cholest-22-en-3β-ol), derived from dinoflagellates [*Volkman*, 1986]. *Jasper and Gagosian* [1993] studied variations in long-chain n-alkanes, n-alcohols, various sterols as well as long-chain alkenones (marine biomarkers) on glacial-interglacial timescales using sediments from Pigmy Basin, which is located close to Orca Basin. Their low-resolution records show increased proportions of terrigenous markers in glacial stages, whereas interglacial sediments contained higher concentrations of alkenones. In addition to source changes, diagenetic alteration of the OM composition was inferred by these authors from differences between biomarker concentrations and bulk $\delta^{13}C_{org}$ values, assuming that the latter is solely influenced by the contribution of terrigenous OM.

However, as mentioned above, bulk $\delta^{13}C_{org}$ values can be influenced by various factors. The carbon isotopic composition of terrigenous material can vary itself due to changes in the abundance of C3 plants with an average isotopic composition of around 27 ‰ and C4 plants with $\delta^{13}C$ values around 14 ‰ [*O'Leary*, 1988]. Such variations in the terrigenous source are not distinguishable from changes in the proportions of terrigenous and marine OM with bulk $\delta^{13}C_{org}$ measurements alone. We therefore measured compound-specific carbon isotopes on long-chain n-alkanes in selected samples from the Orca Basin core in order to assess the effect of such vegetation changes on the bulk $\delta^{13}C_{org}$ values during the last deglaciation.

With the combined optical and biomarker approach for the characterization of OM in Orca Basin sediments we aim to assess the contribution of terrigenous OM and the timing its input

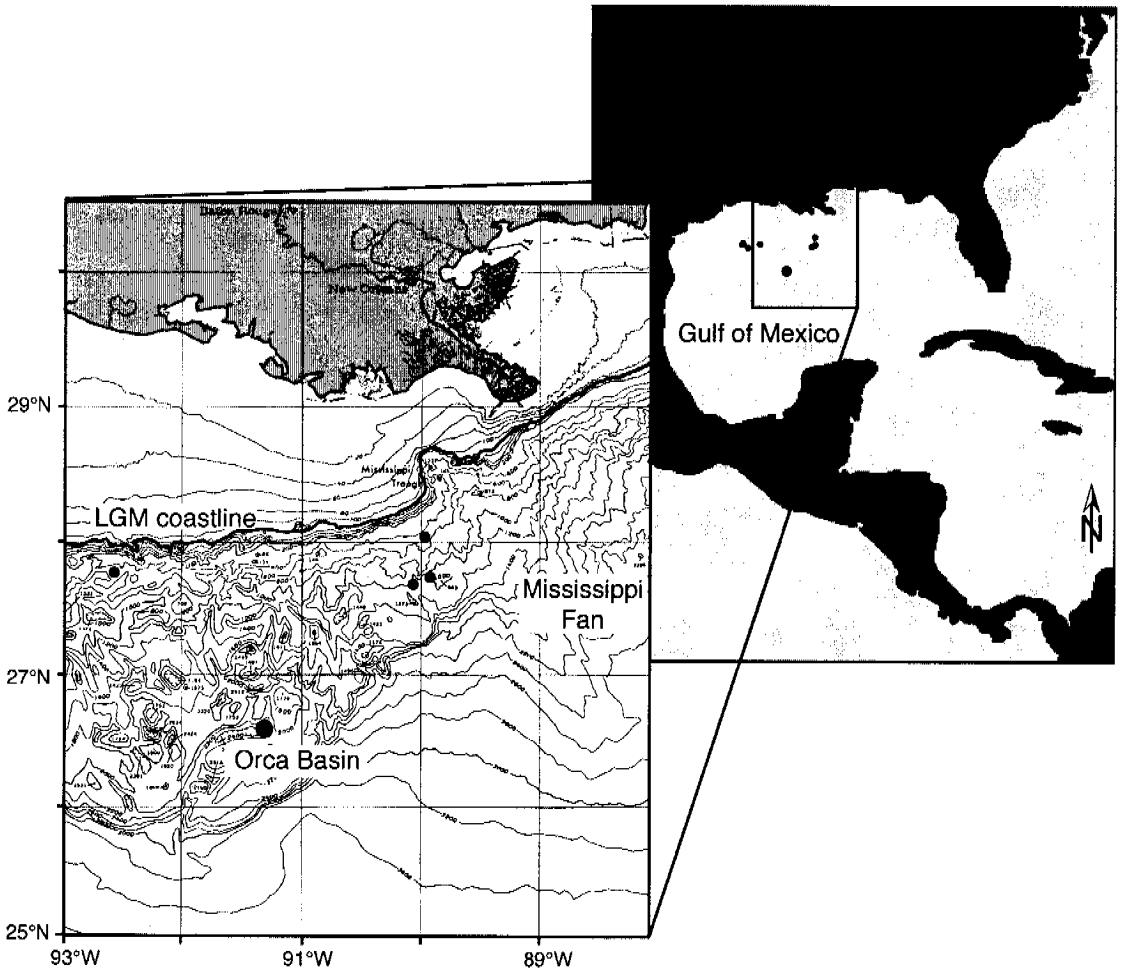

Figure 3.1. Map of the Gulf of Mexico showing the location of Orca Basin (large circle), around 300 km offshore from the Mississippi River mouth. Also indicated are locations of 7 cores (small circles)which were combined into a stacked record [*Aharon*, 2003]. Left panel: Bathymetry of the Louisiana slope and Mississippi Fan. Approximate location of last glacial maximum (LGM) coastline is indicated. Core MD02-2550 was taken from the slope of Orca Basin, in a water depth of 2249 m at 26°56.77N and 91°20.74W.

during the last deglaciation in order to i) better understand the history of meltwater input into the Gulf of Mexico and ii) define sections of the core that are dominated by marine OM and can therefore be used for reconstructions of marine ecosystem changes.

3.2. Materials and methods

Orca Basin is located on the Louisiana continental slope, around 300 km southwest of the Mississippi mouth (Figure 3.1). The basin is 2400 m deep and surrounded by salt diapirs [*Shokes et al.*, 1977], which are the source for a hypersaline brine filling the lowermost 200 m of the basin [*Sackett et al.*, 1979]. The strong density stratification results in anoxic bottom

water, leading to excellent preservation of organic matter in the sediments. The 9.09 m long giant box core MD02-2550 was taken during IMAGES cruise VIII (PAGE) in 2002. The upper 232 cm of the core consist of clearly laminated black sediment. The black color is due to metastable iron sulfides, and the change from grey to black color has been interpreted as the onset of brine accumulation [*Addy and Behrens*, 1980]. However, laminated sediment suggesting anoxic conditions can also be found below this depth. From 232-268 cm, the sediment is clearly laminated, but it lacks the black color. Laminations are less clear and not continuous from 268 to 300 cm and deteriorate further from 300-394 cm. From 394 to 567 cm clear laminations reappear, interrupted by a homogenous interval at 437-456 cm. Smear slide examinations showed that this homogenous interval corresponds to the deglacial peak in the percentage of reworked nannofossils, which has been described by Marchitto and Wei [1995] for neighboring core EN32-PC4. Below 567 cm the sediment is bioturbated. However, bundles of black layers were observed in the bottom section of the core, at 852-863 cm, 875-884 cm, and 896-906 cm. The age model for core MD02-2550 used in this study is based on 13 radiocarbon dates and has been described previously [*Meckler et al.*, submitted; see chapter 2].

3.2.1. Kerogen composition

For the kerogen analysis, freeze-dried material was used, combining 2-5 of the 1cm-sliced samples used for bulk analyses. A total of nine samples was prepared, covering the late Holocene (2 samples), early Holocene (2 samples), Younger Dryas (1 sample), meltwater spike (2 samples), and glacial (2 samples). The material was prepared following standard palynological preparation techniques [e.g., *Traverse*, 1988]. The residue was wet-sieved to obtain particles larger than 10 μm and from that fraction two slides per sample were mounted. An aliquot of the remaining material >10 μm was oxidized with concentrated HNO_3. Two slides per sample were also mounted of the oxidized material. All slides were briefly assessed microscopically. Because some particles were dissolved by the HNO_3 treatment (see below), only slides of un-oxidized material were used for the optical analysis. For 6 samples, around 300 particles were classified into different categories and pictures were taken. Amorphous organic matter was not counted, as it was sometimes present in the form of a diffuse background.

3.2.2. Biomarker analysis

Samples used for the biomarker analyses were taken on board and kept frozen at -80°C. Concentrations of n-alkanes and their isotopic composition were measured at the Limnological

Research Institute of EAWAG (Kastanienbaum) whereas measurements of the other biomarkers (sterols and n-alcohols) were performed at Bremen University as specified in the following.

3.2.2.1. Sterols and n-alcohols

Around 5 g of sediment from selected samples (n = 12) were dried at 40°C for three days. This yielded around 1.5-3.3 g dry sediment, to which 20 µl of a mixture of internal standards were added, amounting to 2 µg of each standard. Subsequently, organic compounds were extracted by addition of 15 ml of a 2:1 mixture of dichloromethane (DCM) and methanol and sonication for 10 minutes. The mixture was centrifuged and the supernatant collected. The extraction was performed 4 times and the extracts combined, before they were evaporated under N_2 to almost dryness. Any water in the extract was removed by filtering the concentrated extract through Na_2SO_4 on pre-combusted glass wool (cleaned beforehand with DCM and methanol), and rinsing with DCM and methanol. Finally, the extracts were evaporated to dryness and kept frozen until further use.

An aliquot of the extract was first separated into asphaltenes (soluble in DCM) and maltenes (in hexane), and the maltenes further separated into different fractions. To this end, solid phase extraction cartridges (Suppelco) were rinsed with first DCM and then hexane, before the sample (in hexane) was added. The different fractions that were subsequently eluted were hydrocarbons (with hexane), ketones (with a 3:1 mixture of hexane and DCM), alcohols (with a 9:1 mixture of DCM and acetone), and fatty acids (with 2% formic acid in DCM). Alcohols were derivatized to trimethylsilylethers with BSTFA (bis(trimethylsilyl)-trifluoroacetamide) and trimethylchlorosilane at a temperature of 70°C and with pyridine as catalyst. Fatty acids were methylated with 10% BF_3 in methanol. The hydrocarbon fraction had to be cleaned from elemental sulfur by reaction with activated copper. Afterwards, all extracts were dried under N_2 and taken up in 50µl hexane for analysis. The analyses were performed using a Thermo Electron Trace GC-MS equipped with a DB-5MS fused silica capillary column (30 m, 0.32 mm ID, 025µm film thickness). He gas was used as carrier. The GC temperature program used was as follows: injection at 60 °C, 2 min isothermal, to 150 °C at 15 °C min^{-1}, to 320 °C at 4 °C min^{-1}, 20 min isothermal. Identification of individual compounds was based on comparison of mass spectra and GC retention times with published data and reference compounds. As the alcohols showed the most variability among the different samples, only the results from this fraction were quantified and will be presented below. We used the two most characteristic alcohols each for marine and terrigenous OM to define the M/T ratio as proxy for the abundance of marine versus terrigenous OM. This ratio was calculated as follows:

M/T = ([brassicasterol]+[dinosterol]) / ([C24 n-alcohol]+[C26 n-alcohol]),

whereby [ ] denotes concentrations in µg/g TOC.

3.2.2.2. n-alkane concentration and isotopic composition

For a total of 47 samples, 2-3 g of sediment each were extracted for 15min at 70°C in a microwave using dichloromethane and methanol to obtain the total lipid extracts. Aliquots of the total extracts were separated after addition of internal standards on an Isolute NH_2 column into four fractions using solvents with different polarity. The hydrocarbon fraction was analyzed by gas chromatography (Carlo Erba HRGC 5160 Mega Series) and gas chromatography–mass spectrometry (Finnigan Voyager) for the quantification and identification of biomarkers, respectively. The isotopic composition ($\delta^{13}C$ against VPDB) was measured on selected samples (n = 10) with a GC (Agilent 6890) connected via a combustion interface to a mass spectrometer (GV instruments, Isoprime). All chromatographical separations were done on a factor four column (Varian, 60 m, 0.25 mm ID, and 0.25 µm film).

The sum of long-chain n-alkanes was calculated from the concentrations of n-alkanes with carbon numbers from 25 to 31 except for C28, as this peak sometimes overlapped with a neighboring peak. Concentrations are given relative to the concentration of total organic carbon (TOC). Analytical precision calculated from duplicate measurements on two samples was better than 5%. Including the extraction, the precision amounts to around 15%. The isotopic analyses were also done in duplicate and precision was better than 0.3‰. The isotopic composition of the C27, C29, and C31 n-alkanes was very similar (mostly within 0.5‰), so that the average of these three values was taken for each sample.

3.3. Results and Discussion

3.3.1. Optical kerogen analysis

The Holocene samples (90 cm and 300 cm; Figure 3.2 A-F) are characterized by a diffuse background of amorphous OM, likely of mainly marine origin. Both contain little reworked material (less than 3% of the palynomorphs; Figures 3.3 and 3.4). Opaque phytoclasts are present in significant numbers (10-15% of total phytoclasts; Figures 3.3 and 3.4), but they could reflect charred material that is not necessarily reworked. The pollen assemblage is composed mainly of extant species, with preferred climates ranging from warm (e.g., *Taxodium*, *Carya*, *Zelkova*) to

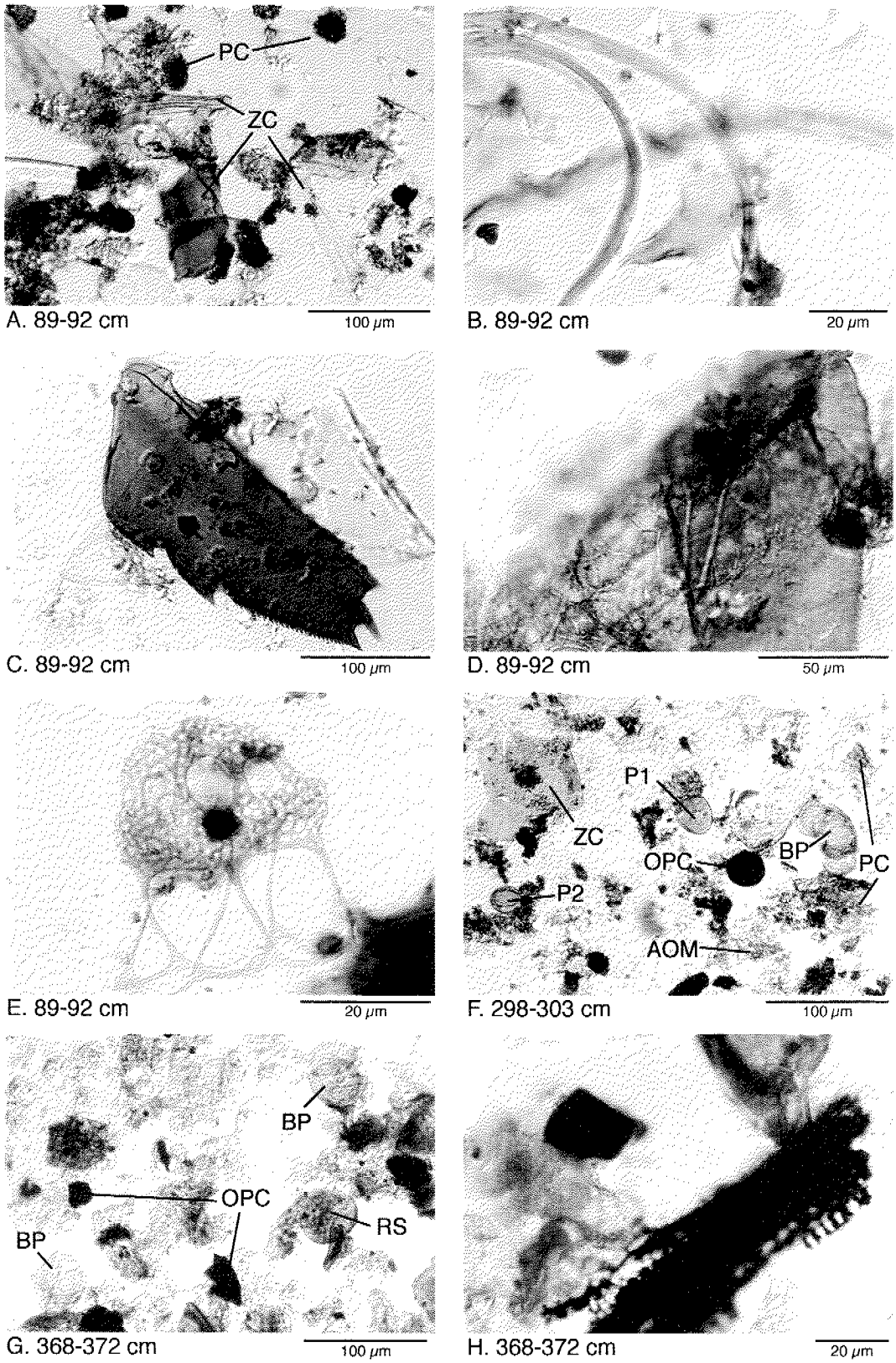

Figure 3.2. Photographs of kerogen in Orca Basin sediments. Sample depths and scales are shown at the bottom of each picture. Some pictures are from oxigenated samples (ox.). A. Overview of late Holocene sample with phytoclasts (PC) and zooclasts (ZC). B. Filaments, possibly of cyanobacterial origin. C. Crustacean limb. D. Biological degradation of crustacean fragment (feeding traces). E. Tintinnid lorica (*Dictyocysta elegans*). F. Overview of early Holocene sample showing PC, ZC, bisaccate pollen grain (BP), opaque phytoclasts (OPC), amorphous OM (AOM), *Carya* pollen grain (P1) indicative of warm climate and a tricolporate pollen grain (P2). G. Overview of Younger Dryas sample showing several BP, OPC, and a reworked spore (RS). H. Charcoal fragment.

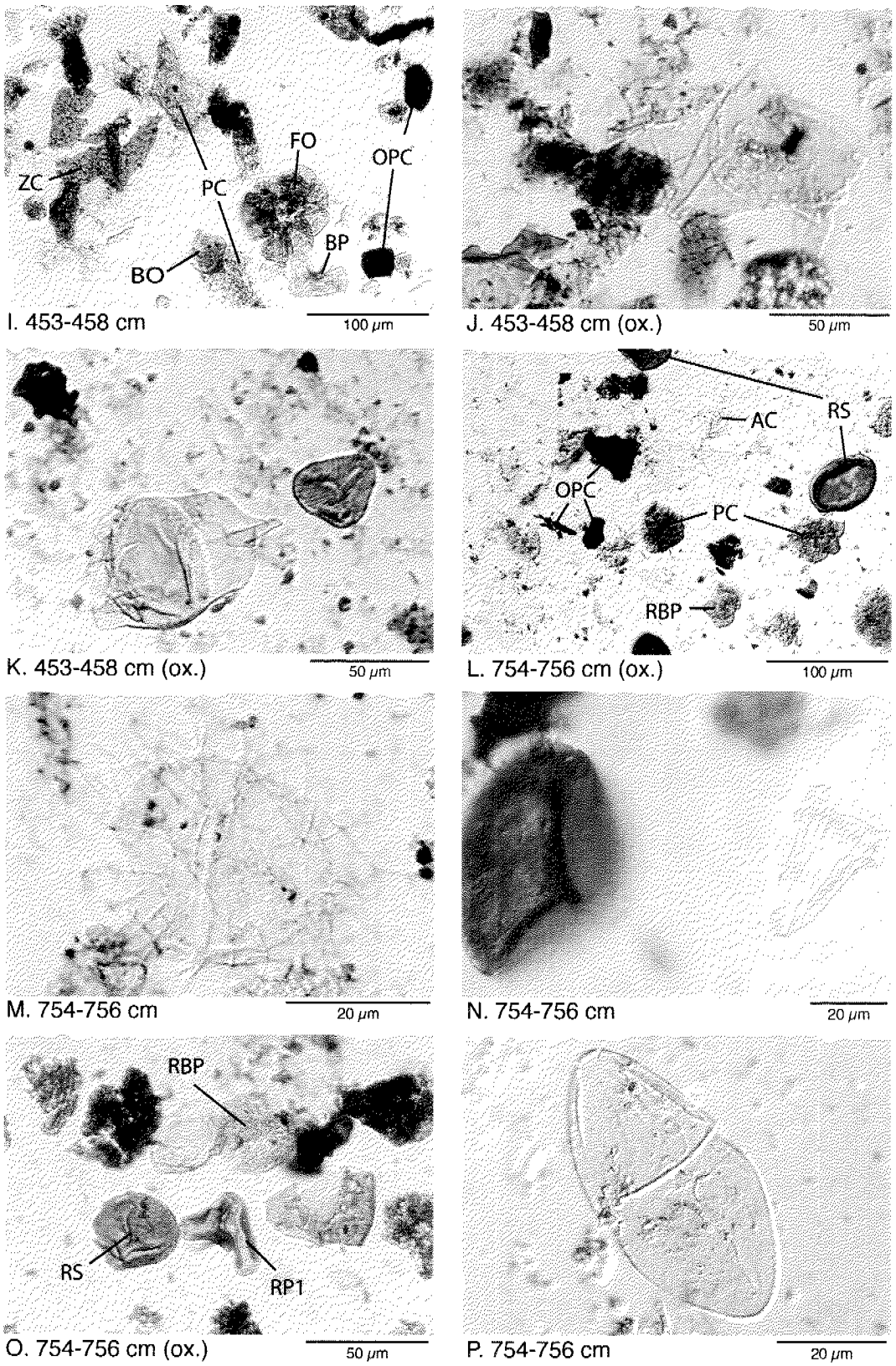

Figure 3.2 (cont.). I. Overview of meltwater spike sample with PC, ZC, BP, and OPC,remains of *Botryococcus* (BO) and a foraminiferal test lining (FO). J. Cretaceous dinocyst *Odontochitina* spp. K. Upper Cretaceous dinocyst *Isabelidinium* spp. (left) and reworked (prob. Cretaceous) spore of *Cicatricosisporites* spp. (right). L. Overview of glacial sample with PC, OPC, reworked bisaccate pollen grain (RBP), reworked spores (RS), and acritarch (AC). M. Upper Cretaceous dinocyst *Paleohystrichophora infusorioides*. N. Paleozoic spore (left) together with an Upper Cretaceous dinocyst (*Dinogymnium* spp., right). O. Reworked Upper Cretaceous pollen grain (*Aquilapollenites*; RP1) together with RBP and RS. P. *Dinogymnium* spp..

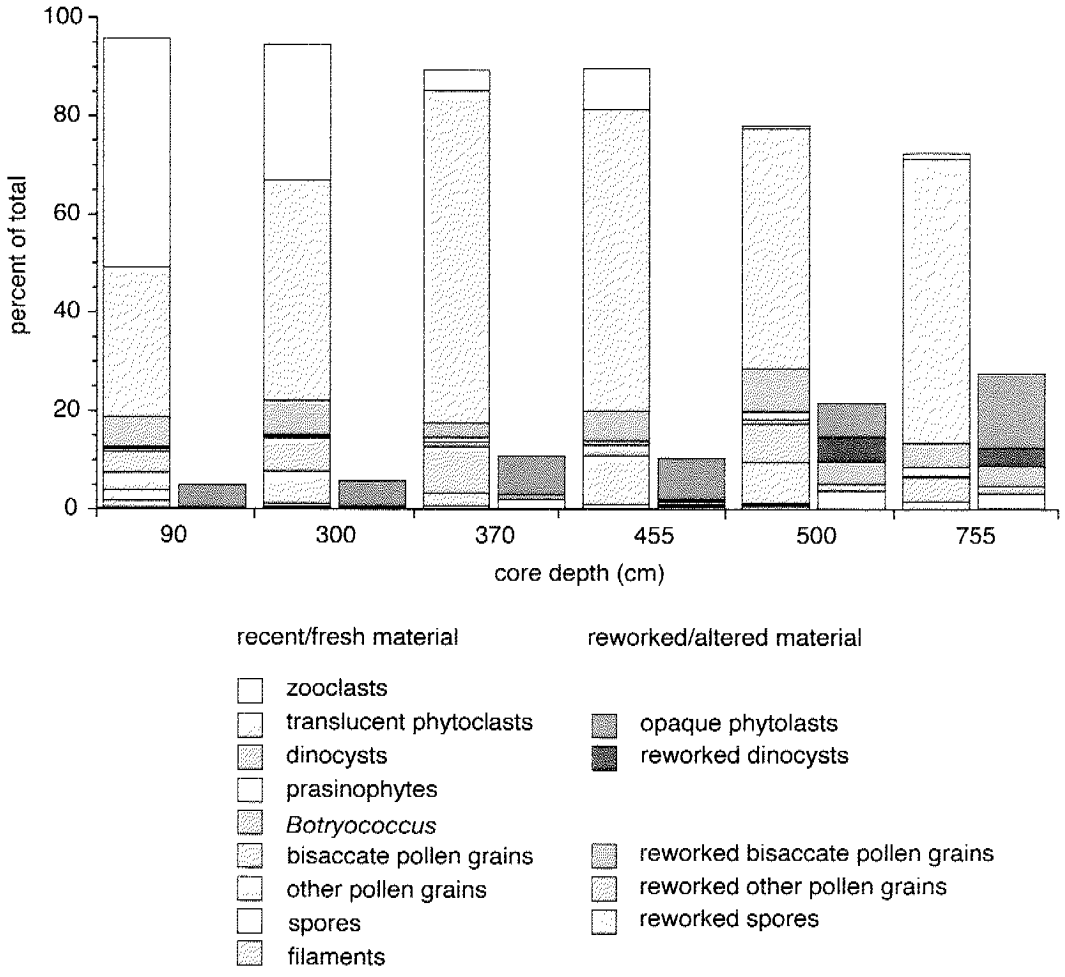

Figure 3.3. Relative abundances of different palynomorph groups (in percent) as revealed by optical kerogen analysis. For each sample, left columns are recent and/or fresh-looking particles, right columns are reworked and/or altered particles. However, opaque phytoclasts are not necessarily reworked (see text). Dynocysts are cysts of dinoflagellates. Around 300 particles were counted in each sample.

temperate (*Quercus*, *Pinus*, *Betula*, *Abies*). The youngest sample contains filaments of unknown, but possibly cyanobacterial origin (Figure 3.2B) as well as loricae of tintinnids (*Dictyocysta elegans*, Figure 3.2E, and *Codonellopsis orthoceras*), a group of ciliates. Very obvious is the much stronger presence of chitinous crustacean remains (zooclasts) in the Holocene samples compared to the older samples (Figure 3.2A, C and D). Some of the fragments were apparently degraded biologically, as revealed by feeding traces (Figure 3.2D). Interestingly, this chitinous material was dissolved by the oxidative treatment with HNO_3, indicating its labile character. Rapid degradation of chitin was also found in laboratory experiments, even under anoxic conditions [*Poulicek and Jeuniaux*, 1991]. The abundance of chitinous crustacean remains in sediments is therefore unusual, as is the presence of tintinnid loricae, attesting excellent preservation of OM in Orca Basin.

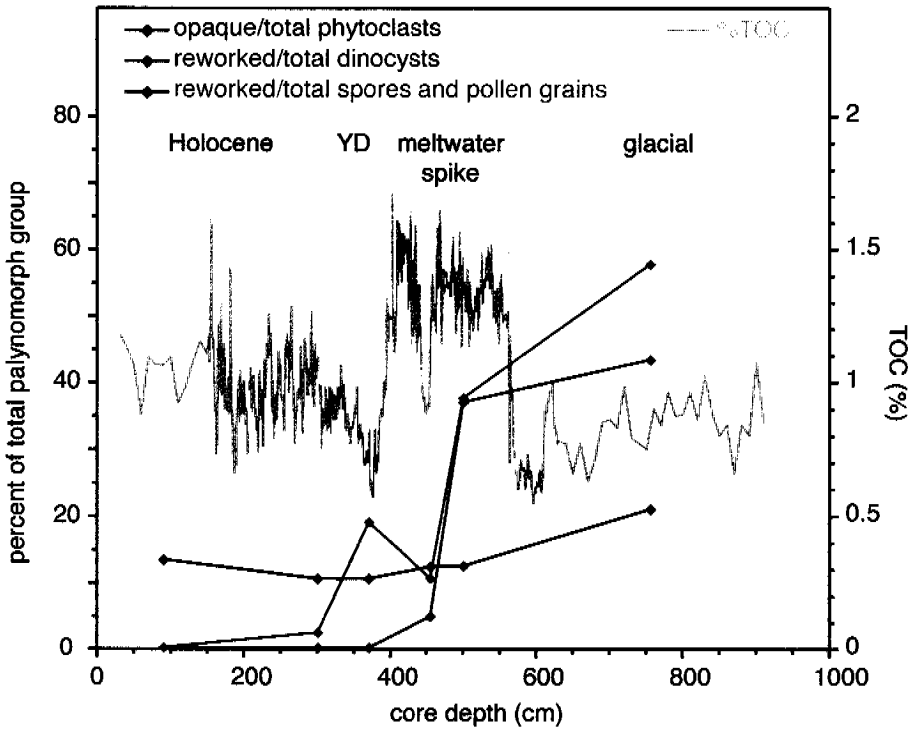

Figure 3.4. Contribution of reworked material in core MD02-2550. Shown are percentages of different palynomorph groups recognized as reworked (dynocysts and spores/pollen grains) or potentially reworked (phytoclasts). The opaque character of phytoclasts can also be due to pyrolization of recent material. %TOC is plotted for comparison. YD means Younger Dryas.

The presence of reworked material is notably increased in the samples from the Younger Dryas (370 cm) and the meltwater spike (455 cm and 500 cm). This can be seen on the photographs (Figure 3.2 G-K) as well as in the fraction of palynomorphs recognized as reworked (Figure 3.3, dark colored bars, and Figure 3.4). In the Younger Dryas interval, 7.5% and 75% of the pollen grains and spores were characterized as reworked, respectively. In addition, opaque phytoclast abundance is increased (Figure 3.2G). The pollen assemblage contains many thermophilic species such as *Carya*, which might be another indication for reworking in a generally cool climate. The meltwater spike samples also contained significant amounts of reworked material, with markedly higher concentrations observed in the deeper sample (500 cm). This sample can probably be considered as more representative of the meltwater spike material, as the shallower sample was taken from the homogenous interval characterized by low TOC concentrations. Around 37%, 27% and 92% of the dinocysts, pollen grains, and spores were counted as reworked, respectively in the sample from 500 cm depth. The reworked palynomorphs in the meltwater samples include pollen grains from the Mesozoic (*Classopollis* spp.), Upper Cretaceous (*Oculopollis* spp., *Aquilapollenites* spp.), and Tertiary or early Quaternary (*Myrica* spp.), as well as Paleozoic and Upper Cretaceous spores (Figure 3.2K). Reworked Cretaceous dinocysts observed were for example *Odontochitina* spp. (Figure 3.2J) and *Isabelidinium* spp.

(Figure 3.2K). Again, many pollen grains from thermophilic species are present (e.g., *Taxodium*, *Carya*, *Juglans*, *Nyssa*). Remains of the freshwater algae *Botryococcus* (Figure 3.2I) were found in both the Younger Dryas and the meltwater spike sediment.

The glacial sample (755 cm depth) contains much less of the mostly marine amorphous OM (not quantified). The abundance of reworked palynomorphs is even higher than in the meltwater samples (Figure 3.3, dark colored bars, and Figure 3.4). 40-50% of dinocysts and pollen grains as well as all counted spores were recognized as reworked in this sample. Examples for ancient material observed are Paleozoic spores (Figure 3.2N), Mesozoic pollen grains (e.g., *Classopollis* spp.), Upper Cretaceous dinocysts (*Isabelidinium* spp., *Dinogymnium* spp., *Palaeohystrichophora infusorioides*; Figure 3.2M, N, and P) and acritarchs (Figure 3.2L). Furthermore, many of the pollen grains of unknown (Tertiary/Quaternary) age again belong to species that are common in warm climatic zones, such as *Nyssa* or *Carya*, indicating reworking as well. In addition to reworked palynomorphs, this sample contains a higher abundance of opaque phytoclasts (Figures 3.2L and 3.4). The opaque character can be due to pyrolization and/or strong degradation. Finally, the observed broad range of different color shadings of palynomorphs also suggests diverse sources with different thermal histories.

As already mentioned, amorphous organic matter, which was not quantified here, constitutes a large part of the overall OM especially in the younger samples. This material can have both terrigenous and marine sources, which are usually distinguishable by fluorescence microscopy. Fluorescence of marine amorphous OM decreases with degradation, whereas amorphous OM of terrigenous origin shows only little fluorescence. However, we observed that the Holocene samples, which probably contain the most marine OM, exhibited almost no fluorescence, while the glacial sample displayed a wide range of different fluorescence grades. The reason could be the influence of the brine, present in Orca Basin since the early Holocene, as it can often be observed that organic matter associated with salt deposits has lost its fluorescence (unpubl. observation). The reasons for this alteration are currently unknown. Therefore, we are limited to using the relative contribution of reworked (ancient or opaque) material as indication of terrigenous input.

In summary, the kerogen analyses confirmed an increased terrigenous input during the glacial period as well as during the meltwater spike and the Younger Dryas interval (Figure 3.4). The increased terrigenous contribution in the Younger Dryas sediments indicates that the negative peak in bulk $\delta^{13}C_{org}$ values during this time, which is not accompanied by higher C/N ratios [*Meckler et al.*, submitted; see chapter 2], indeed reflects terrigenous OM instead of solely changes in terrestrial vegetation. This will be further discussed below in the context of the biomarker records. Another aspect revealed by the kerogen analyses is that much of the glacial OM is probably very old, and therefore caution should be used when interpreting bulk isotopic signatures.

3.3.2. Biomarkers

The results of the biomarker analyses (long-chain n-alkane concentrations and M/T ratios) and the compound-specific $\delta^{13}C$ values ($\delta^{13}C_{n\text{-alkanes}}$) are shown in Figure 3.5 in comparison with the bulk proxies for terrigenous input from the same core and foraminiferal $\delta^{18}O$ from neighboring core EN32-PC6 [*Leventer et al.*, 1983]. The large deglacial minimum in the $\delta^{18}O$ record indicates the interval during which a major deglacial meltwater pulse reached the Orca Basin site. The terrigenous biomarkers studied here, namely long-chain n-alkanes and n-alcohols, do not show a clear trend with time from the glacial to the Holocene (Figure 3.5; n-alcohols not shown). However, the n-alkane record exhibits high concentrations before 22 ka, a single peak at 20.5 ka, a period of large variability between 17.5 and 14.2 ka and two concentration peaks centered around 13 ka (the onset of the Younger Dryas period), and 10.5 ka, respectively. Although in lower resolution and therefore less variable, the record from nearby Pigmy Basin [*Jasper and Gagosian*, 1993] shows similar trends, including an early decrease in n-alkane concentration before the Last Glacial Maximum. In contrast to the terrigenous compounds, the concentrations of the marine biomarkers (brassicasterol and dinosterol) increase in the course of deglaciation, resulting in a positive trend in the M/T ratio (Figure 3.5). Such a trend towards increasing importance of marine OM sources would be expected based on the bulk parameter results (see below) and the kerogen analyses. Interestingly the M/T ratio exhibits a minimum at around 13 ka, coinciding with the peak in long-chain n-alkanes and therefore adding evidence for an increased terrigenous input at that time.

The carbon isotopic composition of the long-chain n-alkanes varies between -29.7 and -32.8 ‰ with no clear trend observable from the glacial to the Holocene. These values are close to the expected isotopic composition for n-alkanes from C3 plants, which are characterized by bulk $\delta^{13}C_{org}$ values of around -27‰ and an offset in n-alkanes compared to total biomass of around -6 ‰ [*Collister et al.*, 1994]. Although the low values suggest C3 plants as the main source, the significant variability indicates admixture of C4 plant material.

3.3.2.1. Comparison with bulk parameters

A comparison of the biomarker results with the bulk parameters such as TOC, C/N, $\delta^{13}C_{org}$, and %detritus (%detritus = 100% - %carbonate - %TOC), reveals several inconsistencies between the different proxies, but at the same time allows additional insight. In the glacial part before 16.8 ka, the previously observed discrepancy between C/N (being lower than during the meltwater interval) and $\delta^{13}C_{org}$ (exhibiting maximum values) was explained by either changes in terrestrial vegetation affecting $\delta^{13}C_{org}$, or inorganic N lowering C/N [*Meckler et al.*, submitted; see chapter 2]. The fact that the compound-specific $\delta^{13}C$ values are not consistently lower in

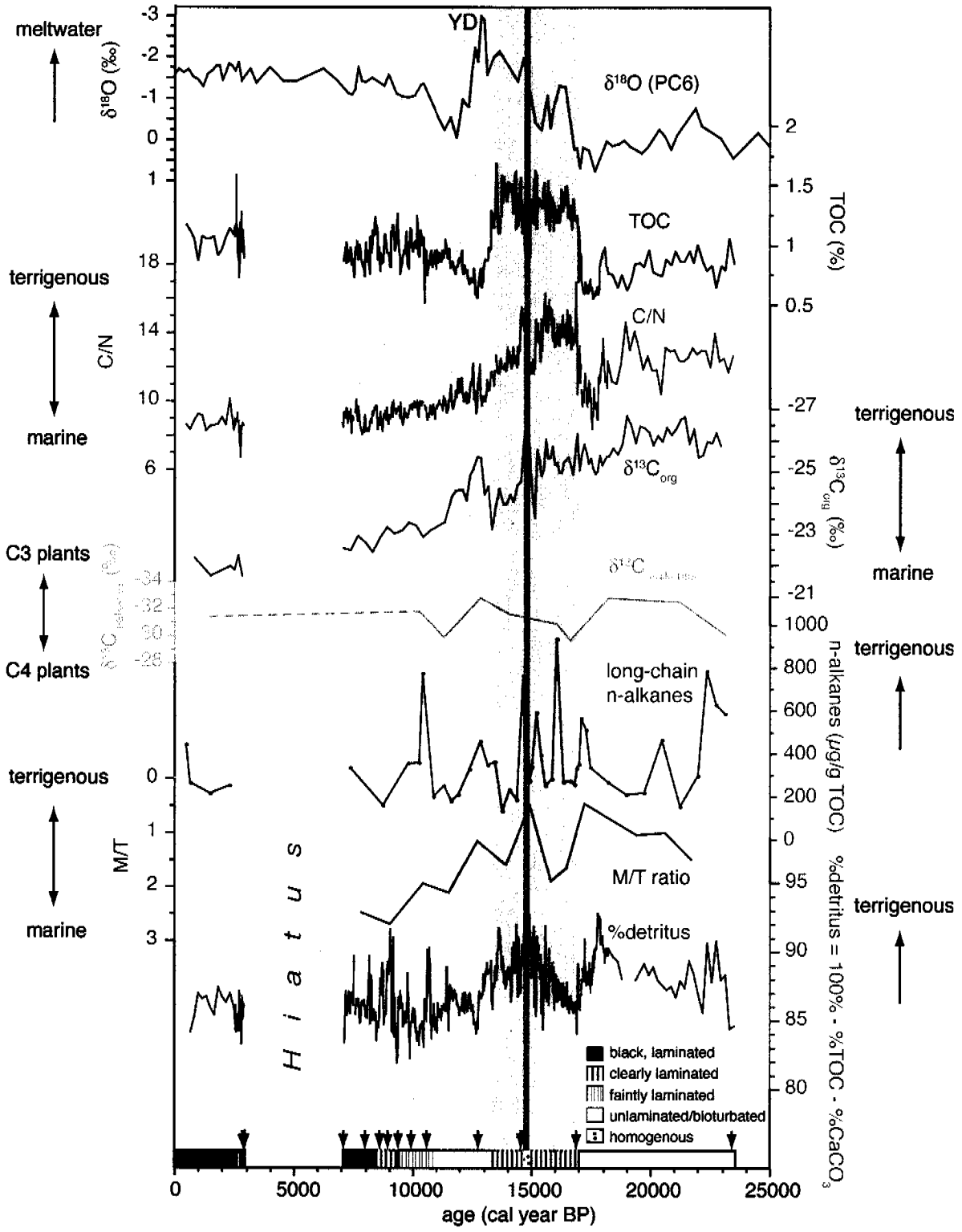

Figure 3.5. Comparison of different proxies for terrigenous input to Orca Basin together with a record of $\delta^{18}O$ from neighboring core EN32-PC6 [*Leventer et al.*, 1983]. Dashed line indicates no data due to few foraminifera. Arrows on top show ^{14}C age control for PC6. TOC concentrations as well as the bulk parameters C/N and $\delta^{13}C$ are from *Meckler et al.* [submitted; chapter 2]. Compound-specific $\delta^{13}C$ values from n-alkanes represent terrestrial vegetation changes (dashed line: unknown mid-Holocene values due to hiatus). Long-chain n-alkanes are a proxy for terrigenous OM input. M/T ratio is calculated from concentrations of different biomarkers (see text) and is a proxy for the abundance of marine versus terrigenous OM. %detritus is the siliciclastic component of the sediment. The core lithology is indicated at the bottom; black arrows (bottom) depict ^{14}C age control. YD is Younger Dryas period. Note the reversed scales for $\delta^{18}O$, $\delta^{13}C$, $\delta^{13}C_{n\text{-alkanes}}$ and M/T.

the glacial argues against the former hypothesis. At the same time, low concentrations of long-chain n-alkanes and n-alcohols contradict strong terrigenous input as an explanation for the low $\delta^{13}C_{org}$. The clue to these discrepancies in the glacial section might be the reworked and degraded nature of much of the organic material, as revealed by the optical kerogen analysis. The low bulk $\delta^{13}C_{org}$ values could be due to isotopically depleted compounds being preferentially preserved [e.g., *Benner et al.*, 1987; *Lehmann et al.*, 2002]. Diagenetic alteration leading to a decreased extractability of biomarkers could be responsible for their low yields. The comparatively low C/N values may indeed reflect a contribution of inorganic nitrogen as discussed previously.

The onset of laminations at 16.8 ka is accompanied by a sharp increase in %TOC and C/N, as well as an increase in the M/T ratio, whereas the other proxies do not show clear changes. This time corresponds to the beginning of meltwater inflow as reflected in decreasing $\delta^{18}O$ in EN32-PC6. The onset of laminations could be related to stratification in the deep part of the basin due to salt leakage, but it could also be due to the increased organic matter flux causing enhanced oxygen consumption [*Leventer et al.*, 1983]. The increase in TOC could therefore either be the cause for or the result of the anoxic conditions. Higher C/N ratios would suggest that much of the OM is terrigenous. However, low n-alkane concentrations and an increased abundance of marine biomarkers (high M/T), as well as low %detritus values at the beginning of the meltwater interval contradict such an interpretation of the high C/N ratios. Alternatively, the increase in C/N might be explained by a decreased dominance of clay-bound inorganic nitrogen relative to organic nitrogen. Therefore, the increased TOC values at this time are likely either due to better preservation under anoxic conditions or to increased marine productivity, or both. Later during the meltwater spike, in contrast, high %detritus values and the group of n-alkane peaks do indicate increased terrigenous input at least until 14.5 ka. This is only contradicted by relatively high M/T values (except for the homogenous layer, see below), which might be explained by increased local productivity due to enhanced nutrient input with the meltwater, and a lack of change in $\delta^{13}C_{org}$. It seems therefore, that both terrigenous and marine OM input increased in the course of the meltwater inflow.

All proxies indicate increased abundance of terrigenous material in the homogenous interval at around 15-14.5 ka, which had been shown to contain a large amount of reworked nannofossils [*Marchitto and Wei*, 1995]. Based on $\delta^{18}O$ records from deep dwelling foraminifera, which revealed a pronounced $\delta^{18}O$ minimum at this time, *Aharon* [2006] argued that meltwater was entrained as a subsurface flow, as a result of increased density due to a large suspended sediment load. If this sediment reached Orca Basin, it might be an explanation for the homogeneity and terrigenous character of this interval of the core. The time of this input corresponds to the so-called meltwater pulse 1-A observed in sea level records [*Fairbanks*, 1989] as a rapid increase in global sea level, thought to have originated from the Laurentide ice sheet.

After the homogenous interval, at 14.5 ka, the drop in C/N, bulk $\delta^{13}C_{org}$, and n-alkane concentrations despite continued meltwater input (low $\delta^{18}O$) might represent decreased terrigenous input due to an increase in distance to the Mississippi River mouth with this sudden rise in sea level. The fact that TOC concentrations remained high could reflect a marine productivity maximum associated with the edge of the low-salinity plume, as proposed by *Jasper and Gagosian* [1993]. However, the low $\delta^{18}O$ based on local foraminifera indicates that Orca Basin was still well in the reach of the meltwater plume. Furthermore, the fact that the M/T ratio does not show a peak at this time argues against this interpretation. Instead, one possible explanation is that peak sediment input was associated with beginning and increasing meltwater flux, when erodable material was most abundant on land. This is augmented by the likely connection of the meltwater pulses to sudden outlet failures of proglacial lakes, which should have resulted in great erosive capacity. The later part of the meltwater pulse could therefore have transported much less material to the Gulf.

3.3.2.2. The n-alkane record: Evidence for transport patterns?

The event-like nature of the n-alkane record contrasts both the sustained shifts in the other proxies for terrigenous input and the smooth salinity record from Orca Basin. Interestingly, however, the n-alkane record resembles in several intervals the stacked $\delta^{18}O$ record from the northern Gulf [*Aharon*, 2003] more than the $\delta^{18}O$ data from Orca Basin (Figure 3.6). Taking both the n-alkane and the stacked $\delta^{18}O$ record at face value, their agreement could potentially indicate that the $\delta^{18}O$ record from Orca Basin is not representative for the meltwater input to the Gulf of Mexico. However, the stacked record has to be interpreted carefully, as the individual records that were combined show some discrepancies, especially during the deglacial meltwater interval (c.f. Fig. 2 in *Aharon* [2003]) and most of the cores have only crude independent age control. This could account for some of the spikiness in the stacked $\delta^{18}O$ record in contrast to the Orca Basin $\delta^{18}O$ record. Nonetheless, some of the discrepancies in the $\delta^{18}O$ record from Orca Basin and the stacked record might be due to low-salinity plumes being too small during times of intermediate meltwater input to be recorded by the foraminifera at the Orca Basin site, whereas the more shoreward sites witness a signal. This could for example be the case for the early Holocene minimum in $\delta^{18}O$ of the stacked record, which coincides with a peak in n-alkanes and % detritus in Orca Basin at around 10.5 ka. These signals could be associated with a brief episode of meltwater flux through the Mississippi after the Marquette readvance, as suggested for example by *Fisher et al.* [2003]. If so, the lack of change in Orca Basin $\delta^{18}O$ would suggest that terrigenous sediment was transported further than the low salinity plume. However, as none of the other proxies in Orca Basin record this input, however, it was probably not of very large magnitude.

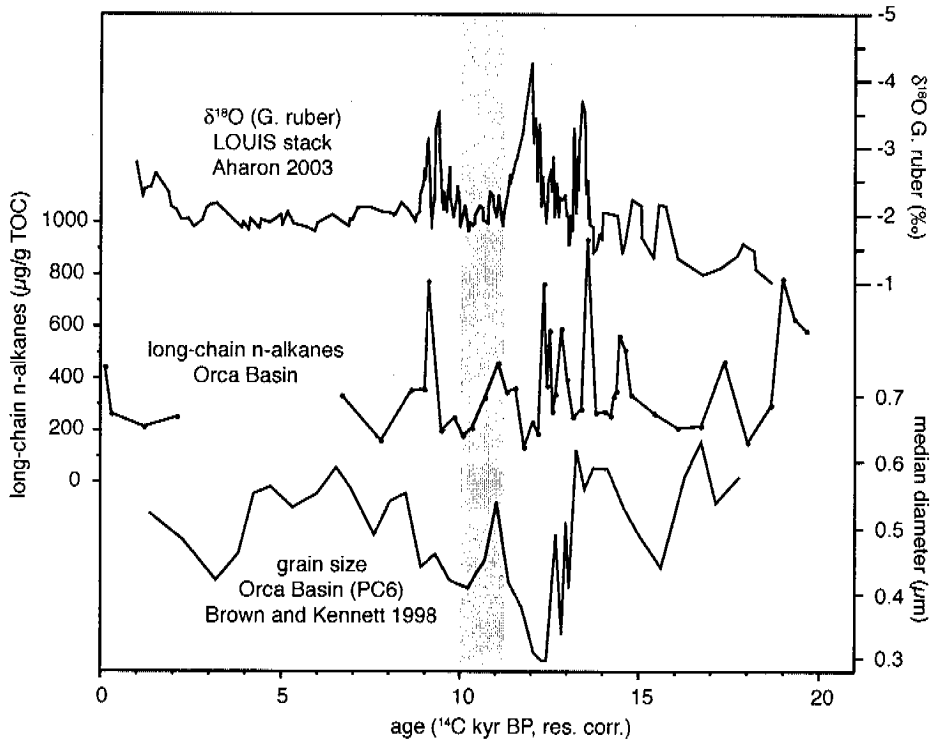

Figure 3.6. The Orca Basin n-alkane record (middle, this study) in comparison with a stacked record of G. ruber d18O from the northern Gulf of Mexico (top) [*Aharon*, 2003] and median grain sizes in Orca Basin core EN32-PC6 (bottom) [*Brown and Kennett*, 1998], which is located next to MD02-2550 used for this study. The stacked record was slightly modified by averaging multiple data with the same age. Ages are in radiocarbon years, corrected for a 400 year reservoir effect.

The differences in the two $\delta^{18}O$ records during the peak phase of meltwater input, reflected in the large negative $\delta^{18}O$ anomaly in Orca Basin, cannot be explained this way and might be due to artifacts in the stacked record. Therefore, the decoupling of the long-chain n-alkane record from the other proxy records and from the much smoother $\delta^{18}O$ record from the neighboring core EN32-PC6 still require an explanation. As discussed above, peak sediment transport is probably associated with the beginning of meltwater fluxes, which could account for some of the spikiness in the n-alkane record. Furthermore, input of terrigenous material could be occasionally decoupled from the surface salinity signal recorded by the foraminifera if meltwater input occurred at depth in the form of turbidity plumes, as argued by *Aharon* [2006] for the homogenous interval in MD02-2550 (see discussion above). Both of these hypotheses can explain a decoupling of terrigenous input and surface salinity. However, for both processes one would expect to see similar signals in n-alkanes and bulk proxies for terrigenous input ($\delta^{13}C_{org}$, C/N, %detritus), which is not the case. Instead, the bulk proxy records are much smoother compared to the record of long-chain n-alkane concentration. Hence, if the n-alkane concentration peaks reflect real input changes, additional factors have to account for the difference to the bulk parameters. Preferential preservation of the refractory n-alkanes could affect their concentration independently of the bulk parameters, but one would expect trends or shifts (if

redox condition changes in the basin were important) rather than spikes. However, a possible way to explain this discrepancy between the different proxies for terrigenous input is an association of n-alkanes with a certain (coarser) size fraction of terrigenous material, giving rise to hydrodynamic sorting [*Prahl*, 1985; *Jasper and Gagosian*, 1993]. Surface sediment studies on the Louisiana shelf have also indicated that preferentially soil derived, small-grained OM is transported to the deeper parts of the Gulf, whereas coarser, lignin-rich particles are deposited close to shore [*Goni et al.*, 1998; *Gordon and Goni*, 2004]. If this mechanism also played a role during transport to Orca Basin, one would expect long-chain n-alkanes to be preferentially associated with coarser particles. Indeed, the record of n-alkane concentrations agrees reasonably well with the grain size record from neighboring core EN32-PC6 [*Brown and Kennett*, 1998] (Figure 3.6).

3.3.2.3. Terrigenous input during the Younger Dryas

At the time of the Younger Dryas period, meltwater input had ceased according to the $\delta^{18}O$ data, which should imply a concurrent decrease in the input of terrigenous material. Indeed, in this interval TOC concentrations are low and C/N ratios almost at Holocene values, suggesting dominantly marine OM, and %detritus values are low. In contrast, bulk $\delta^{13}C_{org}$ exhibits a negative peak, which could reflect increased terrigenous input or a change in vegetation on land. However, the latter interpretation is not fully supported by the isotopic composition of n-alkanes. Although n-alkane $\delta^{13}C$ is low, it is not much lower than in the Holocene. Furthermore, evidence for increased terrigenous input at the beginning of the Younger Dryas comes from a peak in terrestrially derived long-chain n-alkanes and a minimum in the M/T ratio. As revealed by the kerogen composition, reworked OM input was also clearly present in this interval. Finally, a peak in grain size is evident in core EN 32-PC6 (Figure 3.6). Therefore, the combination of the evidence from diverse proxies suggests increased terrigenous input at the beginning of the Younger Dryas.

The evidence of high terrigenous input at this time is surprising, as geomorphologic evidence from the North American continent suggests that the deglacial meltwater was diverted eastwards and therefore away from the Mississippi River at around 10.9 ^{14}C ka, corresponding to 12.9 calendar ka [*Fisher*, 2003; *Teller et al.*, 2005, and references therein]. Furthermore, the high values of foraminiferal $\delta^{18}O$ in both the Orca Basin record and the stacked record argue against meltwater input at that time, and sea level rise had increased the distance to the sediment source. At present, we therefore cannot explain the increased abundance of terrigenous OM during the first half of the Younger Dryas period. However, differences between the early and the late phase of the Younger Dryas were also observed for sea surface temperatures (SST), reconstructed based on foraminiferal Mg/Ca ratios in Orca Basin sediments [*Flower et al.*,

2004]. The first part of the Younger Dryas was characterized by high SST, with a sudden drop at 12.3 ka, which could not be explained. The warm conditions in the early Younger Dryas were probably restricted to the surface water, as cooling at the beginning of the Younger Dryas is suggested by foraminiferal assemblage data [*Kennett et al.*, 1985]. In our records, this warm interval coincides with the peak in long-chain n-alkane concentrations and the lowest bulk $\delta^{13}C_{org}$ values.

It becomes clear from the additional information on terrigenous input that the sequence of events in the Gulf of Mexico during the Younger Dryas episode is not yet understood. An open question is for example, whether deglacial meltwater, albeit in smaller amounts, continued flowing into the Gulf of Mexico. Similarly, the routing of the main meltwater volume in the north as well as the occurrence of a sudden outburst of glacial Lake Agassiz at the beginning of the Younger Dryas period are still a matter of ongoing debate [e.g., *Teller et al.*, 2005, and subsequent discussion in QSR]. As these questions have potentially large implications for the thermohaline circulation [*Broecker et al.*, 1989], more work is clearly needed.

3.4. Conclusions

In this study, we took a combined optical and biomarker approach to determine the nature of organic matter in Orca Basin, with the aim to assess the contribution of terrigenous OM. The results added valuable insights to the existing bulk proxy records, namely C/N and $\delta^{13}C_{org}$ [*Meckler et al.*, submitted; see chapter 2], but also revealed some discrepancies that need further study.

The results confirmed that in the glacial section of the core, the contribution of terrigenous OM was much larger than in the Holocene. In addition, we found that much of the OM was reworked (of Cretaceous age or older). This could influence bulk $\delta^{13}C_{org}$ values and biomarker yields, due to preferential preservation of isotopically depleted compounds and decreased extractability of biomarkers, respectively.

In contrast, sedimentary organic matter in the Holocene part of the core is mainly of marine origin and exceptionally well preserved. The only exception may be a short early Holocene peak in n-alkane concentration centered around 10.5 ka, possibly associated with a brief episode of meltwater influx after a glacial re-advance. However, as the signal is not reflected in the other proxies for terrigenous OM, its significance is unclear. With respect to the applicability of bulk nitrogen isotopes, this study confirms that the Holocene section of the core is well suited for inferring marine ecosystem variations, whereas in the glacial part the signal has most probably been influenced by the large input of old terrigenous material.

The compound-specific $\delta^{13}C$ measurements on terrestrially derived n-alkanes suggest that changes in the relative abundance of C3 and C4 plants are not responsible for the deglacial decrease in $\delta^{13}C_{org}$, as was previously hypothesized.

The deglacial meltwater interval, defined by a minimum in seawater $\delta^{18}O$ as proxy for salinity, is characterized by generally high terrigenous input. However, in some aspects the different parameters yielded equivocal results. While the bulk parameters (C/N, $\delta^{13}C_{org}$, %detritus) show a sustained response during most of the meltwater input, the long-chain n-alkane concentrations are variable, which might be caused by hydraulic particle sorting. Towards the end of the meltwater input period, the link between salinity and the abundance of terrigenous material is not always straightforward. The end of the deglacial peak in freshwater inflow inferred from low seawater $\delta^{18}O$ values was associated with decreasing input of terrigenous material. One explanation could be that the rising sea level moved the sediment source further away from Orca Basin. Alternatively and more likely, it reflects the association of peak sediment load with the beginning of meltwater pulses. In contrast, terrestrial input apparently increased again at the beginning of the Younger Dryas period, although salinity was high, a finding for which we have currently no explanation. However, it might indicate that the timing (and magnitude) of meltwater flux into the Gulf of Mexico during the Younger Dryas interval is not yet fully understood.

Acknowledgements

We would like to thank Laurent Labeyrie, Yvon Balut, and the crew of R/V *Marion Dufresne* for a successful cruise in the Gulf of Mexico. We are furthermore grateful to J. Lipp for assistence with lipid extractions. ANM thanks K.-U. Hinrichs for the opportunity to use the facilities at Bremen University. This work was funded by the Swiss National Science Foundation.

References

Addy, S. K., and E. W. Behrens (1980), Time of Accumulation of Hypersaline Anoxic Brine in Orca Basin (Gulf of Mexico), *Mar. Geol.*, *37*, 241-252.

Aharon, P. (2003), Meltwater flooding events in the Gulf of Mexico revisited: Implications for rapid climate changes during the last deglaciation, *Paleoceanography*, *18*, 1079, doi:10.1029/2002PA000840.

Aharon, P. (2006), Entrainment of meltwaters in hyperpycnal flows during deglaciation super-floods in the Gulf of Mexico, *Earth Planet. Sc. Lett.*, *241*, 260-270.

Benner, R., M. L. Fogel, E. K. Sprague, and R. E. Hodson (1987), Depletion of C-13 in Lignin and Its Implications for Stable Carbon Isotope Studies, *Nature*, *329*, 708-710.

Broecker, W. S., J. P. Kennett, B. P. Flower, J. T. Teller, S. Trumbore, G. Bonani, and W. Wolfli (1989), Routing of Meltwater from the Laurentide Ice-Sheet During the Younger Dryas Cold Episode, *Nature*, *341*, 318-321.

Brown, P. A., and J. P. Kennett (1998), Megaflood erosion and meltwater plumbing changes during last North American deglaciation recorded in Gulf of Mexico sediments, *Geology*, *26*, 599-602.

Collister, J. W., G. Rieley, B. Stern, G. Eglinton, and B. Fry (1994), Compound-Specific Delta-C-13 Analyses of Leaf Lipids from Plants with Differing Carbon-Dioxide Metabolisms, *Org. Geochem.*, *21*, 619-627.

Eglinton, G., and R. J. Hamilton (1967), Leaf Epicuticular Waxes, *Science*, *156*, 1322-&.

Fairbanks, R. G. (1989), A 17,000-Year Glacio-Eustatic Sea-Level Record - Influence of Glacial Melting Rates on the Younger Dryas Event and Deep-Ocean Circulation, *Nature*, *342*, 637-642.

Fisher, T. G. (2003), Chronology of glacial Lake Agassiz meltwater routed to the Gulf of Mexico, *Quaternary Research*, *59*, 271-276.

Flower, B. P., D. W. Hastings, H. W. Hill, and T. M. Quinn (2004), Phasing of deglacial warming and laurentide ice sheet meltwater in the Gulf of Mexico, *Geology*, *32*, 597-600.

Goni, M. A., K. C. Ruttenberg, and T. I. Eglinton (1998), A reassessment of the sources and importance of land-derived organic matter in surface sediments from the Gulf of Mexico, *Geochim. Cosmochim. Acta*, *62*, 3055-3075.

Gordon, E. S., and M. A. Goni (2004), Controls on the distribution and accumulation of terrigenous organic matter in sediments from the Mississippi and Atchafalaya river margin, *Mar. Chem.*, *92*, 331-352.

Jasper, J. P., and R. B. Gagosian (1990), The Sources and Deposition of Organic-Matter in the Late Quaternary Pygmy Basin, Gulf of Mexico, *Geochim. Cosmochim. Acta*, *54*, 1117-1132.

Jasper, J. P., and R. B. Gagosian (1993), The Relationship between Sedimentary Organic-Carbon Isotopic Composition and Organic Biomarker Compound Concentration, *Geochim. Cosmochim. Acta*, *57*, 167-186.

Kennett, J. P., K. Elmstrom, and N. Penrose (1985), The Last Deglaciation in Orca Basin, Gulf of Mexico - High-Resolution Planktonic Foraminiferal Changes, *Palaeogeography Palaeoclimatology Palaeoecology*, *50*, 189-216.

Lehmann, M. F., S. M. Bernasconi, A. Barbieri, and J. A. McKenzie (2002), Preservation of organic matter and alteration of its carbon and nitrogen isotope composition during simulated and in situ early sedimentary diagenesis, *Geochim. Cosmochim. Acta*, *66*, 3573-3584.

Leventer, A., D. F. Williams, and J. P. Kennett (1983), Relationships between Anoxia, Glacial Meltwater and Microfossil Preservation in the Orca Basin, Gulf of Mexico, *Mar. Geol.*, *53*, 23-40.

Marchitto, T. M., and K. Y. Wei (1995), History of Laurentide Meltwater Flow to the Gulf-of-Mexico During the Last Deglaciation, as Revealed by Reworked Calcareous Nannofossils, *Geology*, *23*, 779-782.

Newman, J. W., P. L. Parker, and E. W. Behrens (1973), Organic Carbon Isotope Rations in Quaternary Cores from Gulf of Mexico, *Geochim. Cosmochim. Acta*, *37*, 225-238.

Northam, M. A., D. J. Curry, R. S. Scalan, and P. L. Parker (1981), Stable Carbon Isotope Ratio Variations of Organic-Matter in Orca Basin Sediments, *Geochim. Cosmochim. Acta*, *45*, 257-260.

O'Leary, M. H. (1988), Carbon Isotopes in Photosynthesis, *Bioscience*, *38*, 328-336.

Poulicek, M., and C. Jeuniaux (1991), Chitin Biodegradation in Marine Environments - an Experimental Approach, *Biochemical Systematics and Ecology*, *19*, 385-394.

Prahl, F. G. (1985), Chemical Evidence of Differential Particle Dispersal in the Southern Washington Coastal Environment, *Geochim. Cosmochim. Acta*, *49*, 2533-2539.

Sackett, W. M., J. M. Brooks, B. B. Bernard, C. R. Schwab, H. Chung, and R. A. Parker (1979), Carbon Inventory for Orca Basin Brines and Sediments, *Earth Planet. Sc. Lett.*, *44*, 73-81.

Shokes, R. F., P. K. Trabant, B. J. Presley, and D. F. Reid (1977), Anoxic, Hypersaline Basin in Northern Gulf of Mexico, *Science*, *196*, 1443-1446.

Teller, J. T., M. Boyd, Z. R. Yang, P. S. G. Kor, and A. M. Fard (2005), Alternative routing of Lake Agassiz overflow during the Younger Dryas: new dates, paleotopography, and a re-evaluation, *Quaternary Science Reviews*, *24*, 1890-1905.

Traverse, A. (1988), *Paleopalynology*, 600 pp., Unwin Hyman, Boston.

Tyson, R. V. (1995), *Sedimentary organic matter. Organic facies and palynofacies*, 615 pp., Chapman & Hall, London.

Volkman, J. K. (1986), A Review of Sterol Markers for Marine and Terrigenous Organic-Matter, *Org. Geochem.*, *9*, 83-99.

Seite Leer /
Blank leaf

Chapter 4

Detailed sedimentary N isotope records from Cariaco Basin for Terminations I and V: Local and global implications*

Abstract

For the last deglaciation and Termination V (the initiation of MIS 11 at around 430 ka), we report high-resolution sedimentary nitrogen isotope ($\delta^{15}N$) records from Cariaco Basin in the Caribbean Sea. During both terminations, the previously reported interglacial decrease in $\delta^{15}N$ clearly lags local changes such as water column anoxia as well as global increases in denitrification by several thousand years. On top of the glacial-interglacial change, several $\delta^{15}N$ peaks were observed during the last deglaciation. The deglacial signal in Cariaco Basin can be best explained as a combination of 1) local variations in suboxia and water column denitrification as the reason for the millennial-scale peaks, 2) a deglacial maximum of mean ocean nitrate $\delta^{15}N$, and 3) increasing N_2 fixation in response to globally increased denitrification causing the overall deglacial $\delta^{15}N$ decrease. In the Holocene, much of the decrease in $\delta^{15}N$ occurred between 6 and 3 ka, coinciding with an expected precession-modulated increase in African dust transport to the (sub)tropical North Atlantic and the Caribbean. This begs the hypothesis that N_2 fixation in this region increased in response to interglacial maxima in denitrification elsewhere but that this response strengthened with increased mid-Holocene iron input. It remains to be seen whether data for MIS 11 support this interpretation.

*submitted to *Global Biogeochemical Cycles* as A.N. Meckler, G.H. Haug, D.M. Sigman, B. Plessen, L.C. Peterson, H.R. Thierstein, Detailed sedimentary N isotope records from Cariaco Basin for Terminations I and V: Local and global implications.

4.1. Introduction

In many parts of the ocean, the availability of nitrogen is an important control on primary productivity. Marine productivity, in turn, influences the atmospheric CO_2 content and therefore indirectly the global climate. With regard to the large glacial-interglacial variations in atmospheric CO_2 content, the question of whether the size of the marine nitrogen pool varied on these timescales therefore becomes important.

The main source of nitrogen to the ocean is N_2 fixation, whereas denitrification is its largest sink. Denitrification occurs both in the water column where it is suboxic, such as in the Eastern Tropical North and South Pacific and the Arabian Sea, and in sediments. Despite its importance for the global climate, the nitrogen budget and its regulation are not yet understood. Several factors affect the individual processes. Globally, denitrification rates depend on organic matter fluxes as well as the ventilation of intermediate waters and probably the areal extent of the shelves [*Christensen*, 1994]. Diazotrophic organisms, on the other hand, seem to depend on the availability of iron and/or phosphorus [*Kustka et al.*, 2003; *Mills et al.*, 2004], besides requiring specific light and temperature conditions [*LaRoche and Breitbarth*, 2005]. In addition, it has been proposed that the two processes constitute a feedback: When global denitrification increases, the availability of nitrogen with respect to phosphate decreases, which might make diazotrophic organisms more competitive, leading to an increase in N_2 fixation [*Redfield et al.*, 1963; *Haug et al.*, 1998; *Tyrrell*, 1999].

Both denitrification and N2 fixation can be traced back in time using the isotopic composition of organic nitrogen in sediments. Denitrification results in the preferential loss of ^{14}N, causing the remaining nitrate pool to become progressively enriched in ^{15}N. In systems where some nitrate remains (i.e., most water column settings), the enriched nitrate can be consumed by phytoplankton so that the denitrification signal is recorded in the sediments. The preferential loss of ^{14}N during water column denitrification results in a mean oceanic nitrate $\delta^{15}N$ that is greater than 0‰ (i.e. greater than atmospheric N_2; ($\delta^{15}N$ (‰) = (($^{15}N/^{14}N$ of sample / $^{15}N/^{14}N$ of air) – 1) * 1000)). Its value is mainly controlled by the relative importance of water column and sedimentary denitrification [*Brandes and Devol*, 2002], with the overall rate of denitrification and the size of the nitrate pool as secondary influences [*Deutsch et al.*, 2004]. N_2 fixation introduces fixed N with a $\delta^{15}N$ of ~0-2‰ [*Wada and Hattori*, 1991], which is lower than that of ocean nitrate, so that N_2 fixation inputs may be recorded in sediment records.

A number of high-resolution sedimentary nitrogen isotope records for the last deglaciation exist from denitrification zones, displaying increases in $\delta^{15}N$ after the last glacial maximum [e.g., *Altabet et al.*, 1995; *Ganeshram et al.*, 1995; *Pride et al.*, 1999; *Emmer and Thunell*, 2000; *De Pol-Holz et al.*, 2006], suggesting that the global rate of water column denitrifica-

tion is stronger during interglacials. In contrast, low-resolution records from the South China Sea do not exhibit glacial-interglacial variability and have been interpreted to reflect an unchanged isotopic composition of mean ocean nitrate [*Kienast*, 2000]. These observations can only be explained if feedback mechanisms prevent large changes in the marine nitrogen budget [*Deutsch et al.*, 2004]. One possibility is the N_2 fixation feedback mentioned above. The other potential feedback involves denitrification itself, an increase in which could reduce nitrate supply to the surface ocean and thus primary productivity, leading to decreased oxygen demand for organic matter remineralization [*Codispoti*, 1989]. To assess the importance of these proposed feedbacks, records from N_2 fixation areas are needed. However, diagenetic overprints have been reported from sediments in low-accumulation rate settings with oxygenated bottom waters [*Altabet and Francois*, 1994; *Sigman*, 1997]. Unfortunately, such conditions characterize most regions where N_2 fixation is prominent and the signal not overprinted by denitrification. However, there are exceptions. An N isotope record from anoxic Orca Basin in the Gulf of Mexico indicates that N_2 fixation in that region was similar or weaker in the glacial as compared to present conditions [*Meckler et al.*, submitted; see chapter 2]. Interference by strongly increased input of terrigenous material during glacial times, however, did not permit a more precise assessment from that record.

4.2. Study site

Another site with anoxic bottom water located in a region with current N_2 fixation is Cariaco Basin in the Caribbean Sea off Venezuela (Figure 4.1). The present N cycle in this basin has been studied [*Thunell et al.*, 2004], providing a basis for assessing past changes. Cariaco Basin is a semi-enclosed coastal basin that is up to 1400 m deep, separated from the open Caribbean by a sill with a maximum depth of 145 m. The bottom water of the basin is anoxic below around 300 m, and strong denitrification occurs in the water column just above this depth [*Thunell et al.*, 2004] (Figure 4.2). The oxic/anoxic interface is sharp, leading to very slow exchange with overlying waters. As a result, the entire nitrate is consumed at the interface, such that no ^{15}N enrichment is observed in the overlying thermocline. Sinking flux and surface sediments record low $\delta^{15}N$ values typical for the subtropical North Atlantic thermocline nitrate [*Knapp et al.*, 2005], reflecting the importance of N_2 fixation in the region and/or the basin itself.

The geographic location of Cariaco Basin at the current northern boundary of the seasonal movement of the Intertropical Convergence Zone (ITCZ) results in two distinct seasons: a rainy season in late summer/fall and a dry season with strong, trade wind-induced upwelling in winter/spring. The nutrient supply during the upwelling season stimulates high productivity dominated by diatoms [*Woodworth et al.*, 2004].

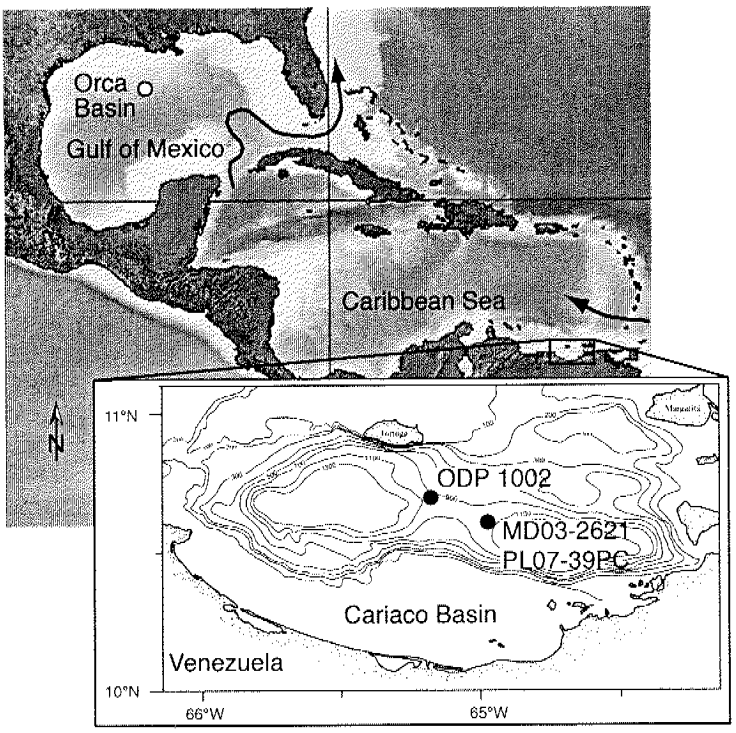

Figure 4.1. Map of the Cariaco Basin, located off Venezuela in the Caribbean Sea. Arrows depict major surface currents. Closed symbols correspond to the locations of the cores used for this study. Isobaths are in meter below sea level. Also indicated is the location of a core from Orca Basin in the Gulf of Mexico used for comparison.

The conditions in Cariaco Basin were very different during glacial times, when sea level was up to 120 m lower than today. Under such circumstances, only a shallow connection remained to the open Caribbean, isolating the basin from the dense and nutrient-rich thermocline water outside. Bioturbated sediments and benthic fauna are found in those intervals, indicating oxygenated bottom waters [*Peterson et al.*, 1991] and implying that there was probably no water column denitrification in the basin during glacial times.

In an earlier study on sedimentary N isotope variations in Cariaco Basin [*Haug et al.*, 1998], lower $\delta^{15}N$ was observed in interglacial sections as compared to sediments from glacial times. It was suggested that the low interglacial values are caused by increased N_2 fixation in response to increased denitrification. A question remaining in that study was, however, whether such a feedback worked locally or globally, i.e. whether the local or the global deglacial increase in denitrification triggered N_2 fixation in the basin and/or the surrounding area. In order to address this question, we are focusing on two terminations in detail, namely the last deglaciation (Termination I) and Termination V at approximately 430 kyrs before present (ka). Thereby, we assess details of the deglacial decreases in $\delta^{15}N$ and, for Termination I, compare those changes to the large body of other proxy data available for Cariaco Basin.

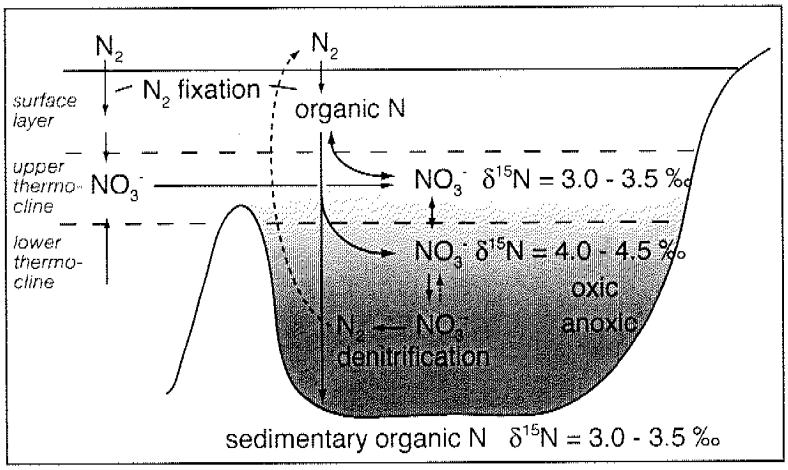

Figure 4.2. The present-day nitrogen cycle in the Cariaco Basin. Isotopic composition of nitrate and surface sediments are taken from *Thunell et al.* [2004]. A significant source of fixed nitrogen is local and/or regional N_2 fixation, reflected in the low $\delta^{15}N$ values of surface nitrate. Strong denitrification occurs in the anoxic bottom waters but currently has only little impact on thermocline nitrate due to almost complete transformation of nitrate to N_2. Surface sediments faithfully record the isotopic composition of surface nitrate.

4.3. Materials and Methods

For this study we used two cores from Cariaco Basin. To examine Termination V, samples were taken from the deep part of ODP core 1002C (119-123 m composite depth) every 2 cm. This core was located on the western side of the central ridge in the basin at around 900 m depth (Figure 4.1). For the last deglaciation, we used core MD03-2621, taken in 2003 during IMAGES cruise XI (PICASSO) from the eastern side of the central ridge (10°40.69 N, 64°58.29 W) at a water depth of around 850 m. Samples were taken every other cm in the upper 12 m of the core.

The sediment in the sampled sections of core MD03-2621 looks very similar to that from other Cariaco Basin cores. In the glacial sections, the sediment appears homogenous and shows signs of bioturbation. A bright blue clay layer occurrs from 8.8-8.3 m depth (centered around 16 ka). The abrupt onset of distinct laminations was observed at 7.9 m depth (14.5 ka), with subsequently lighter sediment color and increased varve thickness between 6.6 m and 5.0 m (corresponding to the Younger Dryas period). Above 5.0 m, the again darker varves become thinner and less distinct, although laminations are present until the top of the core.

Total nitrogen (TN) content and $\delta^{15}N$ were measured with a *Carlo-Erba CN2500* elemental analyzer on-line to a *Thermo-Finnigan DELTAplusXL* mass spectrometer using the reference standards IAEA N1 and N2. For core MD03-2621, roughly one quarter of the samples were measured at least twice, whereas for core 1002, all samples were measured in duplicate. Precision was in most cases better than ± 0.2 ‰ (1 SD) for $\delta^{15}N$ and better than ± 5% of the mean value

for TN. In core MD03-2621, concentrations of total organic carbon (TOC, in weight percent) were determined on acidified samples weighed into silver cups and subsequently dried at 70°C without rinsing. The samples were measured on a *Eurovector* elemental analyzer with a precision of ± 5 % of the mean.

The age model for ODP core 1002C was constructed by correlating *G. ruber* $\delta^{18}O$ from this core [*Peterson et al.*, 2000] to a global stack of benthic foraminiferal $\delta^{18}O$ [*Lisiecki and Raymo*, 2005]. The data and tie-points are shown in Figure 4.3. For the investigated sections of MD03-2621, the age model is based on visual correlation of several parameters to well-dated neighboring cores: Shipboard-obtained lightness data and Ti content measured by XRF-scanning were correlated to grayscale and Ti, respectively, from core 1002, and TOC was correlated to TOC from core PL07-39PC. These correlations were performed simultaneously using the software AnalySeries V2.0 [*Paillard et al.*, 1996].

4.4. Results

The TOC record from core MD03-2621 (Figure 4.3) agrees very well with that obtained previously for core PL07-39PC [*L. Peterson*, unpublished data], which allowed using it for constructing the age model. After 20 ka, TOC decreases from its glacial value of 3 % to a minimum of 0.5 %, which coincides with the blue clay layer. At 14.5 ka, the onset of the Bølling period, a rapid increase to ~ 5.5 % can be seen, concurrent with the onset of clear laminations in the core. TOC stays high, although variable, until the onset of the Younger Dryas period, when it suddenly drops to 2.5 %. However, as earlier studies showed [*Peterson et al.*, 1991; *Hughen et al.*, 1996], sedimentation rates triple during the Younger Dryas, leading to a peak in organic carbon accumulation rates, which will be discussed later. The end of the Younger Dryas coincides again with a rapid increase of TOC to values similar to the Bølling/Allerød interval, staying high until about 9 ka. A minimum with TOC concentrations around 4.0 % is observed for the early Holocene until around 6.5 ka, after which concentrations steadily increase to a present-day value of 5.8 %.

Like TOC, $\delta^{15}N$ is relatively constant until 20 ka (Figure 4.3), with values between 4.5 and 5.0 ‰. After 20 ka, a peak occurs with maximum $\delta^{15}N$ values of 7.5 ‰ at 17 ka, the increase being first gradual and then abrupt. Following a rapid decrease to glacial values in the clay layer, $\delta^{15}N$ increases again sharply with the onset of laminations to around 6.5 ‰. Values are lower during the Younger Dryas, with lowest values (around 5.0 ‰) in the first half of this interval and a step-like increase to 5.5 ‰ in the second half. At the end of the Younger Dryas, $\delta^{15}N$ increases to a third peak of around 6.4 ‰, with a very short maximum of 8.0 ‰ at 11.4 ka.

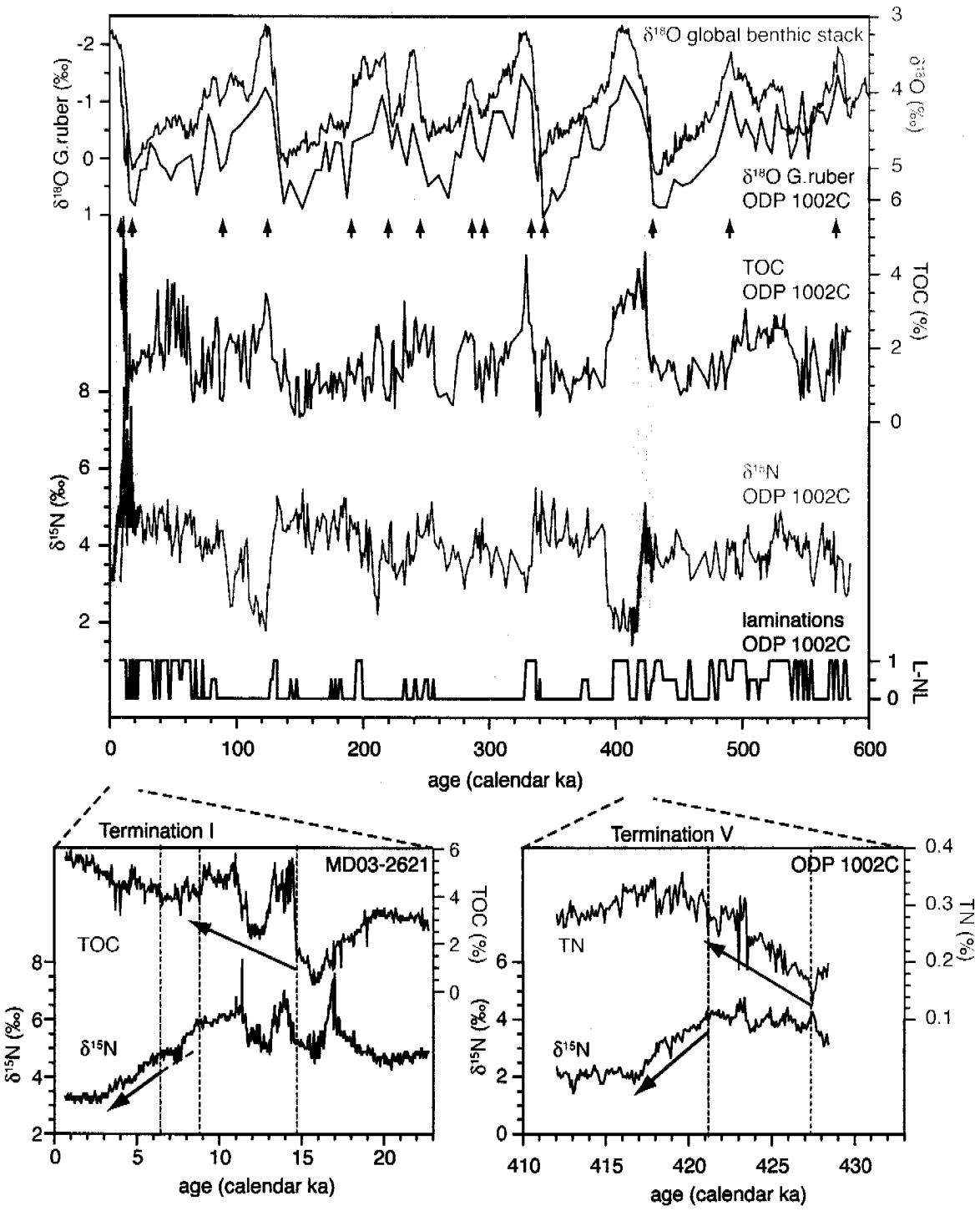

Figure 4.3. Cariaco Basin low- and high-resolution records. Upper panel: $\delta^{18}O$ of *G. ruber* [*Peterson et al.*, 2000] in comparison with a global benthic $\delta^{18}O$ stack [*Lisiecki et al.*, 2004] used for tuning (black arrows are tiepoints). Low-resolution TOC and $\delta^{15}N$ records and lamination data (1 = laminated) are from *Haug et al.* [1998]. Lower panels: High-resolution data from core MD03-2621 and ODP core 1002C.

Afterwards, a stepwise decrease is observed during the Holocene, with more rapid decreases at around 8 ka, 6-5 ka, and 3 ka. Between 7.5 and 6 ka, a plateau with values similar to those from the glacial (around 4.8 ‰) can be noticed. Since around 3 ka, $\delta^{15}N$ has been steady at 3.3 ‰.

Due to the peaks in both TOC and $\delta^{15}N$ during the Bølling/Allerød and the Preboreal, it is not clear exactly where the deglacial increase in TOC and the decrease in $\delta^{15}N$ begin. Nonetheless, it becomes obvious that the $\delta^{15}N$ decrease occurs several thousand years later than the TOC increase and certainly much later than the onset of laminations, which indicate the deglacial turning point in local hydrographic conditions.

For Termination V, the onset of the deglacial changes is easier to determine because peaks, which can also be observed for this earlier deglaciation, are much less pronounced (Figure 4.3). TN (which covaries with TOC) starts to increase around 6 kyrs before the decrease of $\delta^{15}N$. In these sections of core 1002C, laminations are much less developed than for the last deglaciation, which makes a comparison of the $\delta^{15}N$ signal to periods of anoxia more difficult. However, it seems that during this termination, laminations begin before the increase in TOC and are interrupted by short non-laminated intervals during the interglacial. Compared to Termination I, $\delta^{15}N$ is around 1 ‰ lower, but both the magnitude and the duration of the deglacial $\delta^{15}N$ decrease are surprisingly similar during the two terminations. Features analogous to the mid-Holocene plateau and the constant late Holocene $\delta^{15}N$ are apparent during marine isotope stage (MIS) 11 as well.

4.5. Discussion

4.5.1. Glacial-interglacial variability

The observed time lag between changes in TOC or TN and $\delta^{15}N$ of several kyrs implies that the lower interglacial $\delta^{15}N$ is not due to changes in local processes, such as local denitrification, diagenetic overprint, or nutrient utilization, as has already been argued by [*Haug et al.*, 1998]. Such changes would all have been closely associated with sea level rise and anoxia, which clearly precedes the $\delta^{15}N$ decrease. A varying contribution of terrigenous organic nitrogen is also unlikely to have been the reason for the $\delta^{15}N$ changes, as no significant difference is observed between glacial and Holocene C/N ratios. Furthermore, overall low abundances of terrestrial biomarkers with no trend during the last 14 kyrs have been observed [*Werne et al.*, 2000]. The most likely cause for the decreasing $\delta^{15}N$ values is enhanced N_2 fixation, whereby the time lag is an indication that it is not (or not alone) triggered by local denitrification.

When comparing the low-resolution Cariaco Basin $\delta^{15}N$ data to long records from other areas (Figure 4.4), a significant time lag can also be observed between rapid deglacial increases in global denitrification and the $\delta^{15}N$ decreases in Cariaco Basin. Long records of nitrogen isotopic composition from denitrification zones have so far been published for the Arabian Sea

(ODP core 722; Figure 4.4) [*Altabet et al.*, 1999] and the Eastern Tropical North Pacific (ODP core 1012; not shown) [*Liu et al.*, 2005]. Both records show consistent patterns of elevated $\delta^{15}N$ in interglacials, reflecting increased denitrification, whereby $\delta^{15}N$ increases coincide with decreases in global ice volume as indicated by foraminiferal $\delta^{18}O$ in the respective cores. In core 722, even a slight lead of $\delta^{15}N$ with respect to $\delta^{18}O$ has been observed [*Altabet et al.*, 1999]. As a way to circumvent age model artifacts, we therefore compare the $\delta^{15}N$ and $\delta^{18}O$ records from Cariaco Basin to assess the relative timing of N_2 fixation changes and global denitrification. In some cases, the changes in $\delta^{18}O$ (and denitrification zone $\delta^{15}N$) occur much earlier than the decreases in $\delta^{15}N$ in Cariaco Basin. For example, during Termination V, the shift in $\delta^{18}O$ of planktic foraminifera in Cariaco Basin coincides with the increase in TN, around 6 kyrs before the $\delta^{15}N$ decrease (Figure 4.3). At Termination II (around 130 ka), the lag of $\delta^{15}N$ to $\delta^{18}O$ in Cariaco Basin is around 4-5 kyrs. Since estimates of the residence time of nitrate in the ocean currently range between 1.5 to 3.0 kyrs [*Gruber and Sarmiento*, 1997; *Brandes and Devol*, 2002], the time lags at these deglaciations seem too long to explain the $\delta^{15}N$ signal with a simple response of regional N_2 fixation to globally increased denitrification. However, there are two possible explanations. First, the signal of an earlier N_2 fixation increase could be masked by a second process, such as a change in the mean isotopic composition of oceanic nitrate. And secondly, another stimulating factor for N_2 fixation (besides low N:P ratios) could cause the delayed response, which will be further discussed in the context of the Holocene $\delta^{15}N$ decrease.

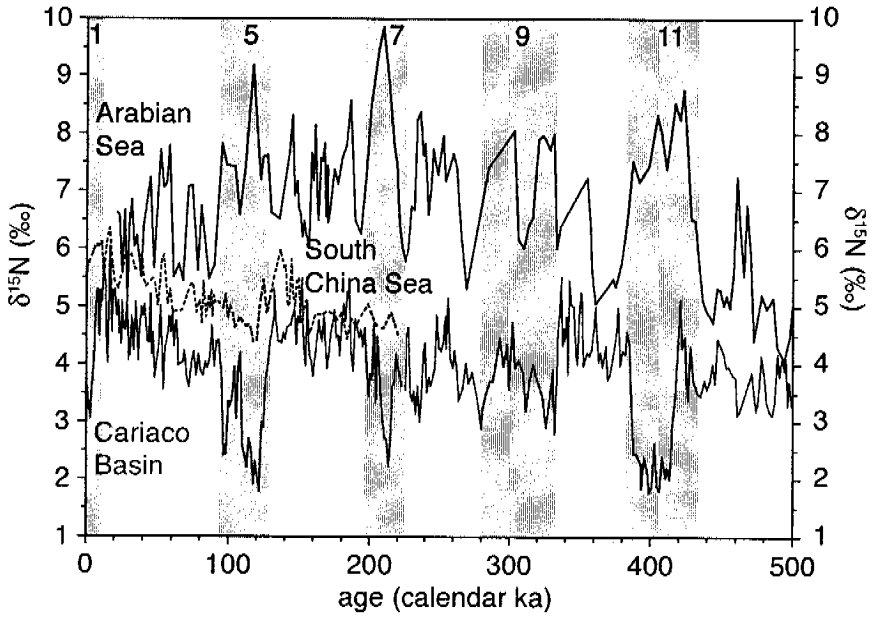

Figure 4.4. The long $\delta^{15}N$ record from Cariaco Basin [*Haug et al.*, 1998] in comparison with records from the Arabian Sea (ODP core 722) [*Altabet et al.*, 1999] and the South China Sea (core 17954) [*Kienast*, 2000]. Shaded bars indicate interglacials, numbers are marine isotope stages. Note the opposite interglacial signals in the Arabian Sea and Cariaco Basin, the former indicating increased denitrification in the oxygen minimum zone of the Arabian Sea. The South China Sea record supposedly reflects the isotopic composition of mean ocean nitrate.

The mean N isotopic composition of oceanic nitrate is supposed to be reflected in $\delta^{15}N$ records from the South China Sea [*Kienast*, 2000], the longest of which covers the last 200 kyrs and is shown in Figure 4.4. Interestingly, in glacial times both the absolute values and the variability of the Cariaco Basin record are similar to those in the South China Sea. Only the negative excursions during the Holocene and the last interglacial stand out with significantly lower values. This suggests that in glacials at least the longer-term signal is mainly affected by the global mean isotopic composition of nitrate. Although the low resolution of the records and the limitations of the age models hamper a more detailed comparison, it is interesting to note that a peak can be observed in the South China Sea record just before the last interglacial (MIS 5), which is also present in the Cariaco record. A deglacial peak in the mean isotopic composition of oceanic nitrate has also been suggested for the last deglaciation [*Deutsch et al.*, 2004; *Meckler et al.*, submitted; see chapter 2] and is probably related to transient changes in the relative importance of water column and sedimentary denitrification. It is therefore possible that part of the deglacial signal in Cariaco Basin reflects such temporary changes in global nitrate isotopic composition.

The high-resolution records from Cariaco Basin allow for a more detailed assessment of this potential influence and the relative timing of the interglacial $\delta^{15}N$ decreases. The records also reveal additional millennial-scale features, such as three peaks during the last deglaciation. We discuss these signals first before returning to the timing of the N_2 fixation increase.

4.5.2. Changes during the last deglaciation

During the deglaciation, large changes occurred both within Cariaco Basin (related to sea level rise) and in the global nitrogen cycle (through increasing global denitrification). The complicated signal of $\delta^{15}N$ during the last deglaciation could therefore either be caused by local changes or be related to global N cycle changes. Most likely, it reflects a combination of these influences. In order to assess the importance of local and global influences, the high-resolution $\delta^{15}N$ record of Termination I is discussed first in the context of other high-resolution data from Cariaco Basin and then in comparison to records from denitrification zones.

Due to the specific bathymetry of the Cariaco Basin, we have to distinguish between two different regimes (Figure 4.5): 1) glacial conditions with an isolated basin and oxygenated bottom water and 2) deglacial to interglacial conditions characterized by a thermocline connection between Cariaco Basin and the open Caribbean and anoxic bottom water (after 14.5 ka). In the first regime, before 14.5 ka, the shallow sill depth of 25-40 m restricted the exchange between Cariaco Basin and the open Caribbean, allowing only mixed layer water to enter the basin. The result was probably a decreased density gradient within the basin, potentially amplified by more

vigorous mixing caused by stronger winds. In addition, climate reconstructions from terrestrial archives indicate that the last glacial maximum was drier than today [*Bradbury et al.*, 1981], implying decreased freshwater input to the basin, which would have further reduced stratification. These changes in local conditions prevented the deep basin from turning anoxic. The first peak in $\delta^{15}N$ occurs under these glacial conditions, which is at first surprising. However, several other local proxies indicate an event at the same time. After 17.5 ka, proxies for terrestrial material (e.g. Ti [*Haug et al.*, 2001, and unpublished data] and detrital mass accumulation rates [*L. Peterson*, unpublished data]; Figure 4.6) indicate a large pulse of terrigenous input, which also encompasses the blue clay layer, represented by the minimum in sediment lightness (L*).

One possibility to explain the large input of terrestrial material is the first flushing of previously exposed shelf area due to the beginning sea level rise, which might have been abrupt [*Clark et al.*, 2004]. The other option is increased freshwater input, which is supported by

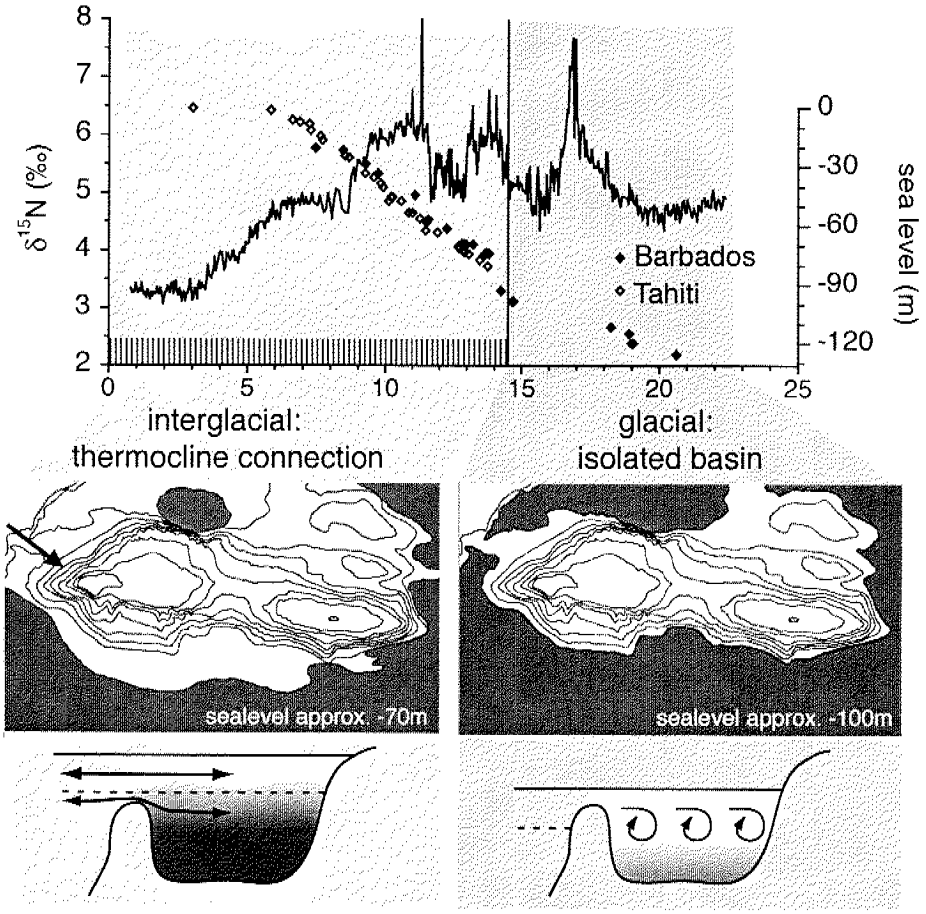

Figure 4.5. Deglacial change of the local conditions in Cariaco Basin due to sea level rise. Sea level data are from *Fairbanks* [1990] (Barbados) and *Bard et al.* [1996] (Tahiti). Isobath spacing is 200 m except for the upper 300 m where spacing is 100 m. In glacial times, Cariaco Basin was almost isolated from the Caribbean Sea due to the shallow sill depth and filled with mixed-layer water. Sea level rise resulted in re-establishment of a thermocline connection and density stratification in the basin. The sudden onset of laminations (hatched bar) at 14.5 ka BP reflects this transition.

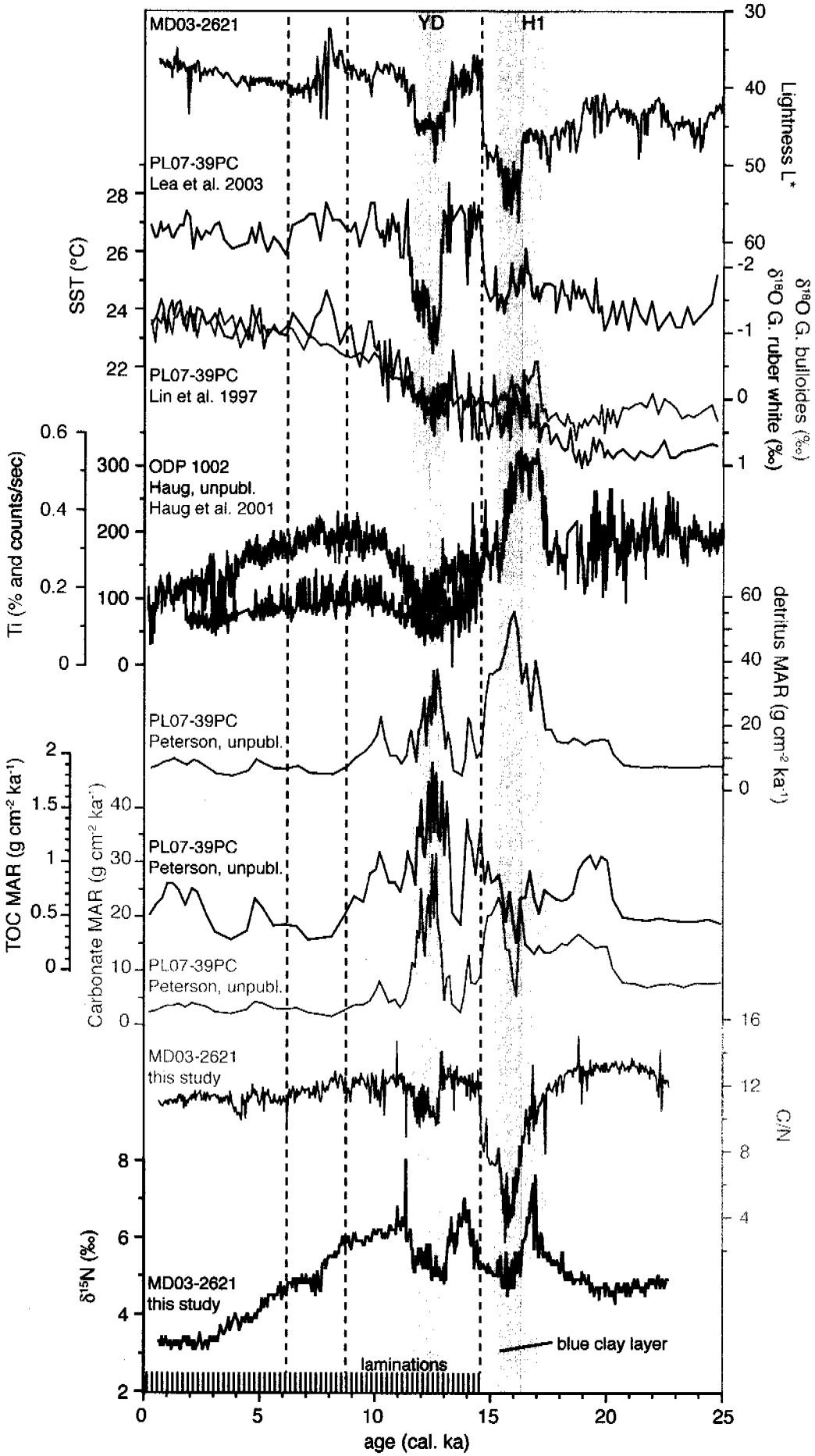
MD03-2621
YD
H1
Lightness L*
PL07-39PC
Lea et al. 2003
SST (°C)
δ18O G. bulloides (‰)
δ18O G. ruber white (‰)
PL07-39PC
Lin et al. 1997
ODP 1002
Haug, unpubl.
Haug et al. 2001
Ti (% and counts/sec)
detritus MAR (g cm-2 ka-1)
PL07-39PC
Peterson, unpubl.
TOC MAR (g cm-2 ka-1)
Carbonate MAR (g cm-2 ka-1)
PL07-39PC
Peterson, unpubl.
PL07-39PC
Peterson, unpubl.
MD03-2621
this study
C/N
MD03-2621
this study
δ15N (‰)
blue clay layer
laminations
age (cal. ka)

Figure 4.6. Compilation of proxy data for the last deglaciation from Cariaco Basin. MAR is mass accumulation rate, YD is Younger Dryas and H1 indicates the time of Heinrich event 1. Dashed lines are for better comparison. Lightness is a mixed signal of carbonates (bright) and organic and terrigenous matter (dark). SST is based on foraminiferal Mg/Ca. Foraminiferal $\delta^{18}O$ is a signal of salinity and/or temperature, superimposed on the global ice volume effect. Ti reflects terrigenous input, as does detritus (= 100% - %TOC - %opal - %carbonate). Note the differences in MAR of detrital material and TOC compared to the respective concentrations (Ti and TOC, c.f. Figure 4.3) due to a large increase in sedimentation rate during the YD. Low C/N in the blue clay layer is probably due to inorganic N.

more negative $\delta^{18}O$ values of planktic foraminifera [*Lin et al.*, 1997]. This would also explain the event character of the terrigenous input, which did not continue with further sea level rise. Interestingly, a similar blue clay layer was observed off the Amazon River mouth at around the same time [*Hemming et al.*, 1998], suggesting a larger-scale hydrologic anomaly. The reason for a freshwater pulse is currently unclear. Around this time, summer insolation increased in the northern hemisphere and northern hemispheric glaciers started to melt. However, this is also the time of Heinrich event 1, and a profound reduction in the formation rate of North Atlantic Deep Water [*McManus et al.*, 2004] and therefore winter cooling. The effect of such increased seasonality [*Denton et al.*, 2005] in the tropics is an open question.

A pulse of freshwater into the well-mixed Cariaco Basin might have led to transient stratification, resulting in suboxic conditions and denitrification in the water column. If denitrification was incomplete, the associated enrichment of subsurface nitrate in ^{15}N could explain the high $\delta^{15}N$ values of up to 7.5 ‰. The sudden decrease in $\delta^{15}N$ afterwards coincides with the blue clay layer and a drop in C/N values to around 4. In face of the evidence for large terrigenous input, these unusually low C/N ratios can only be explained by an increased proportion of clay-bound inorganic nitrogen due to low TOC concentrations and high abundance of clay. If so, the light isotopic composition commonly observed for inorganic nitrogen could add to the rapid decrease after the $\delta^{15}N$ peak ~17 ka. As in all other parts of the core C/N ratios are at values that would be expected for sedimentary organic matter, the influence of inorganic nitrogen on bulk $\delta^{15}N$ is likely limited to the blue clay layer.

2) After 14.5 ka, at the onset of the Bølling period, the sediment suddenly became laminated, indicating permanent anoxia in the deep basin. The reason was probably that sea level rise during meltwater pulse 1A allowed thermocline waters to enter the basin. Since %TOC increases abruptly, it has been thought that the main reason for the anoxia was increased productivity after nutrients became abundant [e.g., *Haug et al.*, 1998]. This is supported by a sudden increase in the relative abundance of the foraminifera species *G. bulloides* [*Peterson et al.*, 1991]. However, the increase of TOC mass accumulation rate [*L. Peterson*, unpublished data], which is an alternative proxy for productivity, is not so clear at this time (Figure 4.6). In any case, a second effect of the tapping of thermocline water was probably that water masses of higher density filled the basin. Together with reduced wind strength due to northern hemisphere

warming, this could have suddenly increased stratification in the basin, leading to anoxia and denitrification. Increased stratification is also consistent with the sudden increase in sea surface temperature [*Lea et al.*, 2003]. High $\delta^{15}N$ values indicate that denitrification was not complete at that time, resulting in heavy residual nitrate being upwelled to the photic zone. The residence time of deep water in the basin was probably short during the Bølling/Allerød interval [*Piper and Dean*, 2002], which could be due to frequent flushing events because continuing sea level rise led to tapping of increasingly dense water.

During the Younger Dryas, sediment accumulation rates peaked, which was due to increases in both terrigenous input (detrital MAR) and productivity (TOC MAR, carbonate MAR) [*L. Peterson*, unpublished data]. In many places, this interval was characterized by a return to (near) glacial conditions. Around Cariaco Basin, it became drier again [*Haug et al.*, 2001; *Hughen et al.*, 2004] and most likely colder. Stronger winds probably resulted in increased upwelling, which is indicated by faunal assemblage shifts [*Peterson et al.*, 1991]. It is unclear whether the increased terrigenous input despite overall drier conditions was caused by increased wind transport or whether single runoff events mobilized the material. Peak productivity and therefore organic matter flux led to increased oxygen demand and might have resulted in increased denitrification rates until complete transformation of nitrate at depth. Thereby the influence of local denitrification on sinking flux $\delta^{15}N$ would have diminished, resulting in sedimentary $\delta^{15}N$ similar to glacial values.

After the Younger Dryas, both upwelling strength and organic matter flux decreased, which could have resulted in decreasing denitrification strength, temporarily restoring its influence on the isotopic composition of the sinking flux. This could explain the higher $\delta^{15}N$ values, especially the very brief peak exceeding 8 ‰ at around 11.5 ka. If so, part of the decrease in $\delta^{15}N$ after 11 ka would have to be caused by a subsequent strengthening of denitrification until completeness, as observed today. The only way such a Holocene increase in denitrification strength could be explained is an increase in the residence time of the deep water, because productivity was decreasing. Such a decrease in ventilation could have been due to the decreased wind strength and upwelling in the Preboreal. We therefore assume that a possible return to complete consumption of nitrate by denitrification occurred within the early Holocene. In summary, the millennial-scale variability in $\delta^{15}N$ observed during the last deglaciation, including the three peaks of up to 8 ‰, could be explained by a variable strength of local denitrification in response to changes in density stratification and productivity.

On the other hand, when comparing the Cariaco Basin record to data from denitrification zones in the east Pacific and the Arabian Sea (Figure 4.7), a striking similarity can be observed for the Bølling/Allerød and Preboreal peaks and the Younger Dryas minimum. By this time, a thermocline connection with the open Caribbean had already been established. A rapid transfer of changes in the isotopic composition of thermocline nitrate in other areas to Cariaco Basin

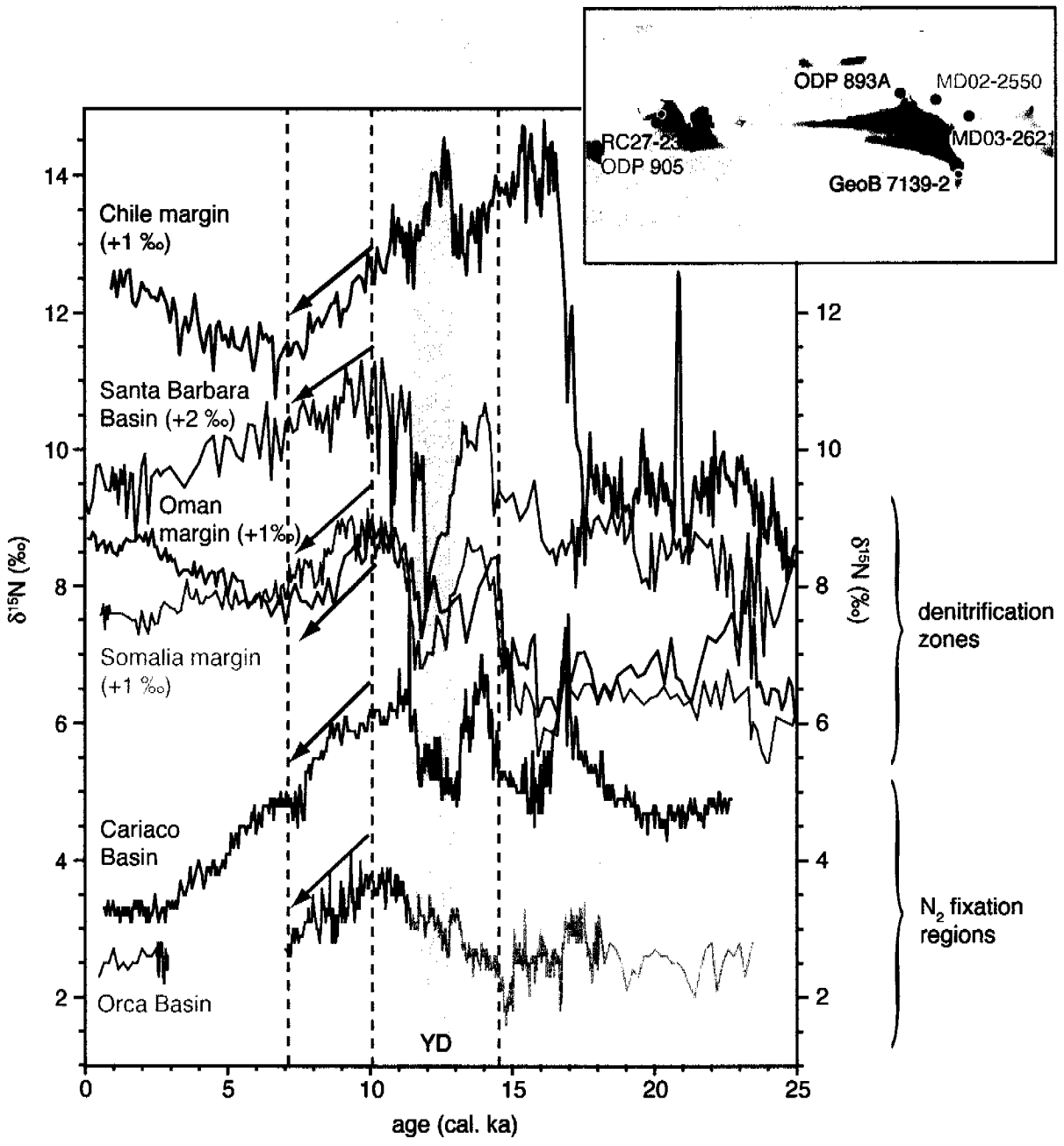

Figure 4.7. Global comparison of $\delta^{15}N$ records for the last deglaciation. Shown are records from denitrification zones in the east Pacific off Chile [*de Pol-Holz et al.*, 2006], off California (Santa Barbara Basin) [*Emmer and Thunell*, 2000], and the Arabian Sea off Oman [*Altabet et al.*, 2002] and off Somalia [*Ivanochko et al.*, 2005] in comparison with the data from Cariaco Basin (this study) and Orca Basin in the Gulf of Mexico [*Meckler et al.*, submitted; see chapter 2]. Glacial data in the Orca Basin record (before 11.5 ka) are probably overprinted by terrigenous nitrogen. Some records are shifted for better comparison. The grey bar indicates the Younger Dryas and dashed lines the rapid increase in denitrification in the northern hemisphere as well as the early Holocene decrease (arrows) common to all records.

could therefore potentially be invoked, assuming thermocline waters of different ocean basins communicated without involving the deep ocean. Even if this was the case, however, the shifts in Cariaco Basin are more abrupt than one would expect if they were reflecting thermo-

cline signals from distant areas. Furthermore, in the denitrification areas of the southern hemisphere, the timing of the deglacial changes was different from the northern hemisphere sites (Figure 4.7), as exemplified by opposite signals during the Younger Dryas period. If the Cariaco Basin signal was imported, it should be influenced by both southern and northern hemispheric changes, whereby opposite trends would have counteracted each other. Therefore it is more likely that the rapid deglacial variations in the Cariaco Basin record reflect mostly local changes in denitrification strength.

It should be noted that this observation does not preclude an imprint of changes in the mean ocean nitrate isotopic composition, as discussed before in the context of the low-resolution record. Such a signal, due to changes in the relative importance of water column and sedimentary denitrification, would be expected to have the shape of a broad peak, reflecting the different timing of denitrification increases (and decreases). In Orca Basin in the Gulf of Mexico, the $\delta^{15}N$ signal is not influenced by local denitrification but should reflect the $\delta^{15}N$ of mean ocean nitrate and/or changes in the strength of regional N_2 fixation [*Meckler et al.*, submitted; see chapter 2]. At that site the glacial part of the record (before 11.5 ka) is difficult to interpret due to interference by terrestrial input and we therefore restrict our comparison to the Holocene. The Orca Basin record exhibits a decrease after around 10 ka, which is similar to the initial part of the Holocene decrease in Cariaco Basin. Decreasing $\delta^{15}N$ values during this interval are furthermore observed in all records from the denitrification zones (Figure 4.7). This agreement of records from very different environments is an indication for a global component in the records. While the onset of such a peak is difficult to determine in the Cariaco record, it is most probably responsible for at least part of the early Holocene decrease. In contrast, the second portion of the Holocene decrease does not appear to be a global signal, and consequently has to be due to local or regional processes.

4.5.3. Timing of the N_2 fixation increase

As discussed before, the overall decrease in Cariaco Basin $\delta^{15}N$ is probably due to increasing N_2 fixation. It is therefore most likely that this process was responsible for the mid-Holocene decrease in $\delta^{15}N$, implying that much of the increase in N_2 fixation recorded in Cariaco Basin occurred later than the influence of the transient global signal. The step-like character of the interglacial $\delta^{15}N$ decrease, including a plateau at $\delta^{15}N$ values similar to those of the last glacial maximum, supports this interpretation. However, what could have caused this delayed increase in N_2 fixation?

The onset of the mid-Holocene $\delta^{15}N$ decrease coincides with climatic changes in the region, which could have stimulated N_2 fixation. Over the course of the Holocene, northern hemispheric summer insolation decreased, which resulted in a southward movement of the Intertropical

Convergence Zone (ITCZ) [*Haug et al.*, 2001]. This caused declining Caribbean precipitation as indicated by decreasing Ti concentrations in Cariaco Basin (Figure 4.6) [*Haug et al.*, 2001]. The reduction in precipitation over northern South America might have led to decreased nitrogen input by the Orinoco River and local rivers, which could have previously suppressed N_2 fixation in the Caribbean Sea and/or Cariaco Basin, respectively. However, a potentially more important effect was the re-establishment of the Saharan desert after an early Holocene humid period [*deMenocal et al.*, 2000]. In the context of this change, transport of dust to the (sub)tropical North Atlantic and the Caribbean probably increased greatly in the mid-Holocene, facilitated by stronger trade winds and a less prevalent ITCZ rain curtain in this region. As N_2 fixation is thought to be sensitive to the availability of iron, an increased iron input by dust potentially stimulated N_2 fixation at times when high interglacial denitrification had decreased the N:P ratio of nutrients in the thermocline. The latter stimulation was absent in glacial times, preventing high N_2 fixation rates despite a Saharan dust input that was probably higher than today [*Mahowald et al.*, 1999]. In contrast, while the deglacial increase in global denitrification created a global surplus of phosphate, Atlantic N_2 fixation was limited by iron and therefore only increased after the dust input recommenced. This proposed mechanism leaves us with the question of whether the Cariaco Basin records a signal of locally increasing N_2 fixation or instead represents a change in the whole region of the (sub)tropical North Atlantic and the Caribbean. We consider the latter as much more likely since the coastal areas receive iron by riverine input and therefore probably do not depend on the dust-bound iron source.

The mid-Holocene decrease in $\delta^{15}N$ is not observable in Orca Basin, although one might expect the signal to be transported to the thermocline of the Gulf of Mexico. The difference between the records could imply that N_2 fixation has a stronger imprint on the Cariaco Basin record, whereas the global changes in mean ocean nitrate $\delta^{15}N$ are the dominant control on the Orca Basin record. Alternatively, N_2 fixation in the Gulf of Mexico could have responded to different forcing factors than in the tropical North Atlantic. Especially the (seasonal) suppression of dust flux to the Caribbean by the ITCZ rain curtain, which was probably stronger with a more northern mean position of the ITCZ in the early Holocene, should not have affected the Gulf of Mexico as much.

In summary, we propose that the step-wise Holocene decrease in $\delta^{15}N$ in Cariaco Basin is due to 1) an early Holocene decrease in mean ocean nitrate $\delta^{15}N$ as part of a deglacial peak, possibly in combination with local changes in denitrification strength as discussed above, and 2) a mid-Holocene increase in regional N_2 fixation due to an increase in Saharan dust input. Mid-Holocene changes also occurred in denitrification zones, albeit in varying ways (Figure 4.7). At the Oman and Chile margins, increasing denitrification after 7 ka has been inferred from increasing $\delta^{15}N$ values [*Altabet et al.*, 2002; *De Pol-Holz et al.*, 2006], whereas at the Somalia margin and in the Santa Barbara Basin, the Holocene decrease in $\delta^{15}N$ continued, suggesting

decreasing denitrification [*Emmer and Thunell*, 2000; *Ivanochko et al.*, 2005]. Although the impact of these different changes on the overall global denitrification rate is yet to be determined, a mid-Holocene increase in global denitrification could have played an additional role in the stimulation of North Atlantic N_2 fixation. Either way, the data suggest that the global nitrogen cycle did not reach stability until at least the late Holocene (around 3 ka).

4.5.4. Comparison of Terminations I and V

The pattern of $\delta^{15}N$ changes observed for the last deglaciation in Cariaco Basin is very similar to the trends during Termination V, except for the larger millennial-scale excursions during the last deglaciation. The reduced signal of such deglacial peaks during the earlier termination could be due to less pronounced shifts between different redox conditions, which is supported by the laminations being less clear in that earlier interval. However, the redox conditions during Termination V are not well constrained at present. In any case, the fact that the remaining trends are similar in timing and magnitude during the two terminations studied here indicates that the shifts represent systematic changes in the nitrogen cycle. During Termination V, a slow increase of around 1 ‰, followed by a decrease of similar magnitude, could represent the transient change in mean ocean nitrate $\delta^{15}N$, similar to that proposed for the last deglaciation. Furthermore, the interglacial decrease seems to occur in two steps, analogous to the Holocene decrease.

Unfortunately, there is presently neither a high-resolution $\delta^{15}N$ record for Termination V from another part of the ocean, nor detailed control on changes in climate during the interglacial period following Termination V (MIS 11) to put these changes into context. The desertification of the Sahara in the mid-Holocene and the southward shift of the ITCZ were likely due to decreasing summer insolation linked to the 23-kyr precessional cycle. The fact that during MIS11 $\delta^{15}N$ stayed low for around 25 kyrs, during which summer insolation exhibited both a minimum and a maximum, would seem to contradict the dust trigger hypothesis. However, other factors could be important in addition to precession and there is presently no detailed control on changes in dust input within this earlier interglacial period.

MIS 11 was an exceptionally long interglacial period, with interglacial climate conditions lasting around 30 kyrs [*McManus et al.*, 1999; *Siegenthaler et al.*, 2005]. This interglacial can therefore be used to assess the stability of the nitrogen cycle in the absence of deglacial perturbations. The constant $\delta^{15}N$ values in the Cariaco Basin record after 417 ka indicate long-term regional and probably also global stability of the nitrogen cycle for much of this interglacial period. As the Holocene is characterized by similar orbital configurations, with reduced amplitudes of insolation changes due to a minimum in eccentricity, the stability inferred for the last 3

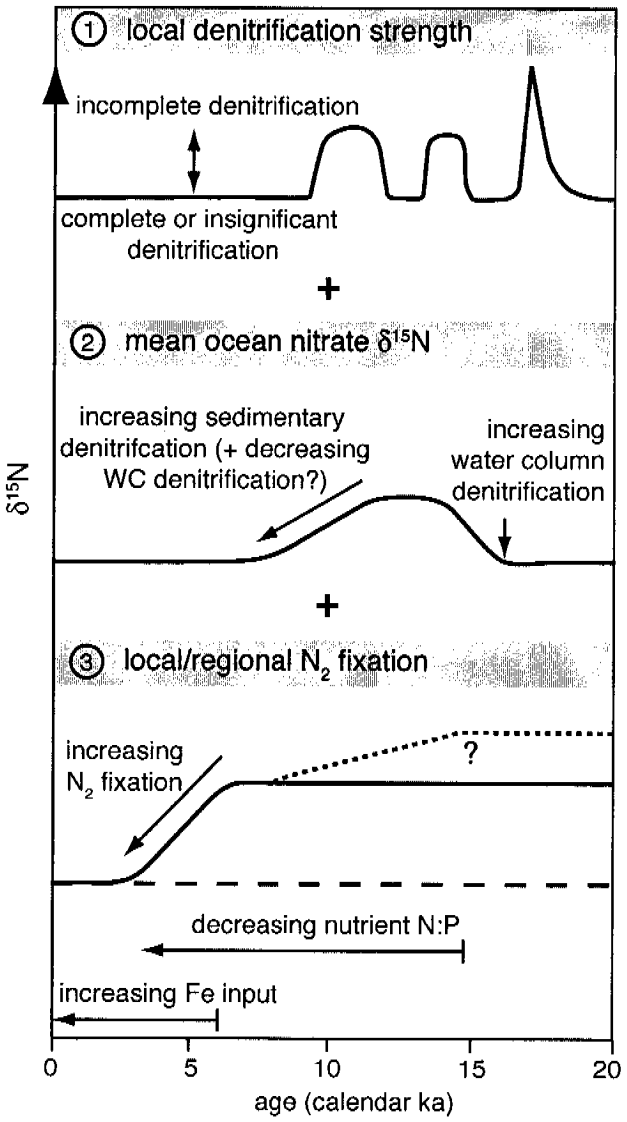

Figure 4.8. Schematic drawing of the different effects thought to cause the observed $\delta^{15}N$ trends in Cariaco Basin during terminations as explained in the text. The exact timing and shape of the mean ocean nitrate signal (2) is unknown.

kyrs could potentially last for some thousand years into the future, in absence of human perturbations of the nitrogen cycle.

4.6. Conclusions

The high-resolution $\delta^{15}N$ data obtained for two terminations in Cariaco Basin allowed a more detailed assessment of changes in the nitrogen cycle at that site than previously possible. An observed time lag of up to 6 kyrs between local changes in productivity and anoxia and the deglacial decreases in $\delta^{15}N$ confirm that the overall decreases are neither related to redox-driven

changes in diagenetic alteration of the signal nor are they due to changes in local processes such as nutrient utilization or denitrification. However, local processes do play a role in the millennial-scale variability superimposed on the glacial-interglacial trends; specifically, a comparison with other available proxy data suggests that variations in the strength of denitrification in Cariaco Basin drove several abrupt $\delta^{15}N$ changes during the deglacial interval (Figure 4.8, part 1). This local influence was apparently more pronounced during the last deglaciation than during Termination V.

The overall deglacial decreases in $\delta^{15}N$ observed in Cariaco Basin were most likely due to increasing N_2 fixation. The Cariaco Basin record therefore adds to the growing evidence that N_2 fixation responds to the higher rates of global denitrification during interglacials. However, a significant time lag was observed between global increases in denitrification and the Cariaco Basin $\delta^{15}N$ decreases. In the Holocene, the $\delta^{15}N$ decrease occurred in two steps, whereby the earlier part of this signal likely represents a decrease in mean ocean nitrate $\delta^{15}N$ as part of a deglacial peak (Figure 4.8, part 2). This is supported by the similarity of the Cariaco Basin data with $\delta^{15}N$ records from various denitrification zones and the Gulf of Mexico during this interval. Furthermore, deglacial peaks in mean ocean nitrate $\delta^{15}N$ are suggested by records from the South China Sea [*Kienast*, 2000].

Much of the Holocene decrease in $\delta^{15}N$ occurred after 6 ka, coinciding with a change in regional climate and, most importantly, the re-establishment of the Saharan desert. We propose that a concurrent increase in dust input triggered a mid-Holocene increase in N_2 fixation in the (sub)tropical North Atlantic, relieving iron limitation that hindered N_2 fixation in the early Holocene (Figure 4.8, part 3). Thereby, this response was probably most pronounced in the southern part of the North Atlantic, as the late decrease in $\delta^{15}N$ is not observable in the Gulf of Mexico [*Meckler et al.*, submitted; see chapter 2]. In glacial times, high $\delta^{15}N$ values in the Cariaco Basin indicate reduced N_2 fixation despite large dust input [*Mahowald et al.*, 1999]. Our hypothesis therefore calls for two requirements to be met in order to trigger N_2 fixation in the North Atlantic: a decreased nutrient N:P ratio and sufficient availability of the micronutrient iron.

The good agreement of the $\delta^{15}N$ signal during the two terminations studied here, regarding the timing, shape and magnitude of the deglacial decreases, suggests a similar sequence of influences during Termination V. However, the long-lasting stability of low $\delta^{15}N$ values during MIS11 seems to contradict the dust trigger mechanism if dust input varied with the 23-kyr precessional cycle. Future work on dust input and climate variability during this interval will allow further testing of the proposed mechanisms. The observed stability of the $\delta^{15}N$ values after the late decrease in both the MIS 11 and the Holocene data suggest that the nitrogen cycle reaches a balance when interglacial conditions prevail long enough.

Acknowledgements

We would like to thank Carlo Laj, Yvon Balut, and the crew of R/V *Marion Dufresne* for a successful cruise in the Caribbean Sea. P. Meier is gratefully acknowledged for help with sample preparation and measurements. Niki Gruber is thanked for helpful comments. This work was funded by the Swiss National Science Foundation.

References

Altabet, M. A., and R. Francois (1994), Sedimentary Nitrogen Isotopic Ratio as a Recorder for Surface Ocean Nitrate Utilization, *Global Biogeochem. Cycles*, *8*, 103-116.

Altabet, M. A., D. W. Murray, and W. L. Prell (1999), Climatically linked oscillations in Arabian Sea denitrification over the past 1 m.y.: Implications for the marine N cycle, *Paleoceanography*, *14*, 732-743.

Altabet, M. A., M. J. Higginson, and D. W. Murray (2002), The effect of millennial-scale changes in Arabian Sea denitrification on atmospheric CO2, *Nature*, *415*, 159-162.

Altabet, M. A., R. Francois, D. W. Murray, and W. L. Prell (1995), Climate-Related Variations in Denitrification in the Arabian Sea from Sediment N-15/N-14 Ratios, *Nature*, *373*, 506-509.

Astor, Y., F. Muller-Karger, and M. I. Scranton (2003), Seasonal and interannual variation in the hydrography of the Cariaco Basin: implications for basin ventilation, *Cont. Shelf Res.*, *23*, 125-144.

Bard, E., B. Hamelin, R. G. Fairbanks, and A. Zindler (1990), Calibration of the C-14 Timescale over the Past 30,000 Years Using Mass-Spectrometric U-Th Ages from Barbados Corals, *Nature*, 345, 405-410.

Bradbury, J. P., B. Leyden, M. Salgadolabouriau, W. M. Lewis, C. Schubert, M. W. Binford, D. G. Frey, D. R. Whitehead, and F. H. Weibezahn (1981), Late Quaternary Environmental History of Lake Valencia, Venezuela, *Science*, *214*, 1299-1305.

Brandes, J. A., and A. H. Devol (2002), A global marine-fixed nitrogen isotopic budget: Implications for Holocene nitrogen cycling, *Global Biogeochem. Cycles*, *16*, 1120, doi:10.1029/2001GB001856.

Christensen, J. P. (1994), Carbon Export from Continental Shelves, Denitrification and Atmospheric Carbon-Dioxide, *Cont. Shelf Res.*, *14*, 547-576.

Clark, P. U., A. M. McCabe, A. C. Mix, and A. J. Weaver (2004), Rapid rise of sea level 19,000 years ago and its global implications, *Science*, *304*, 1141-1144.

Codispoti, L. A. (1989), Phosphorus vs. nitrogen limitation of new and export production, in *Productivity of the Ocean: Past and Present*, edited by W. H. Berger, et al., pp. 377-394, John Wiley, Hoboken, N.J.

De Pol-Holz, R., O. Ulloa, L. Dezileau, J. Kaiser, F. Lamy, and D. Hebbeln (2006), Melting of the Patagonian Ice Sheet and deglacial perturbations of the nitrogen cycle in the eastern South Pacific, *Geophys. Res. Lett.*, *33*, L04704, doi:10.1029/2005GL024477.

deMenocal, P., J. Ortiz, T. Guilderson, J. Adkins, M. Sarnthein, L. Baker, and M. Yarusinsky (2000), Abrupt onset and termination of the African Humid Period: rapid climate responses to gradual insolation forcing, *Quaternary Science Reviews*, *19*, 347-361.

Denton, G. H., R. B. Alley, G. C. Comer, and W. S. Broecker (2005), The role of seasonality in abrupt climate change, *Quaternary Science Reviews*, *24*, 1159-1182.

Deutsch, C., D. M. Sigman, R. C. Thunell, A. N. Meckler, and G. H. Haug (2004), Isotopic constraints on glacial/interglacial changes in the oceanic nitrogen budget, *Global Biogeochem. Cycles*, *18*, GB4012, doi:10.1029/2003GB002189.

Emmer, E., and R. C. Thunell (2000), Nitrogen isotope variations in Santa Barbara Basin sediments: Implications for denitrification in the eastern tropical North Pacific during the last 50,000 years, *Paleoceanography*, *15*, 377-387.

Fairbanks, R. G. (1989), A 17,000-Year Glacio-Eustatic Sea-Level Record - Influence of Glacial Melting Rates on the Younger Dryas Event and Deep-Ocean Circulation, Nature, 342, 637-642.

Ganeshram, R. S., T. F. Pedersen, S. E. Calvert, and J. W. Murray (1995), Large Changes in Oceanic Nutrient Inventories from Glacial to Interglacial Periods, *Nature*, *376*, 755-758.

Gruber, N., and J. L. Sarmiento (1997), Global patterns of marine nitrogen fixation and denitrification, *Global Biogeochem. Cycles*, *11*, 235-266.

Haug, G. H., K. A. Hughen, D. M. Sigman, L. C. Peterson, and U. Rohl (2001), Southward migration of the intertropical convergence zone through the Holocene, *Science*, *293*, 1304-1308.

Haug, G. H., T. F. Pedersen, D. M. Sigman, S. E. Calvert, B. Nielsen, and L. C. Peterson (1998), Glacial/interglacial variations in production and nitrogen fixation in the Cariaco Basin during the last 580 kyr, *Paleoceanography*, *13*, 427-432.

Hemming, S. R., P. E. Biscaye, W. S. Broecker, N. G. Hemming, M. Klas, and I. Hajdas (1998), Provenance change coupled with increased clay flux during deglacial times in the western equatorial Atlantic, *Palaeogeography Palaeoclimatology Palaeoecology*, *142*, 217-230.

Hughen, K. A., T. I. Eglinton, L. Xu, and M. Makou (2004), Abrupt tropical vegetation response to rapid climate changes, *Science*, *304*, 1955-1959.

Hughen, K. A., J. T. Overpeck, L. C. Peterson, and R. F. Anderson (1996), The nature of varved sedimentation in the Cariaco Basin, Venezuela, and its paleoclimatic significance, in *Paleoclimatology and Paleoceanography from Laminated Sediments*, edited by A. E. S. Kemp, pp. 171-183, Geological Society Special Publication.

Ivanochko, T. S., R. S. Ganeshram, G. J. A. Brummer, G. Ganssen, S. J. A. Jung, S. G. Moreton, and D. Kroon (2005), Variations in tropical convection as an amplifier of global climate change at the millennial scale, *Earth Planet. Sc. Lett.*, *235*, 302-314.

Kienast, M. (2000), Unchanged nitrogen isotopic composition of organic matter in the South China Sea during the last climatic cycle: Global implications, *Paleoceanography*, *15*, 244-253.

Knapp, A. N., D. M. Sigman, and F. Lipschultz (2005), N isotopic composition of dissolved organic nitrogen and nitrate at the Bermuda Atlantic time-series study site, *Global Biogeochem. Cycles*, *19*.

Kustka, A. B., S. A. Sanudo-Wilhelmy, E. J. Carpenter, D. Capone, J. Burns, and W. G. Sunda (2003), Iron requirements for dinitrogen- and ammonium-supported growth in cultures of Trichodesmium (IMS 101): Comparison with nitrogen fixation rates and iron: carbon ratios of field populations, *Limnol. Oceanogr.*, *48*, 1869-1884.

LaRoche, J., and E. Breitbarth (2005), Importance of the diazotrophs as a source of new nitrogen in the ocean, *Journal of Sea Research*, *53*, 67-91.

Lea, D. W., D. K. Pak, L. C. Peterson, and K. A. Hughen (2003), Synchroneity of tropical and high-latitude Atlantic temperatures over the last glacial termination, *Science*, *301*, 1361-1364.

Lin, H. L., L. C. Peterson, J. T. Overpeck, S. E. Trumbore, and D. W. Murray (1997), Late Quaternary climate change from delta O-18 records of multiple species of planktonic

foraminifera: High-resolution records from the anoxic Cariaco Basin, Venezuela, *Paleoceanography*, *12*, 415-427.

Lisiecki, L. E., and M. E. Raymo (2005), A Pliocene-Pleistocene stack of 57 globally distributed benthic delta O-18 records, *Paleoceanography*, *20*, PA1003, doi:10.1029/2004PA001071.

Liu, Z. H., M. A. Altabet, and T. D. Herbert (2005), Glacial-interglacial modulation of eastern tropical North Pacific denitrification over the last 1.8-Myr, *Geophys. Res. Lett.*, *32*, L23607, doi:10.1029/2005GL024439.

Mahowald, N., K. Kohfeld, M. Hansson, Y. Balkanski, S. P. Harrison, I. C. Prentice, M. Schulz, and H. Rodhe (1999), Dust sources and deposition during the last glacial maximum and current climate: A comparison of model results with paleodata from ice cores and marine sediments, *J. Geophys. Res. Atmos.*, *104*, 15895-15916.

McManus, J. F., D. W. Oppo, and J. L. Cullen (1999), A 0.5-million-year record of millennial-scale climate variability in the North Atlantic, *Science*, *283*, 971-975.

McManus, J. F., R. Francois, J. M. Gherardi, L. D. Keigwin, and S. Brown-Leger (2004), Collapse and rapid resumption of Atlantic meridional circulation linked to deglacial climate changes, *Nature*, *428*, 834-837.

Meckler, A. N., D. M. Sigman, B. Plessen, and G. H. Haug (submitted), A new N isotope record from Orca Basin, Gulf of Mexico - Evidence for feedbacks in the marine nitrogen cycle, *Paleoceanography*.

Mills, M. M., C. Ridame, M. Davey, J. La Roche, and R. J. Geider (2004), Iron and phosphorus co-limit nitrogen fixation in the eastern tropical North Atlantic, *Nature*, *429*, 292-294.

Paillard, D., L. Labeyrie, and P. Yiou (1996), Macintosh program performs time-series analysis, *Eos Trans. AGU*, *77*, 379.

Peterson, L. C., J. T. Overpeck, N. G. Kipp, and J. Imbrie (1991), A high-resolution late quaternary upwelling record from the anoxic Cariaco Basin, Venezuela, *Paleoceanography*, *6*, 99-119.

Peterson, L. C., G. H. Haug, R. W. Murray, K. M. Yarincik, J. W. King, T. J. Bralower, K. Kameo, S. D. Rutherford, and R. B. Pearce (2000), Late Quaternary stratigraphy and sedimentation at Site 1002, Cariaco Basin (Venezuela), in *Proceedings of the Ocean Drilling Program, Scientific Results*, edited by R. M. Leckie, et al., pp. 85-99.

Piper, D. Z., and W. E. Dean (2002), Trace-element Deposition in the Cariaco Basin, Venezuela Shelf, under Sulfate-Reducing Conditions – a History of the Local Hydrography

and Global Climate, 20 ka to the Present, Professional Paper 1670, US Geological Survey.

Pride, C., R. Thunell, D. M. Sigman, L. Keigwin, M. Altabet, and E. Tappa (1999), Nitrogen isotopic variations in the Gulf of California since the last deglaciation: Response to global climate change, *Paleoceanography, 14*, 397-409.

Redfield, A. C., B. H. Ketchum, and F. A. Richards (1963), The influence of organisms on the composition of seawater, in *The Sea*, edited by M. N. Hill, pp. 26-77, Wiley Interscience, Hoboken, N.J.

Siegenthaler, U., T. F. Stocker, E. Monnin, D. Luthi, J. Schwander, B. Stauffer, D. Raynaud, J. M. Barnola, H. Fischer, V. Masson-Delmotte, and J. Jouzel (2005), Stable carbon cycle-climate relationship during the late Pleistocene, *Science, 310*, 1313-1317.

Sigman, D. M. (1997), The Role of Biological Production in Pleistocene Atmospheric Carbon Dioxide Variations and the Nitrogen Isotope Dynamics of the Southern Ocean, PhD thesis, Woods Hole Oceanographic Institution.

Thunell, R. C., D. M. Sigman, F. Muller-Karger, Y. Astor, and R. Varela (2004), Nitrogen isotope dynamics of the Cariaco Basin, Venezuela, *Global Biogeochem. Cycles, 18*, GB3001, doi:10.1029/2003GB002185.

Tyrrell, T. (1999), The relative influences of nitrogen and phosphorus on oceanic primary production, *Nature, 400*, 525-531.

Wada, E., and A. Hattori (1991), *Nitrogen in the Sea: Forms, Abundances and Rate Processes*, CRC Press, Boston.

Werne, J. P., D. J. Hollander, T. W. Lyons, and L. C. Peterson (2000), Climate-induced variations in productivity and planktonic ecosystem structure from the Younger Dryas to Holocene in the Cariaco Basin, Venezuela, *Paleoceanography, 15*, 19-29.

Woodworth, M. P., M. A. Goni, R. Thunell, E. Tappa, and Y. Astor (2004), Major Sterol Fluxes in Sinking Particles and Surface Sediments in the Cariaco Basin, *Eos Trans. AGU, 85 (47)*, Fall Meet. Suppl., Abstract OS33A-0577.

Chapter 5

Alternative determinations of past changes in N_2 fixation including first tests on coccolith-bound N isotope measurements

5.1. Introduction

The standard method to study past changes in marine nitrogen cycling is the analysis of bulk sedimentary N isotopes ($\delta^{15}N$). This method is well established and allows high sample throughput. However, as became clear in chapters 2 and 4, there are several problems associated with bulk $\delta^{15}N$. Firstly, nitrogen isotopes are affected by many different processes, which are often not easy to distinguish. For example, in the Cariaco Basin record (chapter 4) it is in some parts not discernable whether changes in denitrification or N_2 fixation caused the observed variations in bulk $\delta^{15}N$. Secondly, varying input of terrigenous nitrogen (both organic and inorganic, clay-bound forms) can in some places seriously alter the bulk signal, as is probably the case for the glacial sections of the Orca Basin record (chapter 2). And finally, diagenetic overprint of the original signal is a severe problem in open-ocean sites with low accumulation rates. This is most likely not a problem at the sites studied here, but it prevents obtaining records from areas where N_2 fixation changes are the single most important factor for variations in $\delta^{15}N$.

In order to obtain a signal confined to marine primary producers, one approach is compound-specific measurement of the nitrogen isotopic composition on molecules of marine origin. Unfortunately, the compounds containing most of the organic nitrogen, namely amino acids and amino sugars are very ubiquitous and can therefore not be attributed to marine algae. In contrast, the nitrogen isotopic composition of chlorophyll and its degradation products has been used to obtain the signal from phototrophic biomass [*Sachs and Repeta*, 1999; *Pantoja et al.*, 2002; *Ohkouchi et al.*, 2005]. As this compound is considered to be comparatively labile, one could assume that most of the chloropigments found in sediments are derived from marine phototrophs. However, even if this assumption is valid, a difficulty is the observed offset between the isotopic composition of chlorophyll-N and algal biomass [*Sachs et al.*, 1999; *Pantoja et al.*, 2002], which has been found to be species- and growth rate-dependent. The offset between

the isotopic compositions of chlorophyll-N and marine particulate N might therefore vary over time, complicating the interpretation of chlorophyll-N isotopes with respect to changes in marine nitrogen fixation.

The problem of different overlying influences on the marine $\delta^{15}N$ signal (such denitrification and N_2 fixation in the Cariaco Basin record) could be solved if an independent proxy for the process of interest could be established. Potential approaches to assess N_2 fixation are organism-specific biomarkers [e.g., *Carpenter et al.*, 1997; *Köster et al.*, 1999; *Summons et al.*, 1999] or molecular biological methods. In this study, initial test were performed to assess the applicability of these methods (specific cyanobacterial biomarkers and DNA extraction).

Finally, the problems of terrigenous input and diagenetic overprint can be overcome by measuring $\delta^{15}N$ on organic matter preserved within microfossils, such as diatom frustules. Although time-consuming, this new method has made it possible to obtain $\delta^{15}N$ records from areas where diagenetic changes are a problem [e.g., *Sigman et al.*, 1999; *Robinson et al.*, 2005]. Since a purely marine signal is measured, uncertainties related to terrigenous input are also circumvented. However, diatoms are not present in sediments from all areas, since low abundance and poor preservation are common in nutrient-deplete regions. For this reason, the method needs to be extended to organisms that are abundant in sediments from oligotrophic environments. Thereby, primary producers are the preferred target organisms, as significant increases in $\delta^{15}N$ with trophic level in the food web have been observed [*Altabet and Small*, 1990; *Wu et al.*, 1997]. Furthermore, it would be interesting to compare the diatom signal to that from other organisms to assess the variability due to different growing seasons or different fractionation during N uptake.

The present chapter is organized into two parts. Firstly, alternatives to nitrogen isotope measurements for assessing changes in N_2 fixation are briefly discussed. The focus is on the approaches that were tested in this study, namely biomarker analyses and DNA extraction. The second and main part of this chapter describes initial tests performed towards the measurement of $\delta^{15}N$ on microfossils from oligotrophic regions, mainly coccoliths. Thereby, the methods investigated for separating the coccoliths from the sediment are presented first, followed by the tests carried out regarding the measurement of $\delta^{15}N$ on organic matter contained in carbonaceous microfossils.

5.2. Alternative methods for assessing changes in N_2 fixation

5.2.1. Cyanobacterial biomarkers

Several studies have investigated the composition of lipids derived from cyanobacterial tissue in order to determine characteristic substances that can be used as biomarkers. One compound group that has been proposed are 2-methylated hopanoids, whereby the methylation of the C-2 atom appears to be characteristic for certain cyanobacteria [*Rohmer et al.*, 1984; *Summons et al.*, 1999]. Hopanoids can be directly measured with gas chromatography-mass spectrometry and are regularly identified in sediments. They are fragmented remains of former intact bacteriohopanepolyols (BHPs), which have been degraded gradually during diagenesis. However, not all cyanobacteria produce this compound and therefore *Summons et al.* [1999] stated that these "biomarker probes ... are unidirectional". For example, one of the most important diazotrophic species in the subtropical ocean, *Trichodesmium* spp., does not contain 2-methylated hopanoids [*Roger Summons, pers. comm.*, 2006].

Another group of molecules recently proposed to be characteristic for cyanobacteria are branched *n*-alkanes, mostly methyl-branched heptadecanes with multiple methyl-groups [*Kenig et al.*, 1995; *Köster et al.*, 1999]. So far, these compounds have only been extracted from mat-forming cyanobacteria, however.

In conjunction with the measurement of marine and terrestrial biomarkers at Bremen University (see chapter 3), the abundance of the two groups of suggested cyanobacterial biomarkers were examined in samples from both Orca Basin and Cariaco Basin. At both sites no significant amounts were found of either group. However, since it is not clear whether these compounds are even produced by the diazotrophs in these regions, this result does not allow conclusions about local N_2 fixation.

Recently, a method for measuring the concentration and structure of intact BHPs has been proposed, which employs atmospheric pressure chemical ionization liquid chromatography (APCI-LC) mass spectrometry [*Talbot et al.*, 2003]. This could allow a further assessment of the abundance of these substances in sediments. More research is clearly needed to identify a biomarker that can be used for tracing marine nitrogen fixation in open ocean settings.

5.2.2. Fossil DNA

Another possibility to assess N_2 fixation changes independently of $\delta^{15}N$ measurements would be the determination of the abundance of the gene required for this process, nifH. This

gene has been successfully extracted from water column and culture samples and is well known today [e.g., *Zehr et al.*, 2000; *MacGregor et al.*, 2001; *Falcon et al.*, 2002]. However, since DNA belongs to the most labile fraction of organic matter, it is not clear whether it is stable enough to be found in sediments that are several thousand years old. The exceptional preservation of organic matter in Orca Basin and its location in an area with current N_2 fixation makes this site an ideal location for assessing the presence of the nifH gene in sediments. The extraction of nifH in Holocene sediments from Orca Basin was attempted at USC, Los Angeles by Juliette Finzi and Douglas Capone as well as at ETH during this study. Both tests did not show a significant abundance of this gene in the sediment, indicating that despite the good preservation of organic matter, DNA might be degraded too rapidly to find sufficient concentrations of the nifH gene in sediments. However, more detailed tests are needed to confirm this initial finding.

5.3. Coccolith-bound $\delta^{15}N$ measurements

A group of primary producers that is widely abundant is coccolithophores, or calcareous nannofossils. In this study, preliminary tests were conducted to obtain a $\delta^{15}N$ signal from sedimentary coccoliths by adapting the method established for diatoms [*Robinson et al.*, 2004]. However, several problems were encountered. Firstly, the small size of single coccoliths (2-15 μm in diameter) and the density of carbonate being very similar to that of clay minerals makes it difficult to separate the coccoliths from clays. Since the latter contains inorganic nitrogen in significant amounts compared to the small quantity of nitrogen expected in coccoliths, a separation is crucial. The first set of experiments described in this section is therefore dealing with the separation. Thereby, differential settling and SPLITT separation were assessed.

A second major difficulty was the adjustment of the analysis protocol to carbonaceous material such as to avoid the pH turning too negative (causing dissolution of carbonate) or too positive (resulting in precipitation of carbonate), while still achieving complete oxidation of the organic matter. The preliminary tests towards this aim were performed both on sedimentary fine fractions (which include the nannofossils) and on culture samples of *Emiliania huxleyi* and are described in the second part of this section.

For this test study nannofossil-rich Holocene sediments from different locations with good preservation of carbonates were used. The various samples employed were taken from the following cores: ODP core 925C, located on the Ceara Rise in the tropical Atlantic, ODP core 999A from the Colombian Basin, Caribbean Sea, core MD03-2630 from Walton Basin in the Caribbean Sea, ODP core 1240 from the eastern equatorial Pacific, core MD02-2550 from

Orca Basin, core PL07-69BC from Cariaco Basin, and core KL80 from the North Atlantic. Of these samples, those from cores 999, 1240, and 2630 were used for testing the isotopic measurements.

5.3.1. Separation of coccoliths from sediment samples

Before testing different ways to separate coccoliths from the sediment, the samples were treated as follows. The sediment was suspended in deionized water, which contained a surfactant (Triton® X-100) and had been brought to a pH of 8 by addition of NaOH. In the following, this water will be called pH8-water. The pH was routinely checked and when it fell below 8, more NaOH was added. The next step was the oxidation of the organic matter in the suspended sediments. A combination of H_2O_2 and NaOCl (bleach) was used, which has been shown to yield optimal oxidation results while keeping the pH near neutral [*Bairbakhish et al.*, 1999].Equal amounts of first NaOCl and then H_2O_2 were added to the samples, which caused a vigorous reaction in most cases. The pH of this solution was controlled regularly with a pH electrode and more H_2O_2/NaOCl was added when it increased above 8.5/decreased below 8. In some samples, pH changed significantly, so that large amounts of additional oxidant were needed. The samples were left to react overnight, after which the pH did not change considerably; in some cases the pH was adjusted by addition of a few ml of H_2O_2 or NaOCl. The samples were then wet sieved into different size fractions using pH8-water for rinsing. The coarse fraction was filtered and oven dried, whereas the small fraction (<25 μm) was left to settle and the supernatant was removed after several days. Thereby, the pH stayed between 8 and 9. The fine fractions were examined under the light microscope as well as in some samples by scanning electron microscopy (SEM), which revealed that the oxidation procedure had no effect on the preservation of coccoliths. The samples from ODP site 999 contained very well preserved coccoliths and a large fraction of carbonate, whereas preservation was less good (although still satisfactory) in ODP core 925. In both Orca Basin and Cariaco Basin, a relatively high abundance of carbonate fragments in the fine fraction makes these sites less suitable for measuring coccolith-bound $\delta^{15}N$.

5.3.1.2. Differential settling

In order to separate coccoliths from the remaining fine fraction, different settling methods were tested. First, 50 ml of suspended fine fraction of ODP core 925 with some additional Triton® X-100 was transferred to a 100 ml beaker, and shaken in the ultrasonic bath. Then it was left to settle. Calculations based on Stoke's Law predicted that, in this setup, particles smaller

than 2 µm in diameter take 4 h to settle. However, the supernatant was almost clear after 135 minutes and was therefore taken off. This was most probably due to coagulation of particles. Nonetheless, subsequent SEM analysis of the supernatant showed that it still contained different species of coccoliths, although only of small sizes. In a second set of experiments, settling was performed over a shorter distance (1.8 cm) but repeated 8-10 times. Samples from ODP cores 999 and 1240 were taken for these tests, whereby only particles smaller than 10µm were used, which were obtained by an additional sieving step. This time, the results with Triton® X-100 were compared to those with sodium polyphosphate (Na-PP) as surfactant. Since Na-PP is a strong chelating agent, which would bind Ca ions and thereby dissolve the carbonates, the Na-PP solution was first saturated with $CaCO_3$ before it was used for suspending the samples. The pH of this solution was 9. A third test was performed with ethanol, but this resulted in flocculation and was therefore not useful. Na-PP seemed to keep particles in suspension for a longer time than Triton® X-100. However, when measuring the particle size distributions of supernatants and residues on a Coulter Counter, the distributions of the supernatant were only slightly shifted towards smaller sizes. Under the microscope it was furthermore again observed for both sets of samples that coccoliths were contained in both residue and supernatant. Nonetheless, supernatants and residues from some of these samples were analyzed for their isotopic composition (see below).

5.3.1.2. SPLITT separation

A more sophisticated method for separating particles is split-flow thin fractionation (SPLITT), which has been successfully applied for the separation of diatoms from sediments

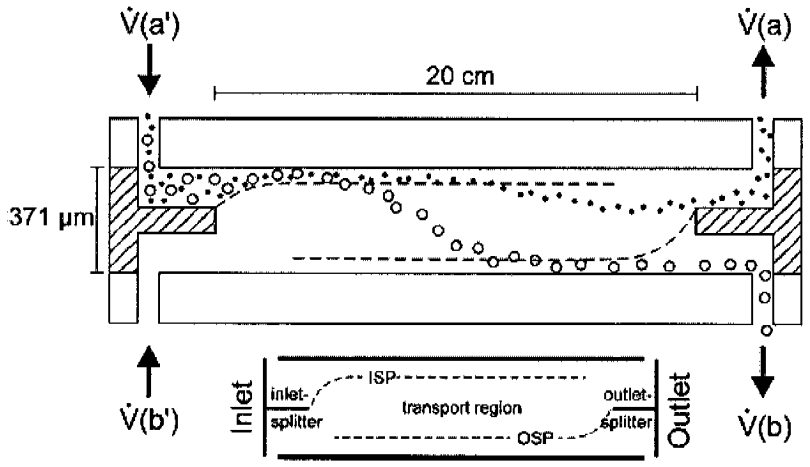

Figure 5.1. SPLITT cell setup used for the initial tests (cross section; not to scale). ISP, OSP: Inner and outer splitting planes. From *Rings et al.* [2004].

[*Rings et al.*, 2004]. However, diatoms are larger than nannofossils and have a higher density, which increases the difference in their settling behavior compared to clay. Nonetheless, experiments were performed in this study to test whether the method could be adjusted to separate smaller and more similar particles as well. The separation with SPLITT is also based on the settling speed of particles, but this time the suspension is introduced horizontally into a flow chamber, which has two inlets and two outlets (Figure 5.1). The sample suspension is added through the upper inlet, while water (in this case, pH8-water) is flowing in below. Over the length of the chamber, the heavier particles sink and leave the chamber through the lower outlet, while the lighter particles exit above. The flow velocity of the incoming suspension can be varied as well as the ratio of outflow velocities through the two exits.

To prepare the samples, they were sieved through 10 μm and 5μm micro-precision sieves (etched Ni-foil, Fritsch). The 5 μm sieve had to be treated with a few drops of the surfactant Agepon beforehand, to avoid clogging. However, for samples with high clay content (such as the one from Orca Basin), microsieving was not possible due to aggregate formation, even when more Triton® X-100 was added and the sample was frequently treated in the ultrasonic bath. The tests were therefore continued with the sample from the North Atlantic (core KL80), which contained much less clay. Light microscopy revealed that coccoliths were most abundant in the smallest size fraction (<5 μm), so this fraction was used for SPLITT. To concentrate the sample after sieving, it was left to settle for 2 days and the clear supernatant was removed.

Different combinations of input velocities (0.8 ml/min., 1.4 ml/min., and 2.0 ml/min) and outflow velocity ratios (2:1, 3:1, 4:1; upper exit:lower exit) were assessed. Since the geometry of the SPLITT cell was designed for the larger diatoms, the flow velocities used here were the lowest possible with this cell. In all cases, only minor separation could be achieved, with most of the material leaving the cell through the same exit. Depending on the velocities chosen, however, it was possible to direct the particle flow to either outlet. Thereby, the lower outlet was taken only with the lowest possible input velocity and outflow ratio (2:1). The cell geometry used for these tests does not allow a finer adjustment of the flow parameters in this low range. Therefore, if this separation method were to be tested further, the geometry of the cell would have to be such that the volume is smaller (allowing for lower flow velocities) while the separation path is longer. Another change worth testing might be the additional application of an electrical current, to take advantage of the different surface loadings of clay and carbonate particles.

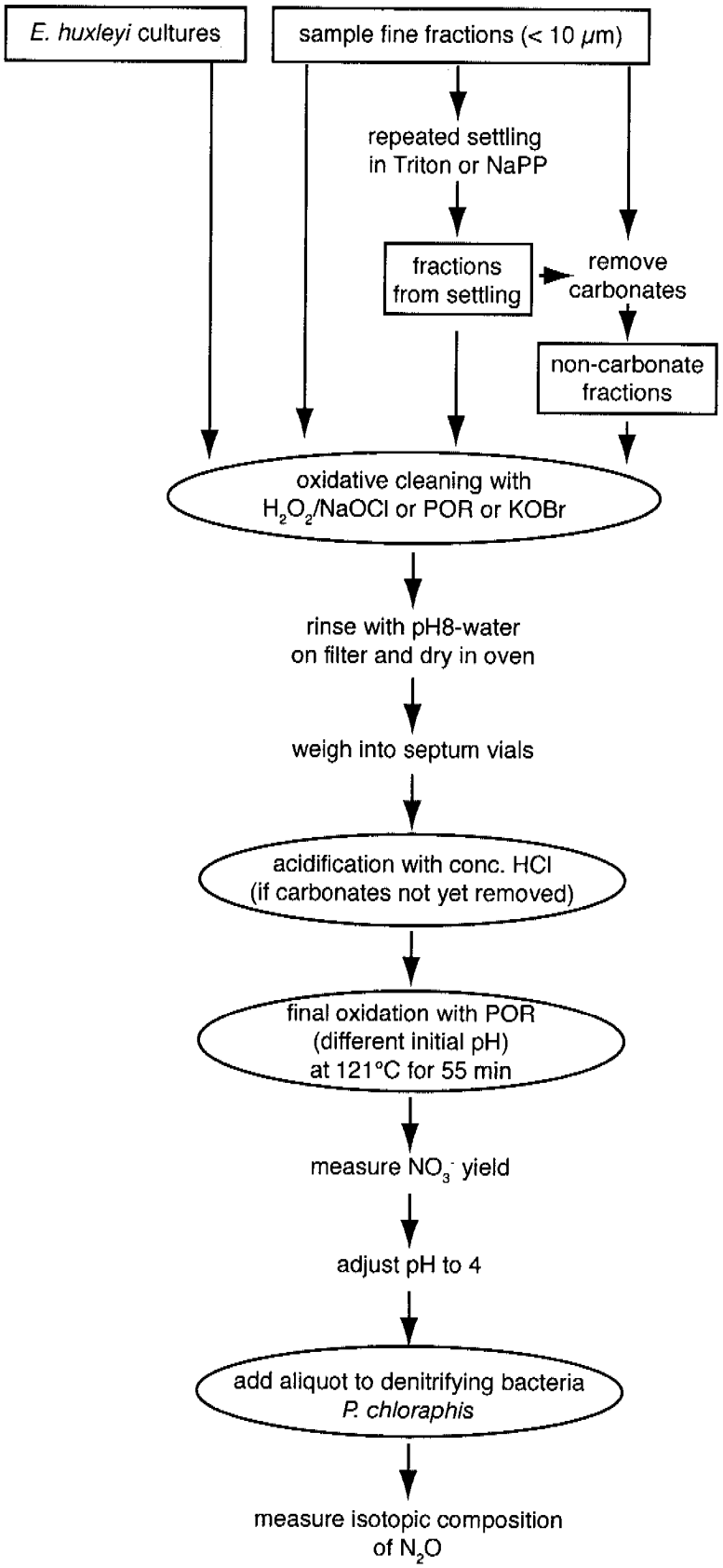

Figure 5.2. Flow chart of the method used for determining nitrogen yields and isotopic composition of coccoliths from cultures and sediments. The procedure is modified from the standard method used for diatoms [*Robinson et al.*, 2004]. NaPP is Na polyphosphate, POR is persulfate oxidation reagent. pH8-water is deionized water with NaOH for pH adjustment and Triton as surfactant.

5.3.1.3. Other separation methods

For the sample from ODP core 999, the fine fraction (<25 μm) was filtered through a 3 μm polycarbonate filter (Nuclepore). The filtering was repeated three times, whereby the remaining material was rinsed off the filter and it was sonicated for a few minutes. Nonetheless, only very little material passed the filter, which is probably rapidly clogged by the small particles.

Another separation method, which seems promising but which was not explored in this study, is froth flotation. This separation method is widely used, e.g., in the metal or the recycling industry. The principle behind is that a substance is added to the suspension, which binds specifically to the material of interest and has a hydrophobic component. Once these molecules are bound to the particles, air bubbles are sent through the suspension, which attract the hydrophobic ends of the molecules and transport them and their load to the surface as froth. There, the froth containing the desired particles can be removed. Only one published study has so far applied the method to enrich coccoliths, and although sediments with very high clay content were used in that study, a successful enrichment was reported [*Baumann and Kaulbach*, 1989]. Due to it its wide application in industry, abundant literature on this method is available and an adjustment towards the separation of coccoliths from clay should be feasible.

5.3.2. $\delta^{15}N$ determination on coccoliths

5.3.2.1. Methods

The method assessed for the analysis of coccolith-bound $\delta^{15}N$ follows closely that established for diatom-bound material [*Robinson et al.*, 2004]. The complete procedure as applied in this study is shown as a flow chart in Figure 5.2 and described in detail below. In short, after the first oxidation, sieving, and settling which have been described above, a second oxidative cleaning was performed on the fine fractions to remove all organic matter not protected inside the nannofossils. Afterwards, the samples were rinsed and dried, and the coccoliths were subsequently dissolved by addition of a strong acid, in order to liberate the organic matter inside. This organic matter was then oxidized by adding a basic potassium persulfate ($K_2S_2O_8$) solution. The amount of nitrate obtained was measured and, after neutralization, an aliquot of the sample was added to cultures of the denitrifying bacteria *Pseudosomonas Chloraphis*, which quantitatively convert nitrate to N_2O. The N_2O was finally measured for its nitrogen isotopic composition on a modified ThermoFinnigan GasBenchII and Delta Plus mass spectrometer [*Casciotti et al.*, 2002].

To test the method for coccoliths, three different sediment samples were analyzed as well as three pure culture samples of *E. huxleyi*. The sediments stem from ODP core 999 (Caribbean, Panama Basin, 139-141 cm depth), ODP core 1240 (equatorial Pacific, 18-20 cm depth) and core MD03-2630 (Caribbean, Walton Basin). Of these samples, complete fine fractions (< 10 μm) were used as well as in some cases the supernatants and residues obtained from repeated settling experiments described above (combining the supernatant solutions from the first 5 settling steps). Additionally, to assess the contribution of clay-bound nitrogen to the signal, all carbonate was removed from subsets of some samples by reaction with hydrochloric acid prior to the usual preparation for the analysis. After acidification, these samples were rinsed and dried, and the clay content was calculated by weighing the samples before and after the acidification.

For the second oxidative cleaning, the following reagents were tested: 1) again a mixture of NaOCl and H_2O_2 (adjusting the proportions so that the initial pH was between 8.5-9), whereby samples were placed in a hot water bath (at 100°C for 1h or 75°C for 2h) or 2) basic potassium persulfate (persulfate oxidation reagent, POR) in the autoclave (121°C for 55 min.), which is also used for the final oxidation step (see below), or 3) KOBr oxidation, which had been originally established to analyze ammonium within clay particles [*Silva and Bremner*, 1966]. Prior to the oxidation, the sample suspensions were centrifuged and the supernatant removed. Samples of which enough material was available were split into aliquots before the oxidative cleaning, to assess the reproducibility of the methods. After the oxidation, the samples were washed on filters and subsequently dried.

For the three culture samples of *E. huxleyi*, different cleaning methods were compared as well. One of the cultures was split into three aliquots to assess 1) the uncleaned culture in pH8-water, 2) cleaning with H_2O_2 and NaOCl at 100°C, and 3) cleaning with persulfate reagent. The two remaining culture samples were each split into two aliquots and all were cleaned twice with H_2O_2 and NaOCl at 75°C.

Of the cleaned and dried samples, around 15-20 mg and 1-5 mg for sediments and culture samples, respectively, were weighed into septum-capped glass vials and acidified by injecting 35 μl of concentrated HCl. The samples were vortexed and allowed to react for 30 minutes, after which 1.5 ml of the basic persulfate solution was added. This reagent was prepared freshly by adding 6 g NaOH and 4.5 g $K_2S_2O_8$ to 75 ml deionized water [*Knapp et al.*, 2005]. Per set of samples, several blanks consisting of different volumes of the persulfate reagent, and in one case a laboratory standard ('BOIL-2', 4 mg) were prepared the same way, but not acidified. To check for nitrate contamination, 12 ml of the pH8-water was also measured, using 2 ml of the persulfate reagent. The final oxidation step was performed in the autoclave at 121 °C for 55 minutes. As precipitates formed due to the high pH, the performance of the oxidation was tested after lowering the initial pH of the reagent solution by adding small amounts of HCl until the

pH was at 9-10, by leaving out the NaOH completely (pH 5-6), and by acidifying a persulfate solution with sulfuric acid.

After the samples had cooled, 1.5 ml of deionized water was added to each vial before nitrate concentrations were measured by chemiluminescence [*Braman and Hendrix*, 1989]. Afterwards, the pH of the samples was adjusted to around 4, and aliquots were added to the tubes containing denitrifying bacteria cultures so that equal amounts of 15 or 20 nmol NO_x were inserted. Were precipitate was present, only the supernatant was taken up. 5 standards (IAEA N3 nitrate) in different concentrations were also denitrified with each batch and the results corrected for any shift in their values.

5.3.2.2. Results and Discussion

Blanks and Standard

Nitrate concentrations in the blanks varied for most runs between 0.7 and 2.0 μM, which is around 1/10 of the concentrations obtained from the samples. An exception is one run where the blank was higher than 3 μM, amounting to 1/3 to 1/2 of the sample nitrate yield. The samples of this run are indicated by asterisks in Tables 5.1 and 5.2. The laboratory standard (BOIL-2) was in the run with the high blank values. Even when corrected for the blank, it yielded nitrate concentrations that were somewhat higher than normal (14.6 μM versus a normal concentration of 11-12 μM) and its isotopic composition was more depleted than normal (1.4‰ versus a normal value of around 2.3‰). This observation indicates that isotopic compositions and nitrate concentrations from that run might contain a bias due to contamination. Nitrate concentration in the pH8-water was negligible.

Non-carbonate material

The determination of non-carbonate concentrations in the sediment samples revealed that the sample from core 999 contained approximately twice as much clay as the equatorial Pacific sample (around 60% and around 30%, respectively; Table 5.1). The data furthermore confirm that no clear separation was achieved by repeated settling. Nitrate yields from the non-carbonate fractions measured are variable, but on the same order as nitrate yields from whole fine fraction samples, implying that nitrogen bound to clay constitutes a major part of the nitrogen measured by our method. This is supported by the fact that the isotopic values of the non-carbonate fractions are similar to those from the whole samples. Nitrogen deliberated from coccoliths during the acid treatment could, however, have been partly adsorbed by clay and might contribute to

Table 5.1. Concentrations of non-carbonate material in fine fractions (<10 μm) of whole samples from ODP cores 1240 (equatorial Pacific) and 999 (Caribbean) as well as in supernatants and residues from settling experiments. Triton® and Na polyphosphate (NaPP) are different surfactants used for settling. Also given are nitrogen yields and isotopic compositions where determined. *high blank nitrate concentrations measured in this run.

sample	Fraction non-carbonate (weight %)	N yield (μmol/g)	$\delta^{15}N$ (‰)
1240 whole fine fraction	28.4	--	--
1240 Triton supernatant	15.6	--	--
1240 Triton residue	28.9	--	--
1240 NaPP supernatant	36.2	--	--
1240 NaPP residue	30.5	--	--
999 whole fine fraction	66.4	1.61*	2.3*
999 NaPP supernatant	55.8	3.31*	3.4*
999 NaPP residue	60.8	1.94*	2.8*

the large concentrations. Nonetheless, these results caution against the measurement of coccolith-bound nitrogen without prior separation from clays.

Oxidative cleaning

With all oxidation methods tested here, the pH increased above 11 after the reaction, which led to precipitation, probably involving carbonates. The precipitate could be problematic because nitrogen liberalized by the oxidative cleaning might bind to these secondary minerals and would therefore not be removed. In addition, the samples that were cleaned with KOBr formed a solid crust after drying, which was hard to homogenize.

Although most oxidations were performed in triplicates, the large variability in both nitrate yields and its isotopic composition (Table 5.2) complicates an assessment of which of the four cleaning methods tested here is suited best. The Persulfate oxidation consistently yielded the lowest nitrate concentrations, which could be a sign of most complete oxidation of organic matter outside the carbonates. However, it could also imply that the oxidation was too strong and nitrogen was leached out of the nannofossils. The most consistent results concerning nitrate yields seem to be reached with either H_2O_2/NaOCl (75°C, 2h) or with KOBr, although it is important to keep in mind that the results from the other two treatments might be affected by contamination, as revealed by high nitrate concentrations in the blanks.

Table 5.2. Comparison of different oxidative cleaning methods for nitrogen yields and isotopic composition. POR is persulfate oxidation reagent. Samples were split into 2-3 aliquots before the oxidation. Samples were from ODP cores 1240 and 999 as well as core MD03-2630 (Caribbean). *high blank nitrate concentrations measured in this run (see text).

Cleaning method	POR		H_2O_2/NaOCl 100°C, 1h		H_2O_2/NaOCl 75°C, 2h		KOBr	
core	N yield (µmol/g)	$\delta^{15}N$ (‰)	N yield (µmol/g)	$\delta^{15}N$ (‰)	N yield (µmol/g)	$\delta^{15}N$ (‰)	N yield (µmol/g)	$\delta^{15}N$ (‰)
1240	2.09*	4.9*	3.86*	2.0*	2.85	-0.5	2.54	5.6
	0.87*	2.9*	3.78*	-2.0*	2.60	5.4	1.95	5.8
	1.90*	-8.2*	--	--	2.43	5.7	2.46	-1.8
999	1.42*	2.5*	1.86*	4.5*	2.31	1.9	2.15	3.0
	1.24*	-0.4*	2.06*	4.7*	2.34	3.8	1.49	3.2
	1.27*	0.4*	--	--	2.41	-3.0	2.88	-6.2
2630	--	--	--	--	16.50	3.5	10.32	3.8
	--	--	--	--	16.05	3.2	8.94	4.4
	--	--	--	--	15.35	3.2	8.91	3.9

pH of final oxidation

The performance of the final persulfate oxidation was tested with a lower initial pH of the reagent compared to the standard method, with the aim to avoid reprecipitation. After autoclaving, the pH was below 1 even for the samples with initial pH of 5-6 and 9-10. Nonetheless, precipitates formed in those samples that had been cleaned with persulfate, whereby precipitation seemed stronger in the samples with initial pH of 9-10 when compared to those with pH 5-6. For the samples cleaned with H_2O_2/NaOCl, no or little precipitation was observed with the

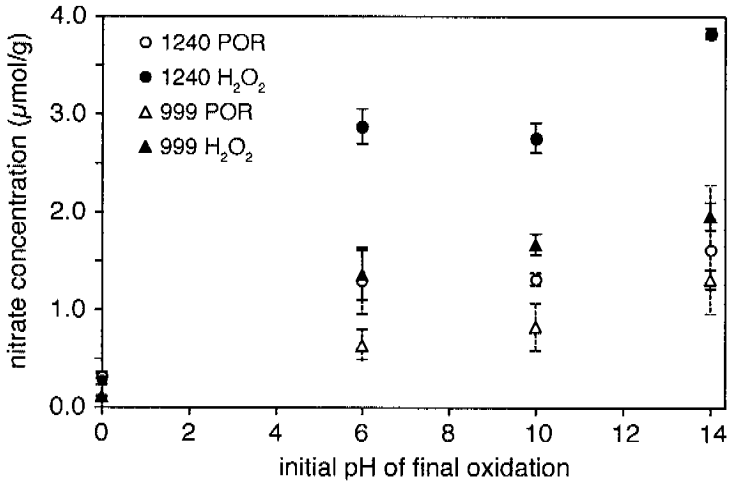

Figure 5.3. Effect of initial pH of the persulfate reactant on the nitrate yield. Shown are the samples from ODP cores 1240 (dots) and 999 (triangles), each treated with two different methods for oxidative cleaning, namely persulfate oxidation (POR, open symbols) and H_2O_2/NaOCl (closed symbols). All samples were cleaned in duplicates (H_2O_2) or triplicates (POR), the standard deviations are shown by the error bars.

Table 5.3. Effect of lowering the initial pH of the persulfate reagent used for the final oxidation on nitrate yields (and isotopic composition). Values for pH 14 are in Table 5.2. Samples were from ODP cores 1240 and 999, treated with different oxidative cleaning methods (POR is persulfate oxidation reagent).

Initial pH of final oxidation	0-1		5-6		9-10	
	N yield (µmol/g)	$\delta^{15}N$ (‰)	N yield (µmol/g)	$\delta^{15}N$ (‰)	N yield (µmol/g)	$\delta^{15}N$ (‰)
1240 POR cleaned	0.30	--	1.68	--	1.29	--
	0.34	--	1.05	--	1.38	--
	0.29	--	1.15	--	1.26	--
1240 H_2O_2/NaOCl cleaned	0.34	--	2.75	--	2.86	--
	0.24	--	3.00	--	2.65	--
999 POR cleaned	--	--	0.80	--	1.10	1.30
	--	--	0.62	--	0.68	5.21
	--	--	0.50	--	0.68	4.06
999 H_2O_2/NaOCl cleaned	0.10	--	1.17	8.31	1.59	8.66
	0.11	--	1.53	0.90	1.74	5.93

lowered pH. The nitrate concentrations measured after the oxidation revealed that the oxidation does not occur under acidic conditions, whereas a reagent with an initial pH of 9-10 and 5-6 yielded significant concentrations of nitrate (Figure 5.3 and Table 5.3). However, nitrate yields decreased with initial pH, indicating incomplete oxidation. This observation cautions against lowering the initial pH of the persulfate reagent. Instead, a different oxidation method needs to be explored which performs well at neutral pH.

Culture samples

Comparison of the results from different treatments of the culture samples of *E. huxleyi* revealed again that the persulfate cleaning leads to lower nitrate yields compared to the H_2O_2/NaOCl treatment (Table 5.4). Repeating the H_2O_2/NaOCl cleaning step, however, yielded similar nitrate concentrations as the POR cleaning. The different nitrate yields from different cleaning protocols might indicate that not all nitrogen has been removed from the outside of the coccoliths. Therefore, it is presently not clear how much nitrogen is bound inside the coccoliths, but it seems to be very little.

The isotopic composition of the liberated nitrate was variable, even among aliquots of the same culture sample. Furthermore no clear relationship between nitrate yield and isotopic composition could be detected. Such a trend would be expected if the obtained nitrate stemmed

Table 5.4. Nitrate yields and isotopic composition of *E. huxleyi* culture samples treated with different cleaning methods. POR is persulfate oxidation reagent. The three available culture samples were split into aliquots before cleaning. One sample was analyzed twice for its isotopic composition.

Culture No.	Cleaning method	N yield (µmol/g)	$\delta^{15}N$ (‰)
1	No cleaning	206.74	-2.77
1	H_2O_2/NaOCl 100°C	76.14	8.11 8.66
1	POR	16.70	2.34
2	H_2O_2/NaOCl 75°C, 2 x	11.28	2.7
2	H_2O_2/NaOCl 75°C, 2 x	17.08	6.2
3	H_2O_2/NaOCl 75°C, 2 x	6.66	2.9
3	H_2O_2/NaOCl 75°C, 2 x	7.09	--

from a mixture of nitrogenous compounds inside and outside the coccoliths, with the latter being removed to a varying degree by the different cleaning treatments.

5.3.3. Conclusions and Outlook

The initial tests on measuring the isotopic composition of coccolith-bound nitrogen revealed several difficulties. Firstly, a good separation of coccoliths from clay minerals seems crucial due to interference of clay-bound inorganic nitrogen with the signal from the small amounts of nitrogen contained in the coccoliths. The methods tested in this study, namely repeated settling and SPLITT separation, did not allow a satisfactory separation. As size, density and shape of clay minerals and coccoliths are very similar, additional characteristics must be exploited in future studies, such as different surface properties. In this regard, froth flotation seems to be a promising method [*Baumann and Kaulbach*, 1989], as well as modifications of the SPLITT cell such as adding an electric field. A second difficulty encountered was precipitation of minerals due to high pH during the oxidation steps in the protocol for the extraction of coccolith-bound nitrogen. For applying this method to carbonaceous fossils, the methodology therefore has to be improved to achieve complete oxidation while keeping the pH near neutral.

In order to circumvent the interference of clay-bound nitrogen, other fossils typically found in sediments underlying oligotrophic regions could be investigated. One possibility is calcareous dinoflagellate cysts, which are abundant in the subtropical and tropical ocean [e.g., *Dale*,

1992; *Karwath et al.*, 2000; *Zonneveld et al.*, 2000]. The most common species in these latitudes, *Thoracosphaaera heimii*, is a phototrophic species (in contrast to many heterotrophic dinoflagellates). Indeed, the cysts (thoracosphaerids) were present in the samples from the tropical and subtropical Atlantic. They were predominantly found in the 10-38 μm size range and could probably be separated from the sediment due to their spherical shape. However, knowledge about the ecology of this species is presently still limited, complicating the interpretation of the nitrogen isotopic signal.

Another large calcareous plankton group are foraminifera, which are ubiquitous heterotrophic organisms. The isotopic composition of foram-bound nitrogen has been first explored by *Altabet and Curry* [1989]. Unfortunately, the heterotrophic nature of foraminifera adds further complication to the interpretation of the isotopic signal due to food web effects [*Altabet and Small*, 1990; *Wu et al.*, 1997]. Advantages of this group are, however, that their behavior has been well studied and that they can be easily picked from sediment samples. In order to minimize food web effects on their nitrogen isotopic composition, species should be selected which do not have symbionts or spines, as the latter are used to catch zooplankton prey. Furthermore, the trophic effects could be best accounted for if the nitrogen isotopic composition is measured in parallel in different species. In order to measure nitrogen bound to these microfossils, however, the method needs to be adjusted to carbonaceous material to avoid precipitation during the oxidative treatments.

In conclusion, although several obstacles have to be overcome, measurement of the isotopic composition of nitrogen preserved in calcareous microfossils is a very promising approach and should be further pursued. Thereby, the best target at present seems to be foraminifera. Together with a development of biomarkers and potentially molecular biological methods for assessing N_2 fixation (see section 2 of this chapter), such a tool would greatly enhance our ability to assess past changes in N_2 fixation and study long-term variations in the marine nitrogen budget.

Acknowledgements

Many people contributed to this work: Julius Lipp and Daniel Birgel aided with the biomarker measurements at Bremen University. The initial assessment of nifH gene abundance at ETH was performed together with Sandra Scherrer. Hans Thierstein, Ursula Brupbacher, Hsin-Chi Lan, and Ruth Prelicz helped with the settling experiments and microscopic analyses at ETH. The SPLITT separation was tested at the Forschungszentrum Jülich together with Jörn Parplies. Gerhard Schleser and Andreas Lücke are gratefully acknowledged for the opportunity to use their facilities and for helpful discussions. Finally, the first tests towards coccolith-bound

$\delta^{15}N$ measurements were carried out at Princeton University together with Rebecca Robinson and Brigitte Brunelle and profited from discussions with Daniel Sigman.

References

Altabet, M. A., and W. B. Curry (1989), Testing models of past ocean chemistry using foraminifera 15N/14N, *Global Biogeochem. Cycles*, *3*, 107-119.

Altabet, M. A., and L. F. Small (1990), Nitrogen Isotopic-Ratios in Fecal Pellets Produced by Marine Zooplankton, *Geochim. Cosmochim. Acta*, *54*, 155-163.

Bairbakhish, A. N., J. Bollmann, C. Sprengel, and H. R. Thierstein (1999), Disintegration of aggregates and coccospheres in sediment trap samples, *Marine Micropaleontology*, *37*, 219-223.

Baumann, M., and R. Kaulbach (1989), Concentrating Calcareous Nannoplankton in Clay-Rich Sediments by Froth-Flotation, *Journal of Sedimentary Petrology*, *59*, 615-617.

Braman, R. S., and S. A. Hendrix (1989), Nanogram Nitrite and Nitrate Determination in Environmental and Biological-Materials by Vanadium(Iii) Reduction with Chemi-Luminescence Detection, *Analytical Chemistry*, *61*, 2715-2718.

Carpenter, E. J., H. R. Harvey, B. Fry, and D. G. Capone (1997), Biogeochemical tracers of the marine cyanobacterium Trichodesmium, *Deep-Sea Res. Part I*, *44*, 27-38.

Casciotti, K. L., D. M. Sigman, M. G. Hastings, J. K. Bohlke, and A. Hilkert (2002), Measurement of the oxygen isotopic composition of nitrate in seawater and freshwater using the denitrifier method, *Analytical Chemistry*, *74*, 4905-4912.

Dale, B. (1992), Dinoflagellate contribution to the open ocean sediment flux, in *Dinoflagellate contributions to the Deep Sea*, edited by B. Dale and A. Dale, pp. 1-32, Woods Hole Oceanographic Institution, Woods Hole, Massachusetts.

Falcon, L. I., F. Cipriano, A. Y. Chistoserdov, and E. J. Carpenter (2002), Diversity of diazotrophic unicellular cyanobacteria in the tropical North Atlantic Ocean, *Applied and Environmental Microbiology*, *68*, 5760-5764.

Karwath, B., D. Janofske, and H. Willems (2000), Spatial distribution of the calcareous dinoflagellate Thoracosphaera heimii in the upper water column of the tropical and equatorial Atlantic, *International Journal of Earth Sciences*, *88*, 668-679.

Kenig, F., J. S. S. Damste, A. C. K. Dalen, W. I. C. Rijpstra, A. Y. Huc, and J. W. Deleeuw (1995), Occurrence and Origin of Monomethylalkanes, Dimethylalkanes, and Trimethylalkanes in Modern and Holocene Cyanobacterial Mats from Abu-Dhabi, United-Arab-Emirates, *Geochim. Cosmochim. Acta*, *59*, 2999-3015.

Knapp, A. N., D. M. Sigman, and F. Lipschultz (2005), N isotopic composition of dissolved organic nitrogen and nitrate at the Bermuda Atlantic time-series study site, *Global Biogeochem. Cycles*, *19*.

Köster, J., J. K. Volkman, J. Rullkötter, B. M. Scholz-Böttcher, J. Rethmeier, and U. Fischer (1999), Mono-, di- and trimethyl-branched alkanes in cultures of the filamentous cyanobacterium Calothrix scopulorum, *Org. Geochem.*, *30*, 1367-1379.

MacGregor, B. J., B. Van Mooy, B. J. Baker, M. Mellon, P. H. Moisander, H. W. Paerl, J. Zehr, D. Hollander, and D. A. Stahl (2001), Microbiological, molecular biological and stable isotopic evidence for nitrogen fixation in the open waters of Lake Michigan, *Environmental Microbiology*, *3*, 205-219.

Ohkouchi, N., Y. Nakajima, H. Okada, N. O. Ogawa, H. Suga, K. Oguri, and H. Kitazato (2005), Biogeochemical processes in the saline meromictic Lake Kaiike, Japan: implications from molecular isotopic evidences of photosynthetic pigments, *Environmental Microbiology*, *7*, 1009-1016.

Pantoja, S., D. J. Repeta, J. P. Sachs, and D. M. Sigman (2002), Stable isotope constraints on the nitrogen cycle of the Mediterranean Sea water column, *Deep-Sea Res. Part I*, *49*, 1609-1621.

Rings, A., A. Lucke, and G. H. Schleser (2004), A new method for the quantitative separation of diatom frustules from lake sediments, *Limnol. Oceanogr.-Methods*, *2*, 25-34.

Robinson, R. S., B. G. Brunelle, and D. M. Sigman (2004), Revisiting nutrient utilization in the glacial Antarctic: Evidence from a new method for diatom-bound N isotopic analysis, *Paleoceanography*, *19*.

Robinson, R. S., D. M. Sigman, P. J. DiFiore, M. M. Rohde, T. A. Mashiotta, and D. W. Lea (2005), Diatom-bound N-15/N-14: New support for enhanced nutrient consumption in the ice age subantarctic, *Paleoceanography*, *20*, PA3003, doi:10.1029/2004PA001114.

Rohmer, M., P. Bouviernave, and G. Ourisson (1984), Distribution of Hopanoid Triterpenes in Prokaryotes, *Journal of General Microbiology*, *130*, 1137-1150.

Sachs, J. P., and D. J. Repeta (1999), Oligotrophy and nitrogen fixation during eastern Mediterranean sapropel events, *Science*, *286*, 2485-2488.

Sachs, J. P., D. J. Repeta, and R. Goericke (1999), Nitrogen and carbon isotopic ratios of chlorophyll from marine phytoplankton, *Geochim. Cosmochim. Acta*, *63*, 1431-1441.

Sigman, D. M., M. A. Altabet, R. Francois, D. C. McCorkle, and J. F. Gaillard (1999), The isotopic composition of diatom-bound nitrogen in Southern Ocean sediments, *Paleoceanography*, *14*, 118-134.

Silva, J. A., and J. M. Bremner (1966), Determination and Isotope-Ratio Analysis of Different Forms of Nitrogen in Soils .5. Fixed Ammonium, *Soil Science Society of America Proceedings*, *30*, 587-&.

Summons, R. E., L. L. Jahnke, J. M. Hope, and G. A. Logan (1999), 2-Methylhopanoids as biomarkers for cyanobacterial oxygenic photosynthesis, *Nature*, *400*, 554-557.

Talbot, H. M., R. Summons, L. Jahnke, and P. Farrimond (2003), Characteristic fragmentation of bacteriohopanepolyols during atmospheric pressure chemical ionisation liquid chromatography/ion trap mass spectrometry, *Rapid Communications in Mass Spectrometry*, *17*, 2788-2796.

Wu, J. P., S. E. Calvert, and C. S. Wong (1997), Nitrogen isotope variations in the subarctic northeast Pacific: Relationships to nitrate utilization and trophic structure, *Deep-Sea Res. Part I*, *44*, 287-314.

Zehr, J. P., E. J. Carpenter, and T. A. Villareal (2000), New perspectives on nitrogen-fixing microorganisms in tropical and subtropical oceans, *Trends in Microbiology*, *8*, 68-73.

Zonneveld, K. A. F., A. Brune, and H. Willems (2000), Spatial distribution of calcareous dinoflagellate cysts in surface sediments of the Atlantic Ocean between 13 degrees N and 36 degrees S, *Review of Palaeobotany and Palynology*, *111*, 197-223.

Chapter 6

Holocene climate variability in the Mississippi catchment as inferred from Gulf of Mexico sediments*

Abstract

We present a high-resolution (decadal scale) Holocene record of elemental composition in sediments from Pigmy Basin in the Gulf of Mexico. The contributions of terrigenous elements, such as Fe, Ti, Si, K, and Al exhibit large and consistent variations throughout the Holocene. Overall higher terrigenous contributions are apparent in the early to mid-Holocene as well as in the late Holocene between 2.5 and 1.0 ka. We interpret increased abundance of terrigenous elements as higher sediment input by the Mississippi River. In the early Holocene, Mississippi input seems mostly related to dynamics of the Laurentide Ice Sheet remains and associated pro-glacial lakes. In contrast, since the mid-Holocene, generally high Mississippi sediment input coincides with periods of strong summer insolation, dry conditions in central North America, warm Gulf of Mexico temperatures and inferred La Niña-like conditions including a northward displacement of the intertropical convergence zone (ITCZ). The most probable explanation for high sediment input under these conditions is increased erosion in the Mississippi catchment due to a combination of reduced plant cover and a higher frequency of extreme hydrological events.

*in preparation as A.N. Meckler, P. Dulski, R.Z. Poore, U.Röhl, G.H. Haug, Holocene climate variability in the Mississippi catchment as inferred from Gulf of Mexico sdiments.

6.1. Introduction

With the increasing availability of high-resolution climate records from the Holocene (the last 10,000 years), it has become obvious that this period has been by far not as stable as previously thought. Holocene climate variability has been observed at a range of timescales: Long-term changes in the earth's orbital parameters caused increased seasonality in the northern hemisphere during the early Holocene, whereas multi-centennial to decadal-scale periodic variability has been linked to changes in solar activity [e.g., *Bond et al.*, 2001; *Mayewski et al.*, 2004]. In addition, many climate records show short events or sudden regime shifts, such as the 8.2 ka cold event in the northern hemisphere [*Alley et al.*, 1997; *Rohling and Pälike*, 2005] or the desertification of the Sahara at about 5 ka [*deMenocal et al.*, 2000]. Much of the observed Holocene variability has not been satisfactorily explained so far.

Many of the observed Holocene climate changes affected the hydrological cycle, which had a large impact on the environment and on human societies. One of the regions that are very susceptible to changes in precipitation is central North America. In this region, major droughts have occurred throughout the Holocene, some of which had a serious impact on human populations in these areas. A well-known example is the Dust Bowl period in the 1930s in the Great Plains. The demise of the ancient pueblo cultures on the Colorado Plateau after 1200 AD might also have been connected to changes in precipitation patterns [*Dean*, 1994; *Polyak and Asmerom*, 2001].

The climate in central North America is influenced by three major air masses: dry Pacific air descending from the Rocky Mountains, cold and dry Arctic air, and warm and moist air coming from the Gulf of Mexico. The main climatic forcing factors are the following: In winter, the north-south temperature contrast is largest and central North American climate is dominated by weather systems following the path of the jet stream (Figure 6.1A). In summer, the jet stream is weak and strong high-pressure systems in the Atlantic (Bermuda High) and the eastern Pacific intensify (Figure 6.1B). In addition, thermal heating of the Colorado Plateau induces low surface pressure in the Southwest and results in the so-called southwest monsoon. The moist monsoonal air masses are derived from both the Pacific and the Gulf of Mexico [*Adams and Comrie*, 1997].

The Great Plains experience semiarid to subhumid climate and rely mainly on summer precipitation associated with mesoscale convective complexes at the confluence of southern and northern air masses [*Woodhouse and Overpeck*, 1998]. Moisture transport to this region is enhanced by nocturnal low-level jets coming from the Gulf of Mexico, which are thought to be westward extensions of the Bermuda High. The flow of southern air to the mid-continent can be hindered when a blocking high develops over the Great Plains, which is probably associated

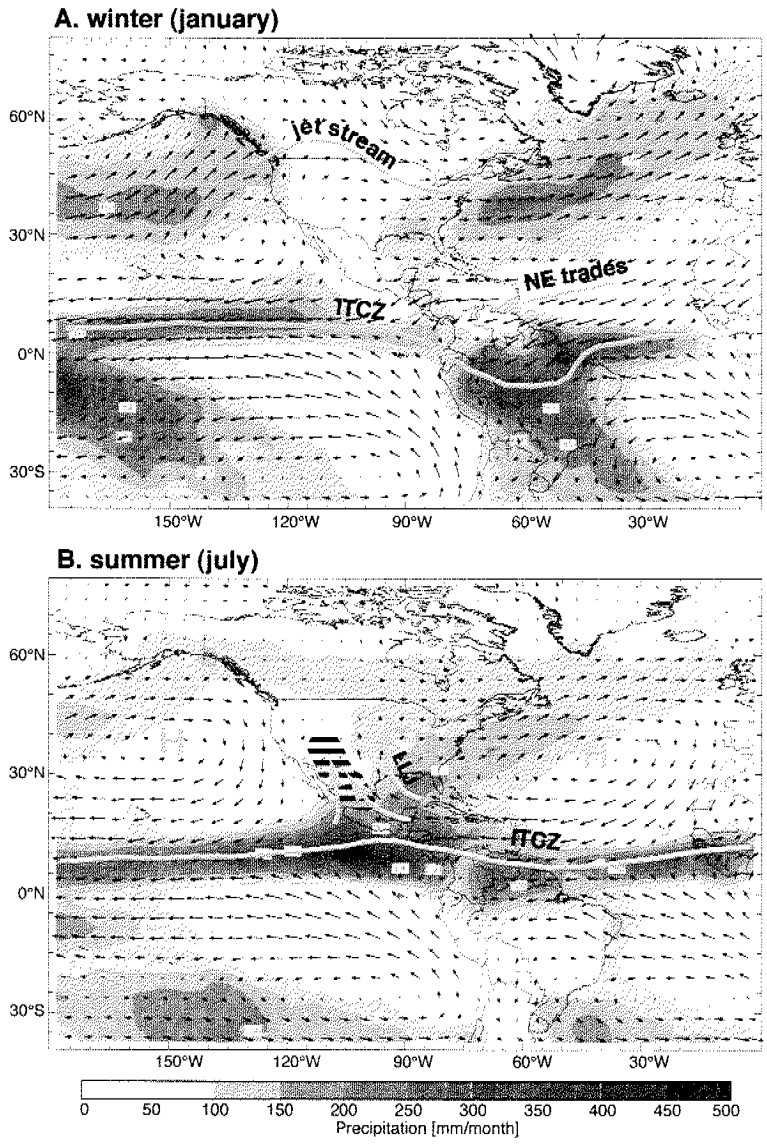

Figure 6.1. General circulation and precipitation (shading) patterns in winter (A) and summer (B). Maps taken from http://iridl.ldeo.columbia.edu/maproom. The hatched area is influenced by the south-west monsoon. ITCZ is intertropical convergence zone and LLJ is low level jet. Black arrows represent surface winds (925 mb).

with a strong heat low in the monsoon region [*Higgins et al.*, 1997; *Woodhouse and Overpeck*, 1998].

Several multi-annual to multi-decadal climate modes influence precipitation over North America. Strong La Niña events lead to dryer winter conditions in the southwest and wetter winters in the northwest [*Cole et al.*, 2002; *Brown and Comrie*, 2004]. The spatial extent of the winter precipitation anomaly, on the other hand, is variable and might be connected to the state of the (North) Pacific decadal oscillation (PDO). Thereby, negative PDO phases, i.e. cool north-east and tropical Pacific and warm central North Pacific, enhance the effect of La Niña conditions [*Cole et al.*, 2002]. The reason for the observed pattern (wet northwest and dry southwest) is that both La Niña and cool PDO phases result in a northward displacement of the average

jet stream position. Dry winters in the southwest, in turn, are often followed by strong summer monsoons [*Higgins and Shi*, 2000]. In addition to the Pacific influence, multidecadal variations in North Atlantic sea surface temperatures (SSTs) have also been invoked as driver for North American precipitation, with warmer SST resulting in decreased central North American rainfall [*Enfield et al.*, 2001; *McCabe et al.*, 2004]. *Hu and Feng* [2001] distinguish between phases when central North American precipitation is coupled to ENSO (El Niño - Southern Oscillation) and those periods when variations in southerly moisture flux are the dominant factor. Two reasons for this shift between forcing factors are discussed: Multidecadal variations in central North Pacific SST, with warm phases favoring an ENSO-response, and northern hemispheric mean temperature, whereby southerly flow is the dominant control under generally warm conditions.

Paleoclimate reconstructions from lake sediments and dune fields revealed very dry conditions in the Great Plains in the early to mid-Holocene, although onset and duration of the dry period varied between the different archives [e.g., *Forman et al.*, 1995; *Laird et al.*, 1996; *Dean*, 1997; *Yu et al.*, 1997]. In the early Holocene, the retreating Laurentide ice sheet still had a significant influence on North American climate, probably resulting in a stronger and southward-displaced jet stream. Another important factor was the northern hemispheric summer insolation maximum and winter insolation minimum [*Laskar et al.*, 2004]. Model results show that summer conditions changed already in the deglacial, while colder winter conditions persisted far into the Holocene [*Bartlein et al.*, 1998].

Whereas the mid-continent experienced prolonged drought periods, most existing data from the southwest indicate wetter mid-Holocene conditions [*Harrison et al.*, 2003, and references therein]. This has been interpreted as increased strength of the southwest monsoon, which could in turn have induced increased subsidence over the Great Plains. Changes in the surface conditions in the Gulf of Mexico, inferred from foraminiferal assemblage shifts, have been related to these variations in monsoon strength [*Poore et al.*, 2005]. Thereby, an increased occurrence of the tropical species *Globigerinoides sacculifer*, for example in the mid-Holocene, coincided with wetter conditions in the monsoon region.

Due to local effects at the respective sites, the abundant North American paleoclimate records are far from being unequivocal. A more integrative signal of North American climate variability might be obtained by assessing changes in Mississippi River discharge. The Mississippi River system drains almost half of the conterminous United States. Integrating over such a big area, this signal overcomes problems associated with local effects on paleo-archives. On the other hand, opposite climate changes in different parts of the catchment could be averaged out. Latitudinal shifts in the climate system, which strongly affect locally confined archives, will not have as much influence on the Mississippi River discharge, which records mainly overall

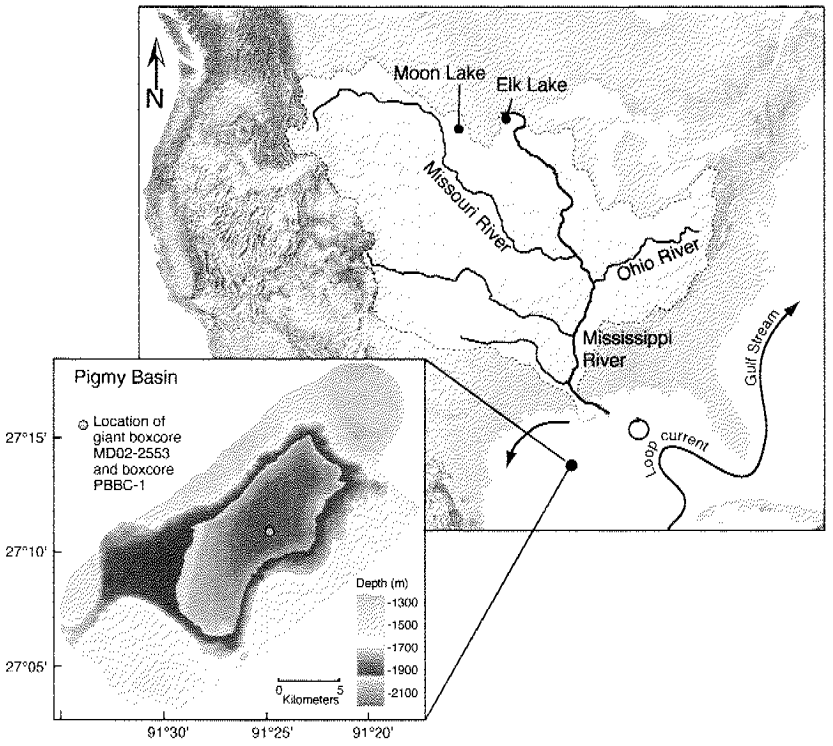

Figure 6.2. Mississippi River catchment and location of cores MD02-2553 and PB BC-1E in Pigmy Basin. Also plotted is the circulation pattern in the Gulf of Mexico with the Loop Current coming from the Caribbean and associated eddies, as well as the coastal current transporting the Mississippi plume westwards. Locations of the lake records used for comparison are also shown.

changes in central North American precipitation. Such a record can therefore not replace the information gained from terrestrial archives but would instead be highly complementary.

The Mississippi River is by far the largest sediment source to the Gulf of Mexico [*Davies and Moore*, 1970]. The tributary contributing most to overall runoff is the Ohio River, reflecting the higher precipitation in the eastern part of the Mississippi catchment. Most of the sediment load, however, is derived from the Missouri catchment [*Turner and Rabalais*, 2004]. At the mouth of the Mississippi River, the highest sediment load is associated with increasing discharge during flood events [*Mossa*, 1996]. Today, Mississippi runoff peaks in April and May.

In this study, we attempt to reconstruct Mississippi transport by assessing variations in the amount of terrigenous material delivered to the Gulf of Mexico. We use the same core as *Poore et al.* [2003; 2005], to allow for a direct comparison with the *G. sacculifer* abundance data.

6.2. Materials and Methods

To assess changes in terrigenous input we measured the elemental composition of two sediment cores from Pigmy Basin in the Gulf of Mexico, located around 250 km southwest of the Mississippi River mouth (Figure 6.2). The basin has a flat bottom at around 2300 m water depth and is surrounded by salt diapirs, which have blocked a former canyon [*Bouma and Stelting*, 1986]. Core MD02-2553 was taken from the basin center in 2002 during IMAGES cruise VIII (PAGE). The giant box core is 10.3 m long and a continuous sub-sample was obtained with U-channels. The U-channels used were designed and developed at the Paleomagnetism and Environmental Magnetism laboratory of the LSCE, Gif-sur-Yvette. Box core PBBC-1 was taken on the RV Longhorn at approximately the same location as the giant box core. The subcore BC-1E was used for this study and has also been sampled with a U-channel.

Pigmy Basin is not anoxic, as shown by the presence of benthic foraminifera [*R. Poore*, unpublished results], and the sediment is not laminated. A few distinct sandy layers were observed in core MD02-2553, occurring at 67-68 cm and at 308-312 cm depth in the Holocene part of the core (approximately the upper 450 cm). Upward grading above some of these layers suggests that they are part of small turbidites. The fact that the sand consists mainly of well-preserved, intact foraminifera indicates that the material was not transported very far and therefore probably stems from the sides of the basin. One much thicker graded interval, consisting of one larger and several small turbidites, was found in the deglacial section of the core (978-996 cm). In addition to the easily visible sand layers, several silt laminae were observed, which were usually very thin but in some cases up to 0.5 cm thick. In the Holocene sections, the thicker silt layers were observed at 122 cm, 225 cm, and 230 cm depth. Otherwise, the sediment appeared very homogenous. No coarse layers were found in core PB-BC1E.

To analyze the elemental composition of the sediment we used XRF core scanning, determining contributions of Fe, Ca, Ti, K, Si, Al, and Mn. Core MD02-2553 was scanned at Bremen with a resolution of 1cm (whole core) and 2 mm (upper 450 cm). Core BC1E as well as, for comparison, the top section of 2553 were scanned in Potsdam at 500 μm resolution (spot size of 400 μm). The Potsdam scanner (EAGLE III BKA; Röntgenanalytik Messtechnik GmbH) obtains point measurements, whereas the Bremen scanner (AVAATECH) measures an area of 1cm width and a length according to the desired resolution. The results were compared for the part of MD02-2553 measured on both machines. In order to assess possible turbidites in the cores, x-radiographs were obtained for some U-channels and grain size measurements were conducted in selected intervals.

The age models for the two cores (Figure 6.3) rely on foraminiferal ^{14}C dates. For core MD02-2553, 20 dates have been obtained from the upper 4 m, covering the last 13 kyrs. The

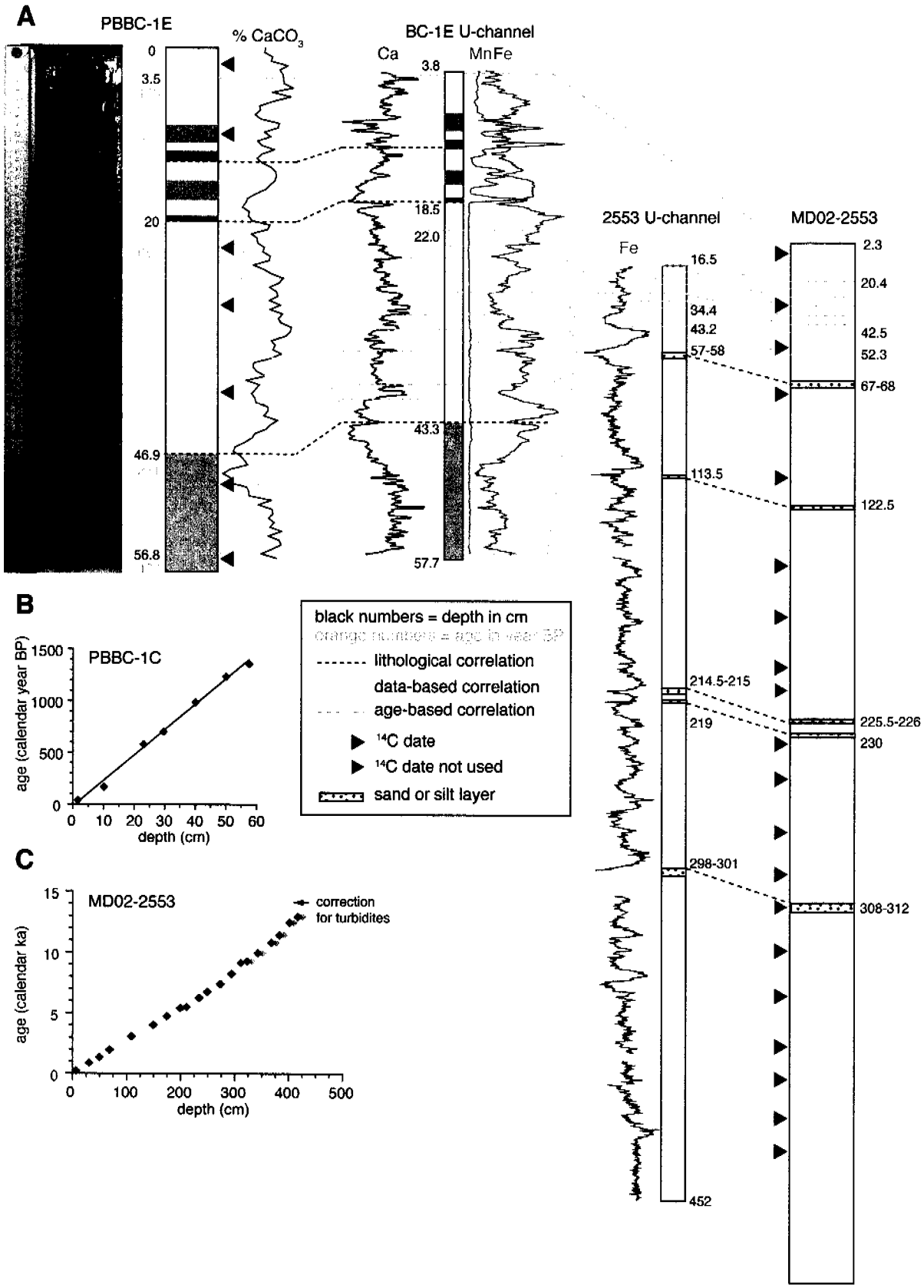

Figure 6.3. A. Correlation between the two cores and the respective U-channels. Correlation of the different cores was achieved with the elemental records (only Fe shown). U-channels and mother cores were correlated using lithologic changes, Ca counts and %carbonate data (BC-1E), and the age models (top of 2553). %carbonate data from *J. Flannery* [unpublished]. B. and C. Calibrated ^{14}C ages from cores PBBC-1C and MD02-2553, respectively. In MD02-2553, two dates were not used (red; see text) and the depths were corrected for two turbidites (grey symbols are at original depths).

dates from the top 2 m (5 ka) have been published by *Poore et al.* [2004]. Two of the remaining dates were not used for the age model because they either coincide with a turbidite (310 cm) or seemed too young with respect to the almost linear age-depth relationship observed for the other dates, with no signs of turbidites explaining the offset (210 cm). The two turbidites occurring in the dated interval (at 64.5-68 cm and 306-312 cm) have been cut out of the record for the construction of the age model, which was derived by linear interpolation between subsequent dates. In this study, we focus on the Holocene period, and therefore no age model was created for the deeper sections of MD02-2553. The age model of core PB-BC1E is derived by correlation to the well-dated twin core BC1C (dated with 7 ^{14}C dates) using carbonate concentrations, foraminiferal assemblage data and oxygen isotopic composition of foraminifera from both subcores. For the short cores, a linear regression of all dates was the basis for the age model [*Richey et al.*, submitted].

Unfortunately, the U-channel depths are shifted relative to the mother cores in some intervals. The sediment in the U-channel from core BC1E is even significantly stretched/compressed in parts, which could be constrained by comparing Ca counts from XRF scanning with carbonate content data as well as by two distinct color changes in the core (Figure 6.3). For MD02-2553, the depth shift was assessed by comparing the depths of the sand and silt layers, which reveal a constant offset of 10-11 cm below 67 cm (the first layer occurs at 57 cm in the U-channel). Above 43 cm, the temporal overlap of cores 2553 and BC1E allows for a correlation of the XRF data and use of the age model of BC1E. The additional error introduced by the correlations of the U-channels to the cores is estimated to be at most 1 cm, corresponding to around 25 years in the age model. When reporting core depths, we use the inferred depths in the original cores instead of U-channel depths unless indicated otherwise.

6.3. Results and Discussion

6.3.1. Implications of the variations in elemental composition

The Holocene part of the core exhibits significant century-scale variability as well as longer-term trends in elemental composition (Figure 6.4). These variations are at the focus of this paper and will be discussed in detail below. The constant values in the deeper part of the core correspond to homogenous intervals, which were probably deposited within very short time as suggested by high deglacial sedimentation rates (6 m/kyr) [*Williams and Kohl*, 1986].

The relative contributions of Fe, Ti, K, Si, and Al (not shown) are well correlated throughout most parts of the core (Figure 6.5), whereas Ca is clearly anticorrelated. The former group of

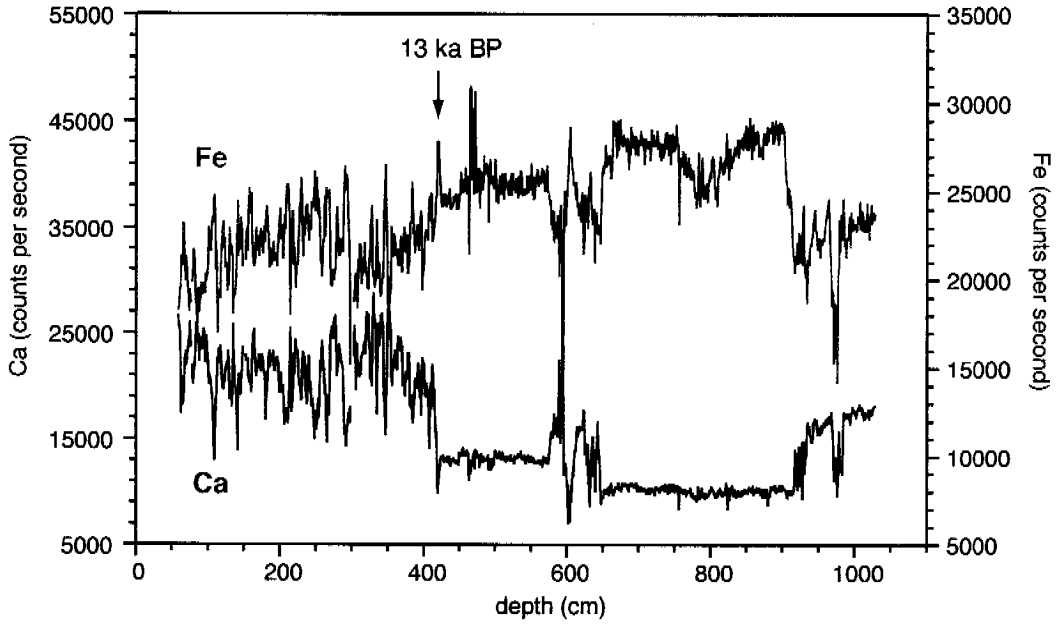

Figure 6.4. Records of Fe and Ca for the whole of core MD02-2553 (1 cm resolution). Note the anticorrelation of the two elements and the long homogenous intervals in the deglacial section. Depths are original U-channel depths. Only the Holocene part of the core was dated and analyzed further.

elements is derived from land. For Ca, mainly associated with carbonates, the anticorrelation with the terrigenous elements indicates that the marine source (calcareous microfossils) dominates over detrital carbonates. Si is contained in aluminosilicates, quartz, and marine opal, but the fact that it covaries with the other terrigenous elements and not with Ca argues against a marine contribution. Although Fe mostly covaries with the other terrigenous elements, intervals where the signals diverge can also be found. These divergences are probably due to remobilization of Fe under changing redox conditions. One example of a peak in Fe without accompanying peaks in the other terrigenous elements was observed at 20-24 cm depth in BC1E. At 24 cm, also a color change from grayish brown to reddish brown occurs, which indicates an increase in iron oxide concentration (Figure 6.3). Just above the Fe enrichment, there are several peaks in Mn, most likely due to manganese oxides. All these indications point towards a redox boundary at this interval. When assessing changes in terrigenous input, we will therefore focus on changes in Ti, which is much less susceptible to remobilization.

As the XRF scanning results reflect concentrations of the different elements, the elemental composition is obtained in relative terms and therefore it is not surprising that the marine and the terrigenous components are anticorrelated. The major question in this case is which component is diluting the other. If an age model could be obtained with a resolution similar to the durations of the peaks, accumulation rates could be calculated instead of concentrations. Unfortunately, this is not possible with the precision of ^{14}C dating. Therefore, we have to rely on comparisons with other data. During the last deglaciation, major meltwater inflows through the Mississippi were recorded in the Gulf of Mexico [*Kennett and Shackleton*, 1975; *Aharon*,

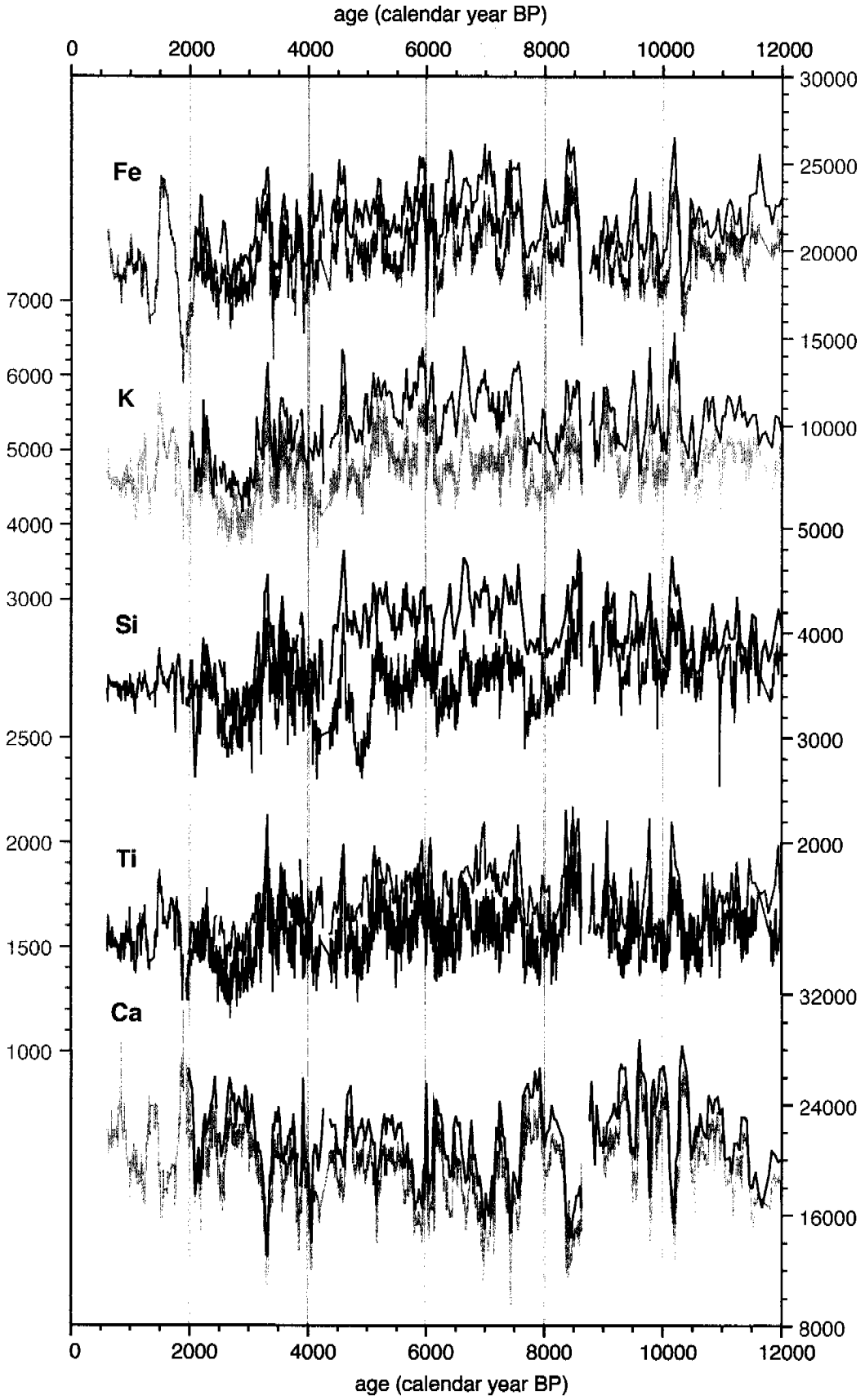

Figure 6.5. Scanning results for the Holocene section of core MD02-2553. Shown are counts of the terrigenous elements Fe, K, Si, and Ti as well as the marine-derived Ca (in counts per second). Dark colors are measurements in 1 cm resolution, light-colored records have been measured separatey with 2 mm resolution. Records have not been corrected for turbidites at around 2 ka and 8.7 ka.

2003; *Flower et al.*, 2004]. The fact that during this period of known increased freshwater flux terrigenous concentrations were at a maximum (Figure 6.4) suggests that input of this material is dominating the signal.

Since part of core MD02-2553 (77-146 cm or 2.5-4.2 ka) was scanned both in Bremen and in Potsdam, the measurements can be used to compare and validate the output from the different scanners (Figure 6.6). The two scanners differ in the scales of their outputs, due to different excitation energies and measurement areas. The values from Potsdam were therefore converted to the Bremen scale using a linear regression between the two records from the interval of overlap. Beforehand, every 4 data points of the data measured at Potsdam were averaged to obtain the same spacing of measurements. The results agree well, despite the different scanning methods and resolutions. A comparison between the two different cores BC1E and 2553 for the time of overlap (0.6-1.5 ka) also shows good reproducibility of the signals. Recognizing that the scanners measure only the very surface of the cores and the results are therefore prone to artifacts due to, for example, smearing of the surface, the consistency between the two cores adds confidence to the results. Furthermore, the good agreement enabled us to produce a composite record of elemental composition for Pigmy Basin. To this end, the results from BC1E were used until almost the end of that record (54.5 cm depth), corresponding to a depth of 48.7 cm in core 2553. From 49-87 cm in core 2553, measurements obtained from the Potsdam scanner were

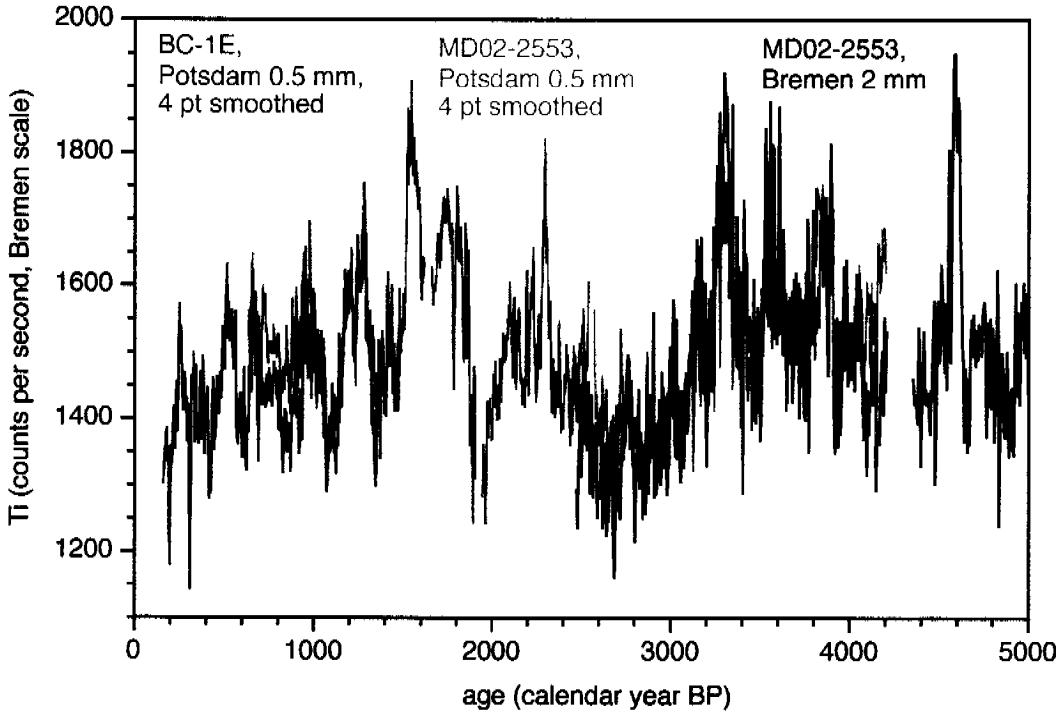

Figure 6.6. Comparison of Ti records obtained from different scanners and different cores. Results have been transformed to the same scale (see text for details).

used as they are the only available data for this interval. Below 87 cm depth, when the record obtained with the Bremen scanner begins, the 2 mm resolution Bremen data were used.

Coarser layers, including silt laminae, show up bright in the X-radiographs (Figure 6.7). A comparison of X-radiographs and Ti counts shows that most of these laminae are followed by peaks in Ti (although not every Ti peak is associated with a coarse layer). Similarly, both of the turbidites identified in the Holocene section of the core (at 64.5-68 cm and at 306-312 cm; c.f. materials section) are followed by peaks in Ti and other terrigenous elements (Fe, K, Al,

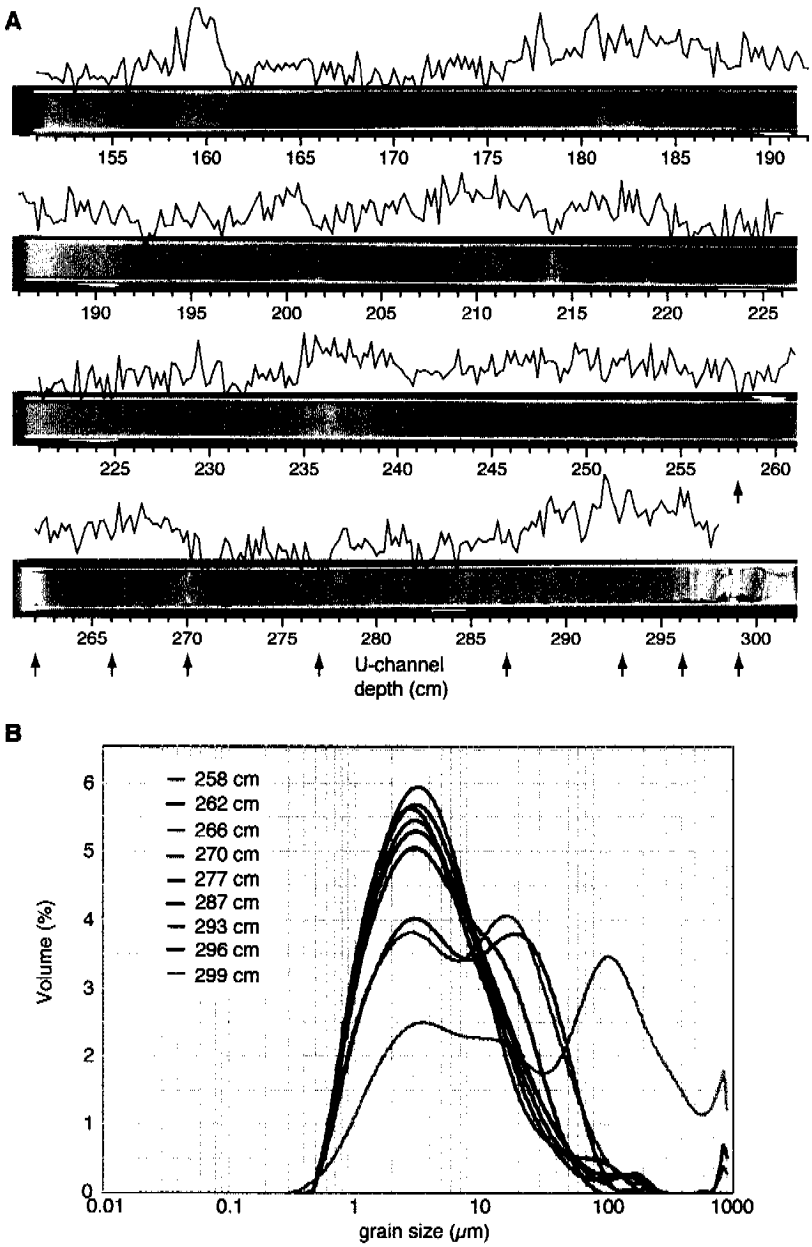

Figure 6.7. A. Comparison of X-radiographs and Ti counts for section II of core MD02-2553. Depths are depth in the U-channel, which is different from that in the original core by about 10 cm (see text). B. Grain size distributions of selected samples. Depths are indicated by black arrows in A and show up as holes in the X-radiograph.Note the similarity of the distributions except for visibly coarser layers at 270 cm (280 cm in the original core) and below 296 cm (306 cm original core depth).

Si). These observations at first sight suggest that the peaks in terigenous element abundance are simply due to particle sorting and associated with the clay-rich upper part of (mini-)turbidites. However, the two terrigenous peaks occurring after the identified turbidites encompass significant layers of sediment, implying that if they were part of the turbidites, changes in sedimentation rate should be observed. In fact, both peaks are bracketed by ^{14}C ages, which do not indicate higher sedimentation rates. Furthermore, grain size analyses between 270 and 310 cm revealed very similar spectra for most samples except for a silt lamina at 280 cm depth (270 cm U-channel depth in Figure 6.7) and the interval between 306-310 cm (296-300 cm in Figure 6.7), which is clearly part of a turbidite and has been removed from the record. This confirms that the remaining variations in elemental composition, even those occurring right above coarser layers, are not due to sorting of the sediment.

6.3.2. Time series analysis

We performed spectral analysis of the composite records of K and Ti with different methods (Maximum Entropy, Blackman-Tukey, and Multi-Taper method). To this end, the timeseries were resampled using a cubic spline interpolation and a sampling period of 6 years. The software used was AnalySeries [*Paillard et al.*, 1996] and the SSA-MTM toolkit [*Ghil et al.*, 2002]. Significant periods (99% confidence level) obtained by all methods and for both elements were centered around 690, 360, and 250 years, whereas periods of 175, 148, 120 and 100 years are not equally significant in the two elemental records (Figure 6.8). However, evolutive spectra (in AnalySeries) and a wavelet analysis (not shown) revealed that the dominance of different frequencies changed in the course of the record. Similarly, visual inspection of the time series (e.g., Figure 6.9) suggests changes in the importance of the different frequencies: higher frequencies appear stronger in the later Holocene, whereas the lower frequencies seem to dominate the early Holocene part of the record.

An important century-scale period in solar activity is the 208 year cycle observed in records of ^{14}C production [*Stuiver et al.*, 1991]. This period is not dominant in the elemental records from Pigmy Basin. However, sedimentary records are imperfect recorders of climatic changes. Already small errors in the age model or short-term variations in sedimentation rates can cause a decrease in the spectral density of a certain frequency or even shifts in spectral density peaks. Furthermore, the fact that we do not see a persistent strong influence of specific cycles in the Pigmy Basin elemental records might reflect the large source area of this signal and the potential combination of different influences. The similar range of the significant century-scale periodicities in the elemental records to those of solar variations therefore might already indicate a solar influence on the climatic changes reflected in Pigmy Basin. If so, this influence was probably larger in the later part of the record.

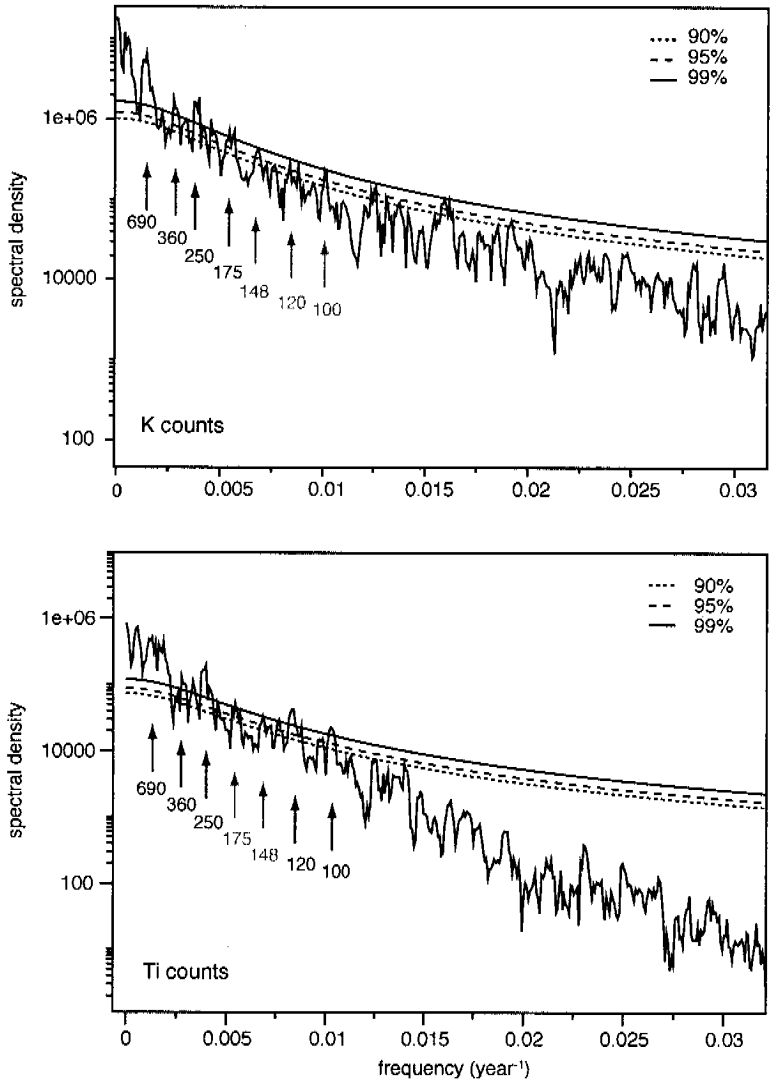

Figure 6.8. Time series analysis of the composite K and Ti records from Pigmy Basin. Spectra were estimated with the multitaper method [*Ghil*, 2002] using the SSA-MTM toolkit. Parameters: Time bandwidth product = 3; number of windows = 2. Numbers with arrows are periods (in years) corresponding to significant peaks at the 99% (black) or 95% (grey) confidence levels. Similar peaks were obtained with the Blackman-Tukey and Maximum Entropy methods.

6.3.3. Comparison with other GOM data

The long-term Holocene trend of the Pigmy Basin Ti record is similar to the trend in the abundance of *G. sacculifer* in the same core (Figure 6.9a), with more Ti in the mid-Holocene corresponding to a higher relative abundance of the Caribbean species. However, little correspondence is observed in the early Holocene, indicating that this relationship only became established in the mid-Holocene. Also, the mid-Holocene maximum is less strong in the Ti data compared to the *G. sacculifer* abundance. The lack of correlation in the early Holocene could be due to the remains of the Laurentide ice sheet still present at that time, which probably had a strong influence on North American climate and might have overprinted southerly influences

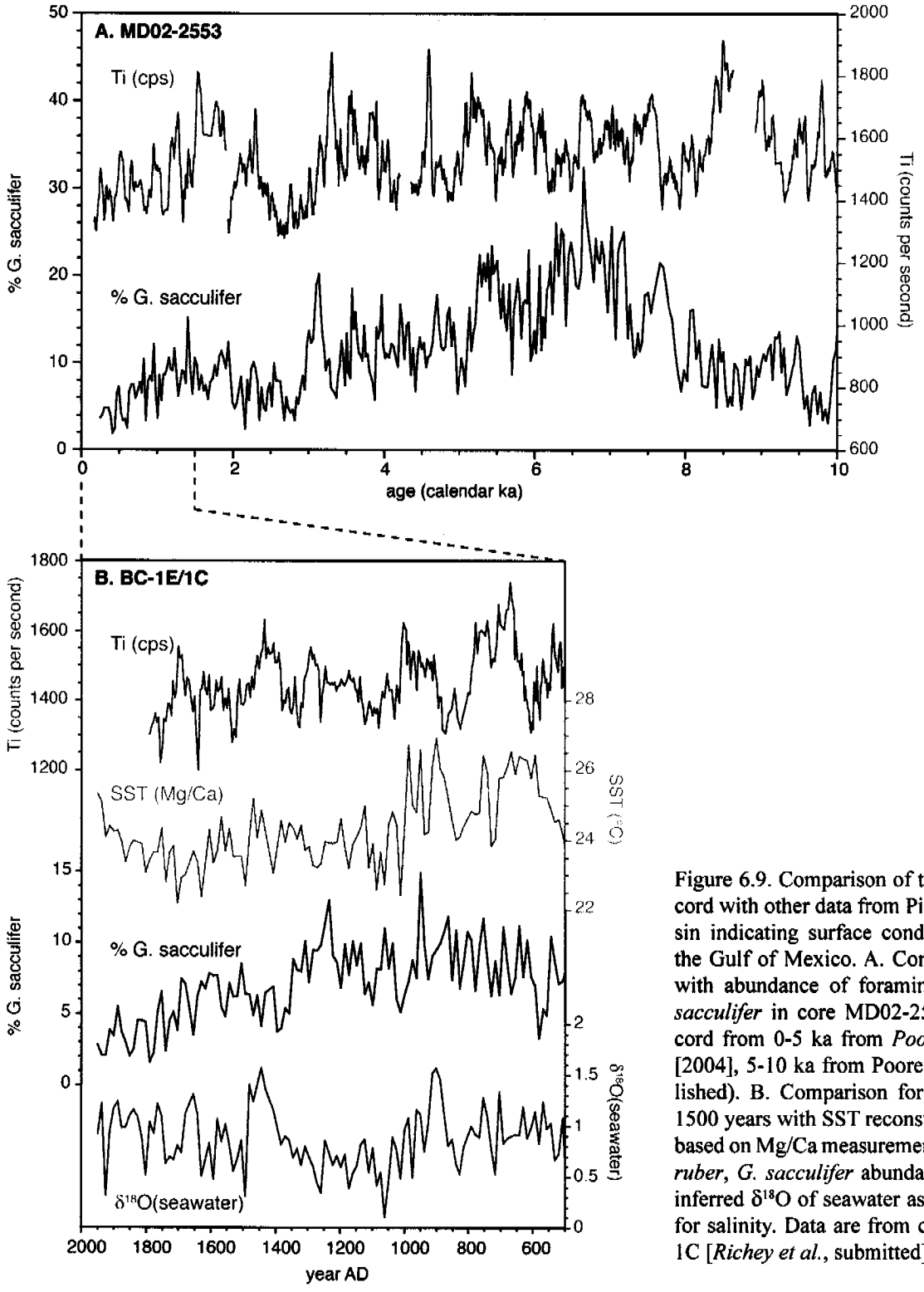

Figure 6.9. Comparison of the Ti record with other data from Pigmy Basin indicating surface conditions in the Gulf of Mexico. A. Comparison with abundance of foraminifera *G. sacculifer* in core MD02-2553. Record from 0-5 ka from *Poore et al.* [2004], 5-10 ka from Poore (unpublished). B. Comparison for the last 1500 years with SST reconstructions based on Mg/Ca measurements on *G. ruber*, *G. sacculifer* abundance, and inferred $\delta^{18}O$ of seawater as a proxy for salinity. Data are from core BC-1C [*Richey et al.*, submitted].

such as monsoon strength and Gulf of Mexico moisture flux. One prominent feature in the early Holocene Ti record with no correspondence in *G. sacculifer* abundance is a peak around 8.5 ka, occurring just before the '8.2-cold event' observed in many records around the globe [e.g., *Alley et al.*, 1997; *Rohling and Pälike*, 2005]. The peak coincides with a well-dated negative excur-

sion in $\delta^{18}O$ of seawater observed in sediments from nearby Orca Basin [*LoDico et al.*, 2006]. It is not clear whether this salinity minimum reflects input of meltwater, as the southern routes via the Mississippi River are thought to have been abandoned by this time [*Fisher*, 2003], or whether a precipitation anomaly is responsible. Climate in the Caribbean region reacted simultaneously to the 'cold event' with a dry spell at around 8.2 ka [*Haug et al.*, 2001; *Lachniet et al.*, 2004], clearly later than the Mississippi signal recorded in the Pigmy and Orca Basins. Therefore, if indeed precipitation-related, the Mississippi runoff peak at around 8.5 ka would have had its source in a northern climate anomaly. However, pollen and lake records from the northern Great Plains suggest an onset of the drier 'prairie period' at around 8.8 ka [*Whitlock and Bartlein*, 1993; *Dean et al.*, 2002], making a precipitation anomaly unlikely and supporting a meltwater-related scenario.

After around 6 ka, the influence of southern climate variations seems to become dominant. After this time, even some of the smaller scale features of the records of *G. sacculifer* and Ti seem related, such as a peak at 5.5-5 ka, several peaks of shorter duration between 4 and 3 ka, a minimum at around 3 ka, and a second broad maximum centered at 1.5 ka. As discussed above, the depth shift of the U-channel-based Ti measurements with respect to the original core could account for minor leads or lags in these data sets. The general correspondence of Ti and *G. sacculifer* holds also true for the most recent trends observed in the short box cores from Pigmy Basin (Figure 6.9b) [*Richey et al.*, submitted]. An even better positive correlation was found between Ti and SST, reconstructed from foraminiferal Mg/Ca ratios. Such a relationship is not unexpected, considering that the Gulf of Mexico is the main moisture source for the Mississippi catchment and higher SST could lead to increased evaporation and therefore moisture flux. However, very little agreement is observed between Ti and $\delta^{18}O$ of seawater, a proxy for salinity. If anything, some of the Ti peaks correspond to maxima in $\delta^{18}O$, that is, to higher salinity, which is surprising, as one would expect increased freshwater flux to accompany the terrigenous input. An explanation could be that the foraminifera did not record the freshwater because they live at a different depth, either too low or, if the plume was transported as a turbidity current, too high. The discrepancy could, however, also indicate that the relationship between Gulf of Mexico SST and Mississippi runoff is not as straightforward as expected. This will be further discussed below in the context of other climate records from the region.

6.3.4. Comparison with North American and Caribbean climate records

As discussed in the introduction, many climate reconstructions from north-central North America indicate much drier conditions in the early to mid-Holocene. The records of reconstructed salinity in Moon Lake (North Dakota) [*Laird et al.*, 1996] and Al content in Elk Lake (Minnesota) [*Dean*, 1997] as a proxy for dust deposition are shown as examples in Figure

6.10. As the early to mid-Holocene corresponds to generally high contributions of terrigenous elements in Pigmy Basin, the reconstructed dry conditions in parts of the catchment contradicts the simple relationship assumed before between foraminiferal assemblage data and the Ti record – a warmer Gulf of Mexico leading to higher Mississippi runoff through increased moisture flux to North America. The same apparent contradiction is found on shorter timescales as well. During the so-called Medieval Warm Period, the American Midwest experienced drought conditions [*Woodhouse and Overpeck*, 1998], while Gulf of Mexico SSTs and terrigenous contributions were high.

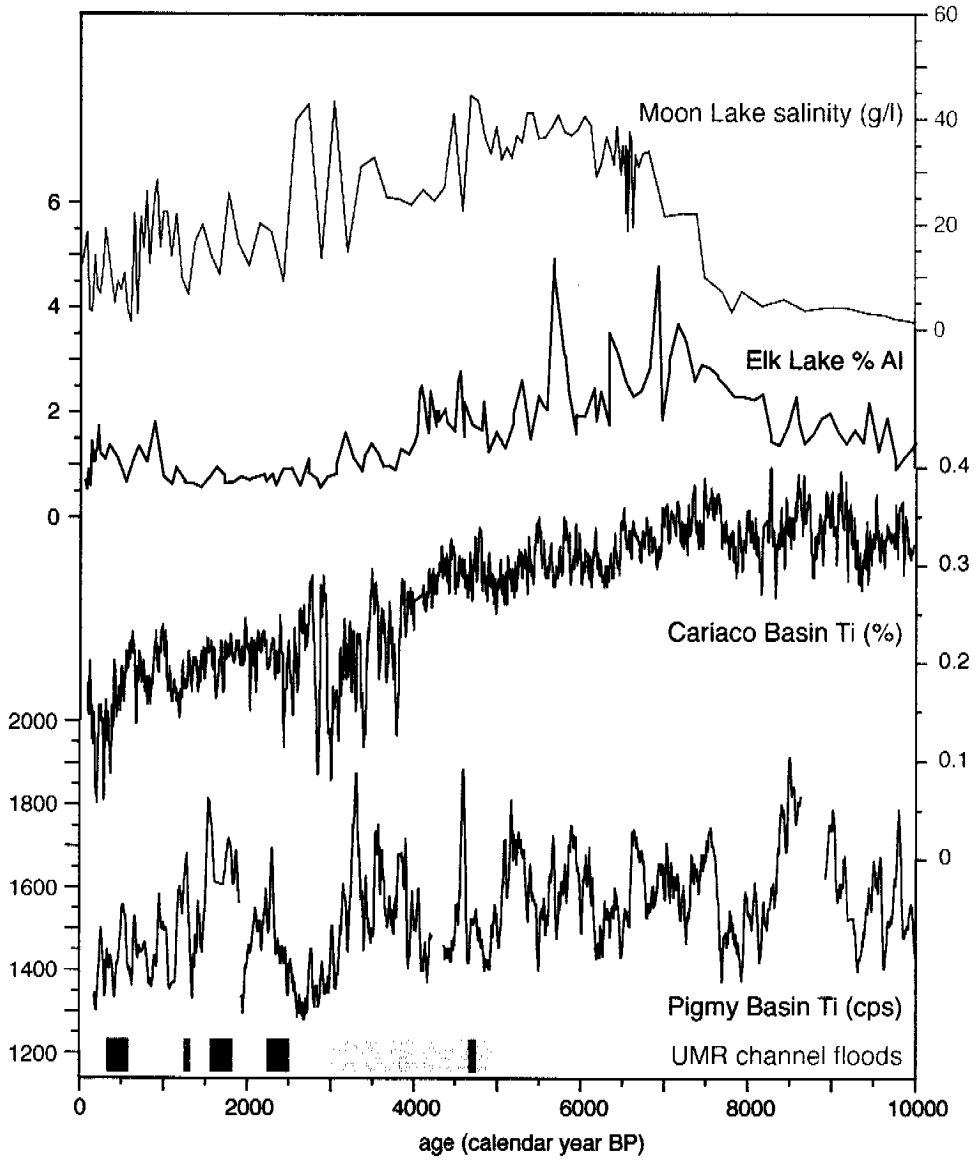

Figure 6.10. Comparison of Pigmy Basin Ti record with climate records from the northern catchment (Moon Lake: *Laird et al.* [1996]; Elk Lake: *Dean* [1997]), the Cariaco Basin off Venezuela [*Haug et al.*, 2001], and Upper Mississippi River (UMR) channel flood episodes [*Knox*, 2003]. For the flood record, dark colors reflect periods of large flooding whereas light color symbolizes large variability but overall smaller floods.

To the south of the Gulf of Mexico, climate is most strongly influenced by the movement of the Intertropical Convergence Zone (ITCZ). In boreal winter, this zone of intensive precipitation is located near the equator, while it moves over the Caribbean Sea in boreal summer, when the northern landmasses heat up (Figure 6.1). On longer timescales, the mean position of the ITCZ is strongly influenced by changes in insolation and SST in the warm pool of the eastern Pacific and the intra-American seas. Ti concentrations in sediments from Cariaco Basin off Venezuela (Figure 6.10) as a proxy for local runoff reveal that the ITCZ migrated southwards during the late Holocene from a northernmost position in the mid-Holocene [*Haug et al.*, 2001]. This is in agreement with the decreasing Gulf of Mexico temperatures inferred from the *G. sacculifer* abundance [*Poore et al.*, 2004]. Comparing the Ti records of Cariaco Basin and Pigmy Basin, it can be seen that the signals covary regarding the general trends and some of the shorter-scale features. Moreover, a surprisingly good correlation can be observed for the last 1000 years (Figure 6.11). Three distinct Ti minima are apparent in both records between 1500 and 1800 AD (the time of the 'little ice age'), when solar intensity was decreased and overall conditions were colder. In contrast, higher Ti input is observed at both sites during the Medieval Warm Period, when solar insolation was high. Several other features correspond in the records, such as another sharp Ti minimum at around 1250 AD.

A general picture of Holocene climate variability in North and Central America emerges from these comparisons. When insolation was high, such as during the mid-Holocene (preces-

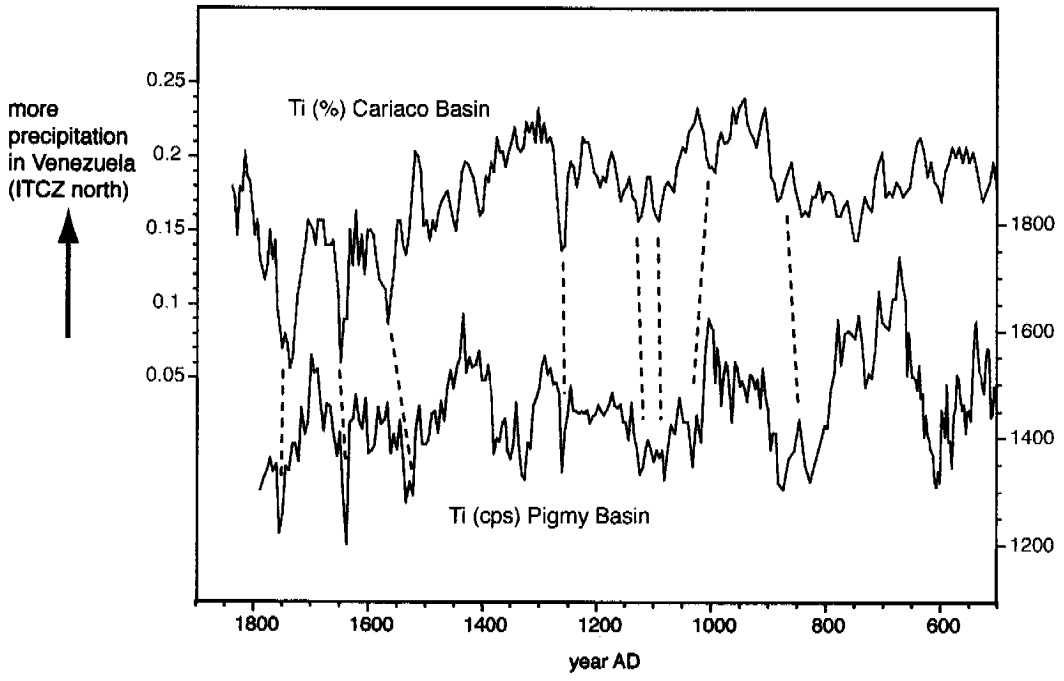

Figure 6.11. Comparison of the Ti records from Pigmy Basin and Cariaco Basin (off Venezuela) [*Haug et al.*, 2001] for the last 1500 years. In the Cariaco Basin, increased Ti input is associated with a more northern position of the intertropical convergence zone (ITCZ).

sion-related) or the Medieval Warm Period (solar intensity-related), both the high-elevation regions in southwestern North America and the warm pool regions like the Gulf of Mexico experienced increased summer warming. This led to stronger monsoons and a northward shift of the mean ITCZ position, respectively. The latter has been recorded as wetter conditions at many sites in the circum-Caribbean region [e.g., *Bradbury et al.*, 1981; *Hodell et al.*, 1991; *Haug et al.*, 2001]. Stronger monsoonal winds and higher Gulf of Mexico SSTs likely resulted in increased moisture flux and precipitation in the southwestern, and maybe also southern, parts of North America [*Kutzbach and Streetperrott*, 1985; *Bartlein et al.*, 1998; *Harrison et al.*, 2003]. At the same time, increased air mass subsidence over the Great Plains, blocking the southerly moisture flux, was probably responsible for the drier conditions in that region. Regarding the wintertime influences, it has been proposed that the early to mid-Holocene climate was similar to current La Niña conditions [*Koutavas et al.*, 2002], with a stronger sea surface temperature contrast along the equator in the Pacific. If this affected the jet stream like La Niña events do today, it could have augmented the summer dryness by decreasing the likelihood of a southern path of the weather systems in winter. Along these lines, *Shin et al.* [2006] find in their modeling study that the observed mid-Holocene dry conditions in central North America can only be reconstructed when both increased summer insolation and the colder equatorial Pacific sea surface temperatures are taken into account. La Niña-like conditions could themselves be associated with positive insolation anomalies, as has been proposed for the early Holocene [*Clement et al.*, 1999].

From the Pigmy Basin Ti record we can infer that terrigenous sediment input into the Gulf of Mexico increased during the times of stronger insolation. This relationship could be due to (i) circulation changes within the Gulf of Mexico or (ii) variations in runoff or erosion on the continent. These different potential influences will be discussed in the following.

Present-day drifter and satellite studies show that near the Mississippi River mouth the average circulation pattern is a predominantly westward coastal current, carrying the plume along the Texas-Louisiana shelf [e.g., *Ohlmann and Niiler*, 2005; *Walker et al.*, 2005]. Cross-shelf transport is mainly associated with passing eddies that are shed from the Loop Current. However, this average flow direction is reversed in summer, when strong southerly winds push the plume towards the east [*Ohlmann and Niiler*, 2005; *Walker et al.*, 2005]. Because the shelf is narrower there and eddies associated with the Loop Current occur frequently, the plume is often carried into the eastern Gulf and towards the Florida Strait during these times. This would decrease transport of Mississippi material to Pigmy Basin, which lies to the southwest of the river mouth. If the relationship of insolation and southerly flow discussed above is correct, then one would expect less terrigenous material in Pigmy Basin sediments when insolation is high. Instead, the opposite is observed, implying that flow direction changes in the Gulf of Mexico are not the reason for the observed variability in terrigenous input. Increased eddy shedding due

to increased loop current strength, however, might affect the offshore transport west of the river mouth. As the Mississippi River is by far the most important sediment source for the Gulf of Mexico [*Davies and Moore*, 1970], changes in the input by other rivers can only have a minor effect.

Another climate feature that was probably more frequent when Gulf of Mexico SST was warmer are tropical storms and hurricanes, which could have significantly affected flow directions. This influence is difficult to assess. However, the few records existing of Holocene hurricane landfalls on the Gulf coast based on sedimentological evidence in lakes suggest a sudden increase in hurricane activity after 3,400 radiocarbon years before present [*Liu and Fearn*, 1993; 2000]. A corresponding shift is not observed in the Pigmy Basin Ti record. Therefore, although we cannot exclude the possibility of an influence of tropical storms and hurricanes, it is unlikely that it dominates the signal.

Since changes in the distribution of Mississippi sediment in the Gulf of Mexico do not appear to be the dominant factor for the observed variability, the driving force was probably climatic changes on the continent. At times when the monsoonal circulation was stronger, precipitation and runoff could have increased in the southern parts of the catchment, leading to the observed higher terrigenous input despite the drier conditions in the northern catchment. Today, the monsoon region (Figure 6.1B) is not part of the Mississippi catchment, but this might have changed with time. An increased southerly moisture flux could have expanded the area affected by the monsoon eastwards. This might have increased runoff contributed by the southern sub-catchments of the Arkansas River and Red River. Unfortunately, the paleoclimate records available to date are either from more northern parts of the Mississippi catchment or from within the monsoon region itself, so we cannot test this hypothesis at present. However, today most of the sediment load of the Mississippi River is derived from the northwestern part of the catchment, namely the Missouri River basin [*Turner and Rabalais*, 2004]. The fact that this is still the case, despite the largest reduction of sediment load due to damming in this sub-catchment [*Mossa*, 1996], suggests that the importance of this sediment source was even larger in the past. Decreased runoff in this sub-basin should therefore have affected overall sediment load stronger than potentially increased precipitation in the southern catchments.

Sediment load, however, does not only depend on runoff but can also be strongly influenced by changes in erosion rates. In the sub-humid climate region of the northwestern catchment, overall drier conditions probably led to reduced plant cover, which could have destabilized the soil. Moreover, the generally drier climate conditions, recorded by lake sediments, dune fields and pollen assemblages, do not preclude the occurrence of extreme precipitation events leading to floods. With the warmer SSTs in the Gulf, a significant moisture source was certainly present. Support comes from a comparison with flood event reconstructions in the Upper Mississippi River channel [*Knox*, 2003]. During the last 5 ka, major erosion events coincided approxi-

mately with Pigmy Basin Ti peaks (Figure 6.10), suggesting that the signal is indeed influenced by processes in the northern catchment. Furthermore, records of channel incision in the central Great Plains reveal stronger erosion during the Medieval Warm Period, when climate conditions were dry [*Daniels and Knox*, 2005]. In that study, reduced plant cover and increased climatic variability have also been invoked as driving factors.

Increased hydrologic variability in combination with greater susceptibility to erosion therefore appears as the most plausible explanation for the observed relationship of increased terrigenous input by the Mississippi River under generally warmer and drier climate conditions. An additional influence by the other processes discussed above can at present not be ruled out, however.

6.4. Summary and Conclusions

The presented high-resolution elemental record from Pigmy Basin in the Gulf of Mexico reveals large variations in the contribution of terrigenous elements over the course of the Holocene, which is interpreted as reflecting varying sediment transport by the Mississippi River. Overall increased and variable input of terrigenous material was observed during the mid-Holocene as well as the late Holocene between 2.5 and 1.0 ka, while less input occurred at around 3.0 ka.

In the early Holocene, the signal seems to be dominated by influences in the northern part of the catchment associated with the remains of the Laurentide ice sheet. For example, the most likely explanation for the peak in terrigenous input shortly before the wide spread cold anomaly at 8.2 ka seems increased meltwater inflow to the Gulf of Mexico, contrasting the general view that the southern routing had been abandoned at that time.

Since the mid-Holocene, on the other hand, Mississippi sediment input appears to have responded to a combination of summer insolation and southern climatic influences, such as sea surface temperatures in the Gulf of Mexico and the eastern equatorial Pacific, as well as the mean position of the ITCZ. Thereby, increased terrigenous input coincided with increased summer insolation and dry climate in central North America. At the same time, elevated sea surface temperatures in the Gulf of Mexico, a stronger monsoonal atmospheric circulation, and a northward displacement of the ITCZ could have led to a more variable climate in the Mississippi catchment. Similarly, decreased insolation during the 'little ice age' period coincided with decreased terrigenous input, low SST in the Gulf of Mexico and a southward displacement of the ITCZ.

Processes that could link the terrigenous input in Pigmy Basin to these climate variations are: increased offshore transport of the Mississippi plume due to more frequent eddy shedding from the Loop current, increased frequency of tropical storms, and increased precipitation and runoff in the southern parts of the catchment. However, the most probable explanation is that stronger Mississippi sediment input reflects increased susceptibility to erosion during dry periods, in combination with an increased frequency and/or magnitude of extreme precipitation events during times of stronger summer insolation.

Acknowledgements

Julie Richey and Ben Flower are gratefully acknowledged for sharing unpublished data and radiocarbon dates as well as for providing a U-channel sub-sample of core PBBC-1E. Brigitte Richert and Heike Pfletschinger are thanked for assisting with XRF scanning. Thomas Schmid contributed to grain size measurements. Ruedi Baumann and Urs Gerber are thanked for the x-radiographs. Laurent Labeyrie, Yvon Balut, and the crew of R/V *Marion Dufresne* are thanked for a successful cruise in the Gulf of Mexico. Julie Richey, Jen Flannery, and Jenna LoDico contributed through interesting discussions. This work was funded by the Swiss National Science Foundation.

References

Adams, D. K., and A. C. Comrie (1997), The North American monsoon, *Bulletin of the American Meteorological Society*, *78*, 2197-2213.

Aharon, P. (2003), Meltwater flooding events in the Gulf of Mexico revisited: Implications for rapid climate changes during the last deglaciation, *Paleoceanography*, *18*, 1079, doi:10.1029/2002PA000840.

Alley, R. B., P. A. Mayewski, T. Sowers, M. Stuiver, K. C. Taylor, and P. U. Clark (1997), Holocene climatic instability: A prominent, widespread event 8200 yr ago, *Geology*, *25*, 483-486.

Bartlein, P. J., K. H. Anderson, P. M. Anderson, M. E. Edwards, C. J. Mock, R. S. Thompson, R. S. Webb, and C. Whitlock (1998), Paleoclimate simulations for North America over the past 21,000 years: Features of the simulated climate and comparisons with paleoenvironmental data, *Quaternary Science Reviews*, *17*, 549-585.

Bond, G., B. Kromer, J. Beer, R. Muscheler, M. N. Evans, W. Showers, S. Hoffmann, R. Lotti-Bond, I. Hajdas, and G. Bonani (2001), Persistent solar influence on north Atlantic climate during the Holocene, *Science*, *294*, 2130-2136.

Bouma, A. H., and C. E. Stelting (1986), Seismic Stratigraphy and Sedimentary Processes in Orca and Pygmy Basins, *Initial Reports of the Deep Sea Drilling Project*, *96*, 563-576.

Bradbury, J. P., B. Leyden, M. Salgadolabouriau, W. M. Lewis, C. Schubert, M. W. Binford, D. G. Frey, D. R. Whitehead, and F. H. Weibezahn (1981), Late Quaternary Environmental History of Lake Valencia, Venezuela, *Science*, *214*, 1299-1305.

Brown, D. P., and A. C. Comrie (2004), A winter precipitation 'dipole' in the western United States associated with multidecadal ENSO variability, *Geophys. Res. Lett.*, *31*.

Clement, A. C., R. Seager, and M. Cane (1999), Orbital controls on the El Nino/Southern Oscillation and the tropical climate, *Paleoceanography* 14, 441-456.

Cole, J. E., J. T. Overpeck, and E. R. Cook (2002), Multiyear La Niña events and persistent drought in the contiguous United States, *Geophys. Res. Lett.*, *29*, 1647, doi:10.1029/2001GL013561.

Daniels, J. M., and J. C. Knox (2005), Alluvial stratigraphic evidence for channel incision during the Mediaeval Warm Period on the central Great Plains, USA, *Holocene*, *15*, 736-747.

Davies, D. K., and W. R. Moore (1970), Dispersal of Mississippi Sediment in Gulf-of-Mexico, *Journal of Sedimentary Petrology*, *40*, 339-&.

Dean, J. S. (1994), The Medieval Warm Period on the Southern Colorado Plateau, *Climatic Change*, *26*, 225-241.

Dean, W. E. (1997), Rates, timing, and cyclicity of Holocene eolian activity in north-central United States: Evidence from varved lake sediments, *Geology*, *25*, 331-334.

Dean, W. E., R. M. Forester, and J. P. Bradbury (2002), Early Holocene change in atmospheric circulation in the Northern Great Plains: an upstream view of the 8.2 ka cold event, *Quaternary Science Reviews*, *21*, 1763-1775.

deMenocal, P., J. Ortiz, T. Guilderson, J. Adkins, M. Sarnthein, L. Baker, and M. Yarusinsky (2000), Abrupt onset and termination of the African Humid Period: rapid climate responses to gradual insolation forcing, *Quaternary Science Reviews*, *19*, 347-361.

Enfield, D. B., A. M. Mestas-Nunez, and P. J. Trimble (2001), The Atlantic multidecadal oscillation and its relation to rainfall and river flows in the continental US, *Geophys. Res. Lett.*, *28*, 2077-2080.

Fisher, T. G. (2003), Chronology of glacial Lake Agassiz meltwater routed to the Gulf of Mexico, *Quaternary Research*, *59*, 271-276.

Flower, B. P., D. W. Hastings, H. W. Hill, and T. M. Quinn (2004), Phasing of deglacial warming and laurentide ice sheet meltwater in the Gulf of Mexico, *Geology*, *32*, 597-600.

Forman, S. L., R. Oglesby, V. Markgraf, and T. Stafford (1995), Paleoclimatic Significance of Late Quaternary Eolian Deposition on the Piedmont and High-Plains, Central United-States, *Global and Planetary Change*, *11*, 35-55.

Ghil, M., M. R. Allen, M. D. Dettinger, K. Ide, D. Kondrashov, M. E. Mann, A. W. Robertson, A. Saunders, Y. Tian, F. Varadi, and P. Yiou (2002), Advanced spectral methods for climatic time series, *Reviews of Geophysics*, *40*, 1003, doi:10.1029/2000RG000092.

Harrison, S. P., J. E. Kutzbach, Z. Liu, P. J. Bartlein, B. Otto-Bliesner, D. Muhs, I. C. Prentice, and R. S. Thompson (2003), Mid-Holocene climates of the Americas: a dynamical response to changed seasonality, *Climate Dynamics*, *20*, 663-688.

Haug, G. H., K. A. Hughen, D. M. Sigman, L. C. Peterson, and U. Rohl (2001), Southward migration of the intertropical convergence zone through the Holocene, *Science*, *293*, 1304-1308.

Higgins, R. W., and W. Shi (2000), Dominant factors responsible for interannual variability of the summer monsoon in the southwestern United States, *Journal of Climate*, *13*, 759-776.

Higgins, R. W., Y. Yao, and X. L. Wang (1997), Influence of the North American monsoon system on the US summer precipitation regime, *Journal of Climate*, *10*, 2600-2622.

Hodell, D. A., J. H. Curtis, G. A. Jones, A. Higueragundy, M. Brenner, M. W. Binford, and K. T. Dorsey (1991), Reconstruction of Caribbean Climate Change over the Past 10,500 Years, *Nature*, *352*, 790-793.

Hu, Q., and S. Feng (2001), Climatic role of the southerly flow from the Gulf of Mexico in interannual variations in summer rainfall in the central United States, *Journal of Climate*, *14*, 3156-3170.

Kennett, J. P., and N. J. Shackleton (1975), Laurentide Ice Sheet Meltwater Recorded in Gulf of Mexico Deep-Sea Cores, *Science*, *188*, 147-150.

Knox, J. C. (2003), North American Paleofloods and Future Floods: Responses to Climatic Change, in *Paleohydrology: Understanding Global Change*, edited by K. J. Gregory and G. Benito, pp. 143-164, John Wiley & Sons, Ltd.

Koutavas, A., J. Lynch-Stieglitz, T. M. Marchitto, and J. P. Sachs (2002), El Niño-like pattern in ice age tropical Pacific sea surface temperature, *Science*, *297*, 226-230.

Kutzbach, J. E., and F. A. Streetperrott (1985), Milankovitch Forcing of Fluctuations in the Level of Tropical Lakes from 18 to 0 Kyr Bp, *Nature*, *317*, 130-134.

Lachniet, M. S., S. J. Burns, D. R. Piperno, Y. Asmerom, V. J. Polyak, C. M. Moy, and K. Christenson (2004), A 1500-year El Niño/Southern Oscillation and rainfall history for the Isthmus of Panama from speleothem calcite, *J. Geophys. Res. Atmos.*, *109*, D20117, doi:10.1029/2004JD004694.

Laird, K. R., S. C. Fritz, E. C. Grimm, and P. G. Mueller (1996), Century-scale paleoclimatic reconstruction from Moon Lake, a closed-basin lake in the northern Great Plains, *Limnol. Oceanogr.*, *41*, 890-902.

Laskar, J., P. Robutel, F. Joutel, M. Gastineau, A. C. M. Correia, and B. Levrard (2004), A long-term numerical solution for the insolation quantities of the Earth, *Astronomy & Astrophysics*, *428*, 261-285.

Liu, K. B., and M. L. Fearn (1993), Lake-Sediment Record of Late Holocene Hurricane Activities from Coastal Alabama, *Geology*, *21*, 793-796.

Liu, K. B., and M. L. Fearn (2000), Reconstruction of prehistoric landfall frequencies of catastrophic hurricanes in northwestern Florida from lake sediment records, *Quaternary Research*, *54*, 238-245.

LoDico, J. M., B. P. Flower, and T. M. Quinn (2006), Sub-Centennial Scale Climatic and Hydrologic Variability in the Gulf of Mexico during the Early Holocene, *Paleoceanography* 20, PA3015.

Mayewski, P. A., E. E. Rohling, J. C. Stager, W. Karlen, K. A. Maasch, L. D. Meeker, E. A. Meyerson, F. Gasse, S. van Kreveld, K. Holmgren, J. Lee-Thorp, G. Rosqvist, F. Rack, M. Staubwasser, R. R. Schneider, and E. J. Steig (2004), Holocene climate variability, *Quaternary Research*, *62*, 243-255.

McCabe, G. J., M. A. Palecki, and J. L. Betancourt (2004), Pacific and Atlantic Ocean influences on multidecadal drought frequency in the United States, *Proceedings of the National Academy of Sciences of the United States of America*, *101*, 4136-4141.

Mossa, J. (1996), Sediment dynamics in the lowermost Mississippi River, *Engineering Geology*, *45*, 457-479.

Ohlmann, J. C., and P. P. Niiler (2005), Circulation over the continental shelf in the northern Gulf of Mexico, *Progress in Oceanography*, *64*, 45-81.

Paillard, D., L. Labeyrie, and P. Yiou (1996), Macintosh program performs time-series analysis, *Eos Trans. AGU*, *77*, 379.

Polyak, V. J., and Y. Asmerom (2001), Late Holocene climate and cultural changes in the south-western United States, *Science*, *294*, 148-151.

Poore, R. Z., T. M. Quinn, and S. Verardo (2004), Century-scale movement of the Atlantic Intertropical Convergence Zone linked to solar variability, *Geophys. Res. Lett.*, *31*, L12214, doi:10.1029/2004GL019940.

Poore, R. Z., M. J. Pavich, and H. D. Grissino-Mayer (2005), Record of the North American southwest monsoon from Gulf of Mexico sediment cores, *Geology*, *33*, 209-212.

Poore, R. Z., H. J. Dowsett, S. Verardo, and T. M. Quinn (2003), Millennial- to century-scale variability in Gulf of Mexico Holocene climate records, *Paleoceanography*, *18*, 1048, doi:10.1029/2002PA000868.

Richey, J. N., R. Z. Poore, B. P. Flower, and T. M. Quinn (submitted to *Geology*), A 1400-year multi-proxy record of climate variability from the Northern Gulf of Mexico.

Rohling, E. J., and H. Pälike (2005), Centennial-scale climate cooling with a sudden cold event around 8,200 years ago, *Nature*, *434*, 975-979.

Shin, S. I., P. D. Sardeshmukh, R. S. Webb, R. J. Oglesby, and J. J. Barsugli (2006), Understanding the mid-Holocene climate, *Journal of Climate*, *19*, 2801-2817.

Stuiver, M., T. F. Braziunas, B. Becker, and B. Kromer (1991), Climatic, Solar, Oceanic, and Geomagnetic Influences on Late-Glacial and Holocene Atmospheric C-14/C-12 Change, *Quaternary Research*, *35*, 1-24.

Turner, R. E., and N. N. Rabalais (2004), Suspended sediment, C, N, P, and Si yields from the Mississippi River Basin, *Hydrobiologia*, *511*, 79-89.

Walker, N. D., W. J. Wiseman, L. J. Rouse, and A. Babin (2005), Effects of river discharge, wind stress, and slope eddies on circulation and the satellite-observed structure of the Mississippi River plume, *Journal of Coastal Research*, *21*, 1228-1244.

Whitlock, C., and P. J. Bartlein (1993), Spatial Variations of Holocene Climatic-Change in the Yellowstone Region, *Quaternary Research*, *39*, 231-238.

Williams, D. F., and B. Kohl (1986), Isotope Chronostratigraphy and Carbonate Record for Quaternary Site-619, Pygmy Basin, Louisiana Continental-Slope, *Initial Reports of the Deep Sea Drilling Project, 96*, 671-676.

Woodhouse, C. A., and J. T. Overpeck (1998), 2000 years of drought variability in the central United States, *Bulletin of the American Meteorological Society, 79*, 2693-2714.

Yu, Z. C., J. H. McAndrews, and U. Eicher (1997), Middle Holocene dry climate caused by change in atmospheric circulation patterns: Evidence from lake levels and stable isotopes, *Geology, 25*, 251-254.

Seite Leer /
Blank leaf

Chapter 7

Conclusions and outlook

7.1. Terrigenous input by the Mississippi River

Examining variations in the input of terrigenous material by the Mississippi River proved to be valuable in several aspects. On the one hand, the assessment of the contribution and nature of terrigenous organic matter in Orca Basin sediment set the basis for the interpretation of the bulk nitrogen isotope record. On the other hand, the multi-proxy investigation showed that terrigenous material might be a useful additional proxy for assessing the timing of deglacial meltwater flow to the Gulf of Mexico, which had previously been exclusively inferred from foraminiferal $\delta^{18}O$ values. Finally, variations in the abundance of Mississippi-derived material in Pigmy Basin yielded valuable information on hydrological changes in the catchment over the course of the Holocene.

More specifically, the results indicate that:

- In Orca Basin, organic matter in the glacial sediment is to a large part of terrestrial origin and strongly degraded. This seriously affects the use of bulk sedimentary proxies such as $\delta^{15}N$ for inferring changes in marine ecosystem during that time. In contrast, the sediment younger than around 11 ka contains exceptionally well-preserved organic matter of mostly marine origin.
- During the deglacial period characterized by strong meltwater flow to the Gulf of Mexico, peak input of terrigenous organic matter does not always coincide with salinity minima reconstructed previously from foraminiferal $\delta^{18}O$. This potentially indicates additional influences on organic matter transport, but also calls for further assessment of the timing of meltwater input, for example during the Younger Dryas period. In addition, differences observed among various applied proxies for terrigenous organic matter contribution caution against relying on one single parameter.

- In the course of the Holocene, Mississippi sediment input to Pigmy Basin was largest during generally dry conditions in parts of the catchment. Some potential influences such as climate conditions in the eastern catchment or changes in sediment distribution in the Gulf of Mexico are currently not well constrained. Nonetheless, this observation is best explained by more extreme climate conditions facilitating erosion during these times, which were generally associated with strong summer insolation.

Although the interpretation of the elemental record from Pigmy Basin would benefit from further investigations, for example on variations in the sediment distribution pattern in the Gulf of Mexico, the results from this study already suggest that in climatic regimes like central North America riverine sediment input could be used as a proxy for the extremity of hydrologic conditions, in contrast to many archives recording changes in the mean state.

7.2. Deglacial changes in N_2 fixation

The nitrogen isotope records presented here are the first high-resolution deglacial records from areas with active N_2 fixation, which are located far from the influence of denitrification in the major oxygen minimum zones. The results therefore provide much-needed evidence for the behavior of N_2 fixation during deglaciations and complement existing evidence for changes in global denitrification. This is a further step towards constraining variations in the marine nitrogen reservoir on glacial-interglacial timescales. However, in both records, additional local factors influenced the $\delta^{15}N$ signal and had to be separated from the effect of N_2 fixation changes.

The following conclusions can be drawn:

- Although the interpretation of the $\delta^{15}N$ record from the Orca Basin is compromised by the interference of terrigenous organic matter in the glacial section, the data imply that glacial N_2 fixation was not stronger than in the Holocene, but probably weaker.
- The timing of the clear deglacial $\delta^{15}N$ decreases in Cariaco Basin implies that these changes can best be explained by regional increases in N_2 fixation. Local effects of variations in hydrography and nutrient cycling added superimposed millennial-scale variability to the overall signal.

- The results from both Orca Basin and Cariaco Basin therefore show that N_2 fixation in the North Atlantic was not enhanced in glacial times, despite potentially larger dust input. Instead, N_2 fixation was most likely stronger in interglacials and responded to a global loss of fixed nitrogen due to enhanced denitrification causing global nutrient N:P ratios to decrease upon deglaciations.

- The Cariaco Basin data suggest that iron-containing dust input is a second important requirement for N_2 fixation. This is reflected in the Holocene decrease in $\delta^{15}N$ being delayed until the mid-Holocene re-establishment of the Saharan desert. However, the long stability of low $\delta^{15}N$ values during an earlier interglacial (MIS11) seems to contradict a significant influence of dust input if that flux is connected to the 23-kyr precessional cycle. A further assessment of the dependence of N_2 fixation on iron input therefore requires a high-resolution record of Saharan dust flux for MIS11.

- The comparison of the detailed Cariaco Basin record from the last deglaciation with that from termination V proved a useful approach for testing how representative the results are. However, the lack of other high-resolution records for this earlier termination currently limits the insight that can be gained.

- An early Holocene decrease in $\delta^{15}N$, which Orca and Cariaco Basin have in common with records from denitrification zones likely represents a deglacial alteration of the mean ocean nitrate isotopic composition. This signal is probably related to a transient change in the relative global importance of water column versus sedimentary denitrification.

With regard to the regulating mechanisms within the marine nitrogen cycle and its stability on glacial-interglacial timescales, the results of this thesis provide answers but also new challenges. The new records showed that increasing N_2 fixation in the western North Atlantic from glacials to interglacials balanced some of the increased global N loss through denitrification. One major question is how representative the results from the Atlantic are for global N_2 fixation. While it is now likely that N_2 fixation did not augment a glacial increase in nitrate availability, the question remains how much this process contributed to keep the nitrogen budget in balance. If N_2 fixation responded globally several thousand years after the rapid deglacial increase in denitrification, the ocean could potentially have lost, in the absence of other regulating mechanisms, a considerable amount of fixed nitrogen. Records of N_2 fixation from other ocean basins, with a different deglacial history of dust flux, are therefore needed to assess whether the lateness of the N_2 fixation response is a global phenomenon.

Besides adding valuable new evidence, this work has also confirmed the limitations of bulk nitrogen isotope measurements in sediments, as different overlying influences are some-

times difficult to distinguish and varying organic matter sources can potentially turn the signal unreliable. Although these interferences could be reasonably well constrained in the settings of this study, further investigations of deglacial changes in N_2 fixation at continental margin sites will depend on the development of alternative methods. This is also a prerequisite for obtaining records from open ocean areas, where bulk sedimentary nitrogen isotopes cannot be used as proxy. Therefore, there is a strong need to further investigate nitrogen bound to carbonaceous microfossils, potential biomarkers characteristic for marine diazotrophs, molecular biological methods for reconstructing past N_2 fixation activity, and compound-specific $\delta^{15}N$ measurements. The preliminary results from this study suggest that cyanobacterial biomarkers proposed so far might not be applicable to the open ocean system. With regard to fossil-bound nitrogen, this study illustrated that coccoliths are probably not the ideal target, as contamination by clay-bound nitrogen proved difficult to evade. Further method development should therefore concentrate on fossils that are better to separate from clay, such as foraminifera or thoracospheres. The good preservation of organic matter in Orca and Cariaco Basin as well as the information about likely changes in N_2 fixation obtained in the present study make these sites ideal candidates for further testing of new methods.

Appendix

A. Organic matter composition in core MD02-2550 (Orca Basin)

A1. Kerogen composition

A2. Concentrations of marine and terrigenous biomarkers and M/T ratio

A3. Concentrations and $\delta^{13}C$ of long-chain n-alkanes

B. High-resolution geochemical data ($\delta^{15}N$, %TN, %TOC, C/N, %carbonate, %detritus, $\delta^{13}C_{org}$) from core MD02-2550 (Orca Basin)

C. $\delta^{15}N$, %TN, %TOC and C/N data from core MD03-2621 (Cariaco Basin)

D. $\delta^{15}N$ and %TN data for termination V from ODP core 1002C (Cariaco Basin)

E. Elemental composition of cores PBBC-1E and MD02-2553 (Pigmy Basin)

The high-resolution data from Orca Basin, Pigmy Basin, and Cariaco Basin (Appendix B-E), are available in electronic form.

A1. Kerogen composition in Orca Basin core MD02-2550. Given are abundances of different palynomorph groups in percent of total counted particles. For some palynomorph groups, the percentage of particles classified as opaque/reworked out of the total particles in that group is given as well.

core depth (cm)	90	300	370	455	500	755
No. of particles counted	283	310	308	331	295	325
zooclasts	46.6	27.7	4.2	8.5	0.7	1.2
translucent phytoclasts	30.4	44.8	67.5	61.3	48.8	57.9
opaque phytolasts	4.6	5.2	7.8	8.5	6.8	15.1
% opaque/total phytoclasts	13.1	10.3	10.3	12.1	12.2	20.7
dinocysts	6.0	7.1	2.9	6.0	8.8	4.9
reworked dinocysts	0.0	0.0	0.0	0.3	5.1	3.7
% reworked/total dinocysts	0.0	0.0	0.0	4.7	36.6	42.9
prasinophytes	0.4	0.3	1.0	0.0	1.7	1.9
Botryococcus	0.7	0.3	1.0	0.9	1.0	0.3
bisaccate pollen grains	4.2	6.8	9.4	2.1	7.8	4.9
reworked bisaccate pollen grains	0.0	0.3	1.0	0.6	4.8	4.0
other pollen grains	3.5	6.5	2.6	10.0	8.5	1.5
reworked other pollen grains	0.0	0.0	0.0	0.3	1.4	1.5
% reworked/total pollen grains	0.0	2.4	7.5	6.9	27.3	46.2
spores	2.1	0.7	0.7	0.9	0.3	0.0
reworked spores	0.0	0.0	2.0	0.6	3.7	3.1
% reworked/total spores	0.0	0.0	75.0	39.7	91.6	100.0
% reworked/total spores+pollen gr.	0.0	2.3	18.7	10.4	37.2	57.2
filaments	1.4	0.3	0.0	0.0	0.7	0.0

A2. Concentrations of characteristic marine and terrigenous biomarkers (alcohols) in core MD02-2550. Concentrations are normalized to TOC content. The M/T ratio was calculated as ratio of marine biomarkers (brassicasterol + dinosterol) versus terrigenous biomarkers (C24 + C26 n-alcohols)

core depth (cm)	age (ka BP)	brassicasterol (µg/g TOC)	dinosterol (µg/g TOC)	C24 n-alcohol (µg/g TOC)	C26 n-alcohol (µg/g TOC)	M/T
215	7.8	83.62	151.91	49.36	45.62	2.48
255	9.0	31.45	86.5	20.15	23.71	2.69
300	10.4	47.13	69.8	29.72	30.46	1.94
335	11.5	31.11	75.18	21.38	28.95	2.11
375	12.7	35.63	67.72	42.69	47.28	1.15
415	13.9	41.39	80.62	39.6	37.09	1.59
455	14.9	0.00	19.25	16.88	22.26	0.49
500	15.8	19.51	58.3	15.99	25.07	1.90
535	16.4	23.27	53.86	20.21	26.37	1.66
575	17.2	0.00	37.32	18.9	61.63	0.46
695	19.4	17.93	23.57	15.5	24.33	1.04
755	20.6	32.03	36.69	27.59	41.23	1.00
815	21.7	19.93	39.72	13.09	26.89	1.49

A3. Concentrations and isotopic composition of terrigenous (long-chain) n-alkanes in Orca Basin core MD02-2550. Values are summed concentrations of C25 to C31 n-alkanes except C28 (see Chapter 3), given relative to dry weight (dw) of sediment as well as normalized to TOC content. $\delta^{13}C$ of n-alkanes is mean of $\delta^{13}C$ of C27, C29, and C31 n-alkanes.

core depth (cm)	age (cal. ka BP)	long-chain n-alkanes (µg/g dw)	long-chain n-alkanes (µg/g TOC)	$\delta^{13}C$ n-alkanes (‰)
30	0.5	5.17	441.78	
40	0.7	2.94	262.73	
90	1.5	2.23	212.85	-31.4
140	2.3	2.86	250.44	
200	7.4	3.31	334.30	
245	8.7	1.67	159.02	
280	9.8	3.73	355.59	
295	10.3	3.75	357.43	-31.8
300	10.4	7.96	773.20	
315	10.9	1.79	198.44	
330	11.3	2.40	250.32	-29.9
340	11.6	1.52	179.23	
350	11.9	1.80	209.45	
365	12.4	2.23	327.39	
380	12.9	3.11	458.06	-32.8
390	13.2	3.10	348.24	
400	13.5	4.42	362.53	
410	13.8	1.82	134.65	
420	14.1	3.40	230.96	-31.6
430	14.4	2.35	186.70	
440	14.7	10.30	762.99	
445	14.8	3.46	372.55	
450	14.8	5.25	583.73	
455	14.9	3.01	273.35	
460	15.0	4.14	339.75	
470	15.2	6.74	591.41	
480	15.4	5.37	395.07	
490	15.6	2.93	250.50	
505	15.9	3.87	282.20	
515	16.1	11.59	934.53	-30.9
530	16.4	3.60	268.42	
545	16.6	3.31	273.18	-29.7
555	16.8	3.18	256.25	
560	16.9	3.94	331.04	
565	17.0	3.59	352.03	
570	17.1	4.01	564.17	
580	17.3	3.43	511.23	
590	17.5	2.19	336.95	
630	18.2	2.05	265.85	-32.8
670	19.0	1.30	209.74	
710	19.7	1.78	216.79	
750	20.5	3.44	464.57	
790	21.2	1.32	153.44	-32.5
830	22.0	3.01	297.64	
850	22.4	6.19	783.92	
870	22.8	4.09	628.75	
890	23.1	4.62	585.43	-30.1

Seite Leer /
Blank leaf

Acknowledgements

I would like to thank

Gerald Haug for the idea to this project and his support and motivating enthusiasm.
Hans Thierstein for his generous support and insightful discussions.
Judith McKenzie and Nicolas Gruber for valuable input and for joining the committee.

Tom Pedersen for introducing me to paleoceanography and the marine nitrogen cycle, and for continued interest in my work.

Daniel Sigman for challenging discussions about the nitrogen cycle, be it at summer school dinners, amongst cacti on Catalina Island or while he's driving in a "bumpy car"...
Larry Peterson and Ben Flower for generously sharing data and their knowledge about Cariaco and Orca Basin.
Julie Richey, Jen Flannery and Dick Poore for sharing their data and cores.
Curtis Deutsch, Eric Galbraith, Sam Jaccard, Brigitte Brunelle, and many other "nitrogen people" for stimulating discussions about the most important element.

Birgit Plessen for running thousands of samples on the mass spec in Potsdam.
Georg Schettler, Ursula Kegel, and Petra Meier for aiding with sample preparations at GFZ Potsdam.
Peter Dulski and Brigitte Richert for μXRF scanner measurements at GFZ Potsdam.
Carsten Schubert for measuring n-alkanes at Eawag and for helpful discussions.
Rebecca Robinson and Brigitte Brunelle for helping to look for nitrogen in coccoliths.
Peter Hochuli for the introduction to palynology and for classifying the kerogen particles.
Daniel Birgel and Julius Lipp for help with the biomarker measurements at Bremen and for making the long hours in the lab seem shorter.
Ulla Röhl, Kai Hinrichs, Gerhard Schleser, and Daniel Sigman for the opportunity to use their facilities.
The groups at GFZ Potsdam, Princeton, Bremen, FZ Jülich, and USF for all their help and openness.
The chief scientists, participants, and crews of the research cruises on the Marion Dufresne.

Ursula Brupbacher and Regula Schälchli for keeping the administrative jungle out.
Urs Gerber for millions of pixels of sediment and Robert Hofmann for always finding a technical solution.
The micropal group members: Hsin-Chi, Sam, Sandra H., France, Ralf, Jörg, Patrick Q., Jens, Andy W., Sandra S., Magali, and Ursi.
Adi, Andy M., Beat, Beno, Flavio, Florian, Katrin, Michi Sch., Michi St., Miriam A., Miriam D., Monica, Patrick M., Stefan, and Uli for their help and the good times in the office, the institute, and beyond.
Stefano Bernasconi and Maria Coray for making the work in the isotope lab both instructive and fun.
All the other people at the Geological Institute who make this place great to work at.

My family and friends for their interest and for reminding me that there is also a world outside science.
And Haresh for being at the same time the most critical and the most supportive of all.

Curriculum Vitae

Anna Nele Meckler

born 22 April 1977 in Frankfurt am Main

citizen of Germany

Education:

2002-2006	Doctoral student and research assistant at the Geological Institute, ETH Zürich, Switzerland
	Supervision: Prof. G.H. Haug and Prof. H.R. Thierstein
1996-2002	Studies in Geoecology at the University of Bayreuth, Germany
	Specialization in Climatology and Hydrology
	Diploma thesis: "Assessment of organic matter degradation in lake sediments" at Eawag, Kastanienbaum, Switzerland
	Supervision: Prof. S. Peiffer, Dr. M. Dittrich
1998-2001	Undergraduate studies in Economics at the University of Bayreuth, Germany
1999-2000	Studies in Oceanography at the University of British Columbia, Vancouver, Canada
	Scholarship from the German Academic Exchange Service (DAAD)
June 1996	Allgemeine Hochschulreife (Abitur)
1993-1996	Gymnasium Nidda, Germany